Underground Hydrogen Storage in the Taranaki region, New Zealand

Authors:

Andrew Nicol; David Dempsey; Edward Yates; Karen Higgs; Mac Beggs; Ludmila Adam

Date:

March 2022

Acknowledgments:

This report presents independent research led by the University of Canterbury and commissioned by the Firstgas Group. We gratefully acknowledge contributions from Alan Bischoff and Jonathan Ennis-King.

Table of contents

Executive summary

Green hydrogen, generated from excess renewable electricity, will be an important component of the future zero-emissions energy system. Hydrogen has a wide range of applications including transport fuel, industrial feedstock, and electricity generation to meet excess demand.

Hydrogen is projected to account for at least 10% of the global energy system in 20 years. At current energy demand, this corresponds to 72 PJ (~600,000 tonnes) of hydrogen annually in New Zealand, of which 7 to 18 PJ may need to be held in storage. Storage allows production to take advantage of intermittent renewable surplus at low cost, to accommodate peaks in energy demand, and to provide a strategic reserve.

Meeting this storage demand would require up to 200 cryogenic tanks of the most advanced design, or about 500 vertical shafts, which are currently an unproven technology. It could also be met through subsurface storage in a small number (e.g., <10) of porous reservoirs. The large storage volumes of porous reservoirs, which are here referred to as Underground Hydrogen Storage (UHS), will permit larger-scale hydrogen production and provide sufficient capacity for managing out-of-phase supply and demand cycles.

Globally, underground storage of pure (>98%) hydrogen has only been achieved in caverns excavated from salt deposits, which are not present in New Zealand. Instead, this report focuses on the potential for UHS in subsurface porous rock formations of Taranaki. Two types of storage systems are considered here, depleted oil and gas reservoirs and saline aquifers.

Depleted oil and gas reservoirs are the most attractive of the two options because containment of buoyant fluids over geological time is proven, they are usually associated with extensive subsurface characterization, and have existing infrastructure that could be repurposed (e.g., wells and pipelines). Optimism in the published literature is high for storage in both aquifers and depleted natural gas reservoirs with foundational research and technical trials showing promising results.

Effective UHS in porous-media requires the geological system to have sufficient storage capacity, deliverability and security of containment to meet operational specifications. Taranaki UHS systems require three key elements; i) a porous reservoir sandstone to store the hydrogen, ii) an effective geological cap rock (top seal) to prevent hydrogen migrating upwards out of the reservoir, and iii) a suitable geological trap to prevent the hydrogen migrating around the cap rock.

The preponderance of hydrocarbon accumulations in the Taranaki region demonstrate that sedimentary strata commonly form effective reservoir-cap rock trap systems. The largest and geologically simplest traps are at the crests of anticlines at depths of <2.5 km. The suitability of five reservoir sandstone formations and three cap rock mudstone formations are considered here. These rocks range in age, mineral composition, physical properties, and burial depths. Reservoir sandstones range in thickness from 10s to 100s of metres, with permeabilities of mainly 10-100 mD. The Tariki Sandstone in the Ahuroa field and McKee Sandstone in the McKee field have the greatest potential for UHS. Cap rocks typically comprise fine silt and clay sized particles with porosities of a few percent, permeabilities of <5 mD and thicknesses of >10 m.

Reservoir and seal rocks in Taranaki are dominated by silicate minerals (quartz, feldspars, clay) that are unlikely to undergo significant alteration over a typical hydrogen storage cycle.

Geochemical modelling of hydrogen-brine-rock systems suggests that reservoir and cap rocks containing sulphates, carbonates (e.g., calcite or dolomite) or pyrite could react with injected hydrogen resulting in mineral dissolution and/or precipitation. Sulphate minerals are generally absent in New Zealand reservoir and seal rocks; many also do not have significant carbonate or pyrite and are considered unlikely to produce adverse reactions. However, carbonate and pyrite content is variable and will need to be assessed for each UHS site. Furthermore, hydrogen-rock reactions are dependent on sub-surface conditions (e.g., temperature, pH, pressure, chemistry) and studies are recommended to predict the degree of rock reactivity and potential resulting changes in rock properties.

Preliminary reservoir models were constructed for UHS at three depleted gas fields (Ahuroa, McKee and Rimu) and one saline aquifer (Ahuroa shallow sand). These were characterized using data from well and field reports and published literature. Dynamic (annual) modelling suggests that the depleted reservoirs could have storage capacities up to 850 TJ per well. The McKee scenario has the largest storage due to its high permeability and porosity, thick storage interval and relatively large pressure depletion. Dynamic storage between 55 and 290 TJ at Rimu per well is probably sufficient to accommodate (10 to 15% of) the ~600-770 TJ of hydrogen production estimated for a nearby Waipipi windspill scenario.

Static modelling suggests total storage capacity could be 5 PJ at Ahuroa (if converted from natural gas), and 1 PJ at Rimu, which collectively are approaching the estimated requirements of a future hydrogen economy (7 to 18 PJ). These volumes exceed the capacity of other large storage options (cryogenic storage, artificial caverns, linepack). Modelled hydrogen transfer rates are lower at Rimu and McKee (0.45 and 7.0 TJ/d) than Ahuroa (18 to 33 TJ/d). These hydrogen rates are less than the current estimated energy transfer performance for natural gas at Ahuroa (65 TJ/d).Monitoring of UHS is likely to be a regulatory and operational requirement for storage sites. It will ensure that infrastructure (e.g., wells and pipelines) and reservoir performance are within specifications, confirm containment and help manage adverse rock reactions and leakage, which could result in contamination and loss of the recovered hydrogen. Stored hydrogen can be monitored using atmospheric techniques, monitoring wells or geophysical methods. Monitoring wells are widely used in industry and are the most prospective means of confirming stored hydrogen and reservoir-cap rock conditions (pressure, temperature and chemistry). The number of wells will depend on a range of factors including, site conditions, desired resolution and implementation budget.

Published studies emphasise the need for case-by-case evaluation using research tailored to a region or reservoir's particular characteristics. Despite the large datasets available for many depleted oil and gas reservoirs in Taranaki, additional information may be required to support UHS operationalisation by reducing uncertainties. These investigations may include characterisation of 3D geological models, reservoir-cap rock properties, chemical reactions, microbiological activity, reservoir engineering performance and UHS monitoring requirements.

1. Introduction

Hydrogen is a versatile energy carrier that can be used for a wide range of purposes across domestic, industrial and export sectors (Concept, 2019b, 2019a, 2019c; MBIE, 2019). Green hydrogen, a zero-carbon fuel produced using water electrolysis and surplus renewable electricity, is a potential supplement for fossil fuels (CCC, 2021; ICCC, 2019; IEA, 2019; MBIE, 2017, 2019). Green hydrogen can be used for downstream industries (process heat, fertilizer production), transport, export, or electricity generation when demand exceeds supply over time periods of days to months (e.g., NZ dry-year scenario)(MBIE, 2019; Tapuae Roa, 2019).

Hydrogen storage facilities will be required to support continuity of supply during peak feedstock and electricity demand. According to future scenarios, as hydrogen demand rises, the need for storage options (Figure 1) will increase and storage capacity greater than on-site industrial tanks will be required to realise the full potential of hydrogen (Andersson & Grönkvist, 2019; IEA, 2019; IRENA, 2018; Kruck et al., 2013; Ozaki et al., 2014).

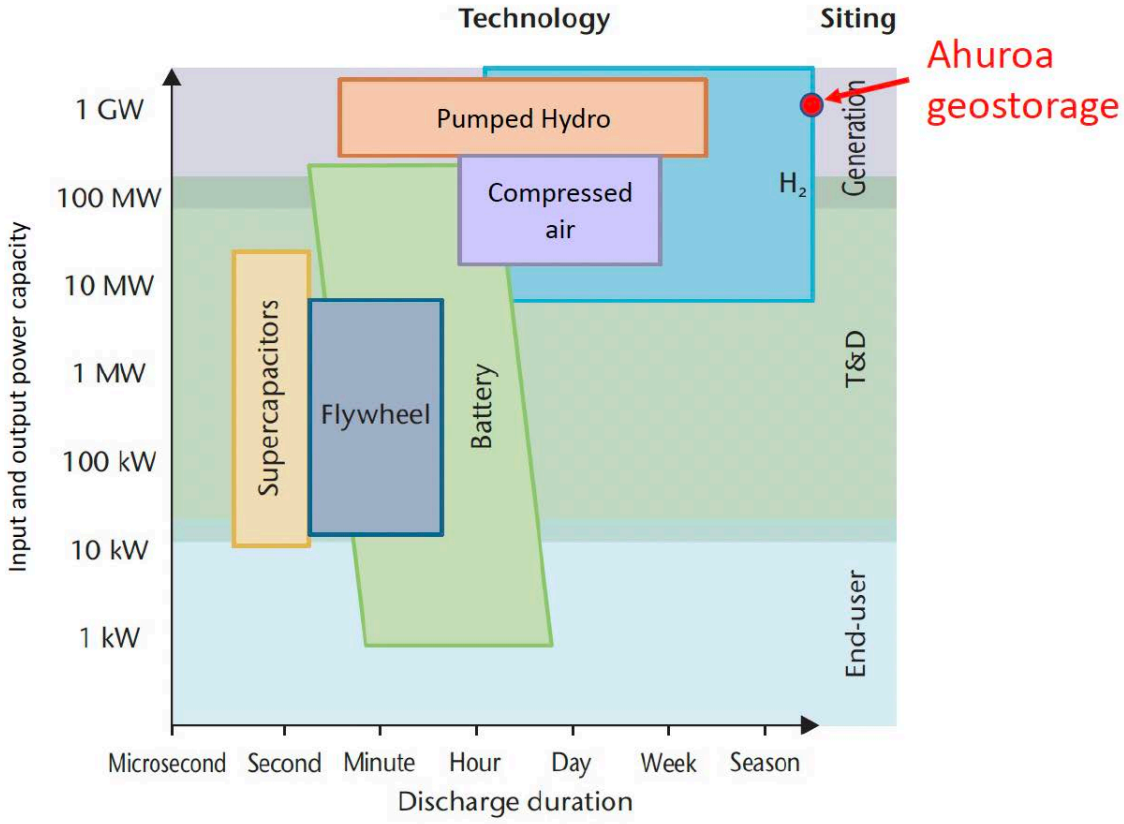

Figure 1: Electricity storage applications and technologies as a function of capacity and discharge duration (modified from Körner et al., 2015). Hydrogen-based electricity storage covers large-scale and long-term peaks in energy demand typically met using fossil fuels. For scale comparison, a single natural gas reservoir in NZ (Ahuroa field – GSNZ SPV1, 2020) stores the equivalent of ~18 PJ of electricity.

Subsurface storage in anthropogenic caverns and natural porous rock reservoirs are viable options for large volumes of hydrogen (Kittinger et al., 2017; Lord, 2009; Lord et al., 2014;

Zivar et al., 2020). These storage options are here referred to as Underground Hydrogen Storage (UHS) and individual sites are capable of storing energy exceeding 3.6 PJ. Although there are presently few UHS operations in porous rocks, hydrogen reservoirs occur naturally (Prinzhofer et al., 2018) and subsurface storage of natural gas is a mature industry (Lord, 2009). International studies support the view that porous rock reservoirs could have sufficient volume, containment capacity, and biogeochemical stability to store commercially viable quantities of hydrogen (Amid et al., 2016; Ennis-King et al., 2021; Hassannayebi et al., 2019; Lord et al., 2014).

No UHS investigations have been conducted in or with reference to New Zealand geology. This report reviews the current state of knowledge for international UHS, with emphasis on porous rock storage systems. This study is a pre-feasibility assessment using published information that focuses on the subsurface geological and reservoir engineering requirements for deployment of UHS in Taranaki, New Zealand. In addition to reviewing the literature, preliminary calculations of reservoir performance are presented for certain storage sites. The geological conditions (reservoir, cap rock and structural containment), reservoir engineering, and monitoring requirements for hydrogen storage are reviewed. Practical steps for the appraisal and development of UHS in New Zealand are proposed. Economic and above-ground engineering considerations are not addressed in this report.

The report addresses seven main topics, which are briefly outlined below.

1. *Energy landscape.* A discussion of past developments in the NZ energy sector, the current context and decarbonisation transition, and future trajectories in which green hydrogen, and storage thereof, play an important role (Section 2).
2. *Hydrogen storage technologies.* Potential caverns and porous sandstone reservoirs are reviewed, including depleted oil and gas reservoirs, and aquifers. Storage options are compared, with their strengths and weaknesses discussed (Section 3).
3. *Geological conditions.* Consideration is given to general requirements for hydrogen storage. Geological structural controls and potential reservoir/cap rocks are examined. Geochemistry, possible hydrogen-rock (mineral and pore fluid) chemical interactions, and microbiological activity that could impact reservoir performance and/or hydrogen purity are considered (Section 4).
5. *Taranaki storage opportunities*. A brief outline of subsurface storage options in Taranaki accompanied by more detailed consideration of key sites (Section 5).
6. *Reservoir engineering.* A review of injection, storage and extraction requirements for UHS in Taranaki reservoirs is presented. Static and dynamic storage models are developed for key reservoir rocks at four potential storage sites and a range of depths (Section 6).
6. *Monitoring and hazards.* A summary of the main monitoring techniques for safe and economic hydrogen storage are discussed. Focus is given to subsurface monitoring of reservoir and cap rock performance, discussion of atmospheric contamination. Monitoring of infrastructure performance (e.g., wells, pipelines and compressors), and ground-surface environmental impacts are not considered (Section 7).

7. *Future work.* Identifies and prioritises key unknowns where additional examination may facilitate the safe and economic implementation of UHS (Section 8).

A glossary of key acronyms is provided in Appendix A1.1, while information and discussion in the main body of the report is supported by supplementary material in appendices 2-5.

2. New Zealand Energy Landscape

As a relatively small economy situated remote from global centres, New Zealand's energy markets can be differentiated from developed world norms. Whereas petroleum liquids (including LPG) are traded readily in and out of the country, electricity is a closed system. The electricity generation portfolio has been dominated by renewables: hydro, geothermal and, more recently, wind. The gas market (excluding LPG) is confined to the North Island, with an important global interface via methanol, which is primarily exported. Methanol production consumes up to 90 PJ of gas as feedstock and energy from New Zealand fields per year, which is up to 45% of the total output.

This section draws on recent studies from a range of perspectives to consider the outlook for hydrogen in New Zealand's future energy system (Concept, 2019a; Ennis-King et al., 2021; FirstGas, 2021; MBIE, 2019; Tapuae Roa, 2019). In particular, we consider when and how UHS would be required to meet green hydrogen's growth trajectory as it supplants natural gas in industrial, electricity, commercial, domestic and transport sectors. The historic context includes previous transitions and dislocations in New Zealand's energy system, especially in relation to natural gas and its infrastructure.

Global production of hydrogen is significant, however, it is typically generated and used at source in refining and other petrochemical processes. Since about 2018, the potential of hydrogen as an important component of a sustainable decarbonized energy system has been widely recognized. To date hydrogen has had limited use in energy systems as a whole. Supplanting the current carbon-based energy system with new technology and fuel will be an ambitious exercise, but will not be the first significant transition in the history of New Zealand's energy system.

2.1. Previous relevant transitions in New Zealand's energy system

New Zealand's extant energy system is in large part a legacy of major investments made in the third quarter of the 20th century, which have been sustained and modernized but not greatly altered structurally. These include major electricity generation projects, an oil refinery, and infrastructure for natural gas utilization including a petrochemicals industry.

2.1.1. Leveraging the Natural Gas Opportunity (1970's–1980's)

Discovery of the Maui gas (for location see Figure 2) field in 1969 presented an opportunity to develop an abundant new energy source for economic transformation and growth, which introduced new energy-intensive industries and diversified energy supply. The growth of the gas industry is illustrated in Figure 3. The counterpart challenge was to finance and implement considerable green field infrastructure in a coordinated way.

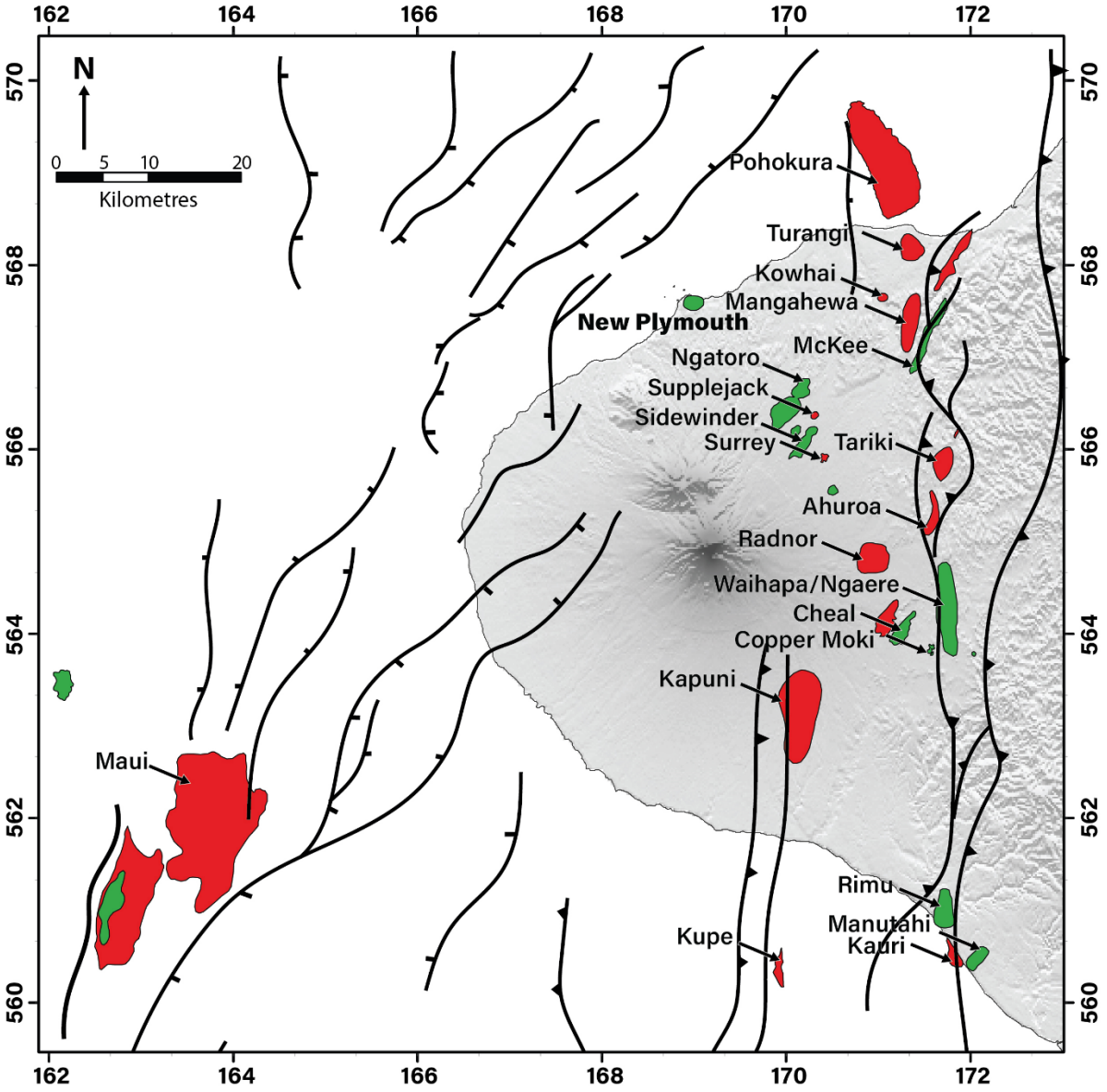

Figure 2: Map showing the locations of oil and gas fields and geological faults in the Taranaki Peninsula area. Oil (green) and gas (red) field locations are from (NZP&M, 2021)*. Geological faults modified from King and Thrasher (1996).*

The Maui gas field was discovered in offshore Taranaki by Shell, BP and Todd in 1969 following their success onshore at Kapuni a decade earlier. The government-led decision to develop Maui required ambitious companion investment in gas processing, transmission, distribution and consumption.

With technological advances, new elements were added to the system, including several combined cycle gas turbines for power generation. Most have been retired as new geothermal and wind generation has proven more economic in the face of rising carbon

charges, gas supply terms, and competition for base load dispatch. Some energy intensive industries that benefitted from natural gas infrastructure, especially wood processing, have diminished in output in the face of increased gas prices and reduced availability (New Zealand Herald, 2021a).

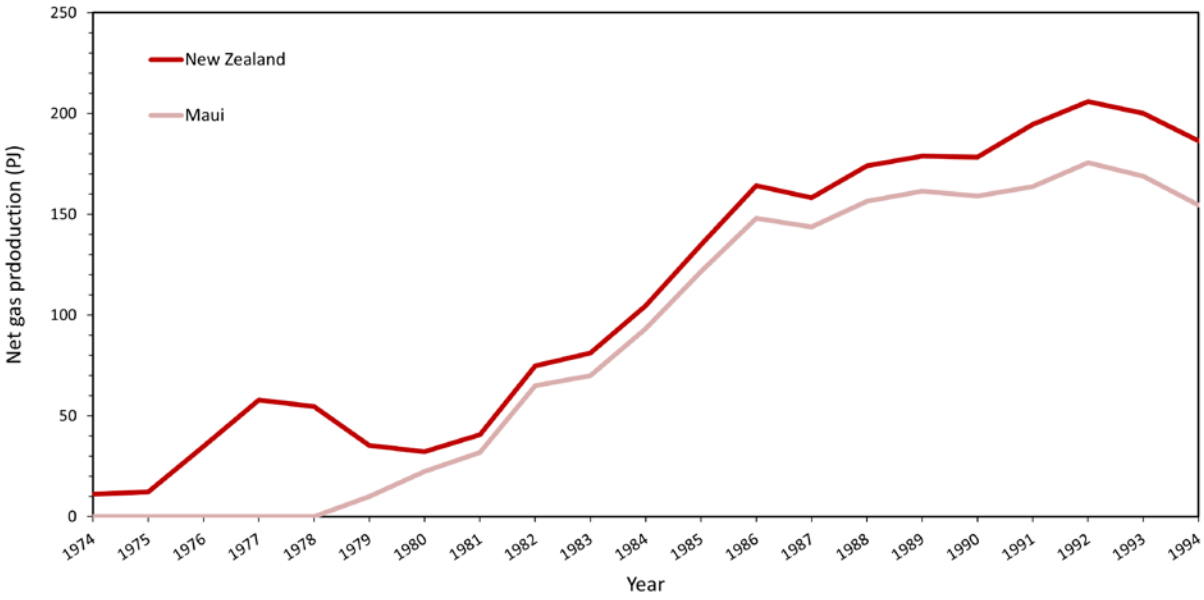

Figure 3: Natural gas production (and consumption) in New Zealand expanded rapidly with the development of the Maui field, to its present scale of around 200 PJ per year. The industry more than trebled between 1981 and 1986, as new midstream and downstream infrastructure was commissioned. Figure from MBIE (2021).

In common with the present transition to decarbonisation, the response (to discovery of a large natural gas resource) was driven by government policy with much investment in transformational infrastructure through state owned enterprises.

2.1.2. Consequences of Maui field redetermination (mid 2000's)

The most significant adaptions to the "Think Big" system occurred around the turn of the millennium, with the price of natural gas released from the 1970's Maui contracts when the field's reserves were revised downwards.

In 2002/3, the Maui contracts were restructured following a downward redetermination of the field's contractual reserves, driving significant changes in the energy system. For example, methanol manufacture was severely curtailed for a period of time. Gas prices rose, stimulating the development of additional gas fields – Pohokura and Kupe offshore, and the Mangahewa and Turangi fields onshore north Taranaki (Figures 2 and 4).

Previously, during the long heyday of New Zealand's natural gas production (~1986-2003), the main gas fields, in particular Maui, featured highly productivity reservoirs, with changes in demand managed by opening and closing wells. In the late 1990's, this feature of the energy system, combined with take-or-pay contracts and a large inventory of pre-paid gas held by the newly-corporatised Contact Energy, encouraged commissioning of combined-cycle gas turbines to meet growing electricity demand.

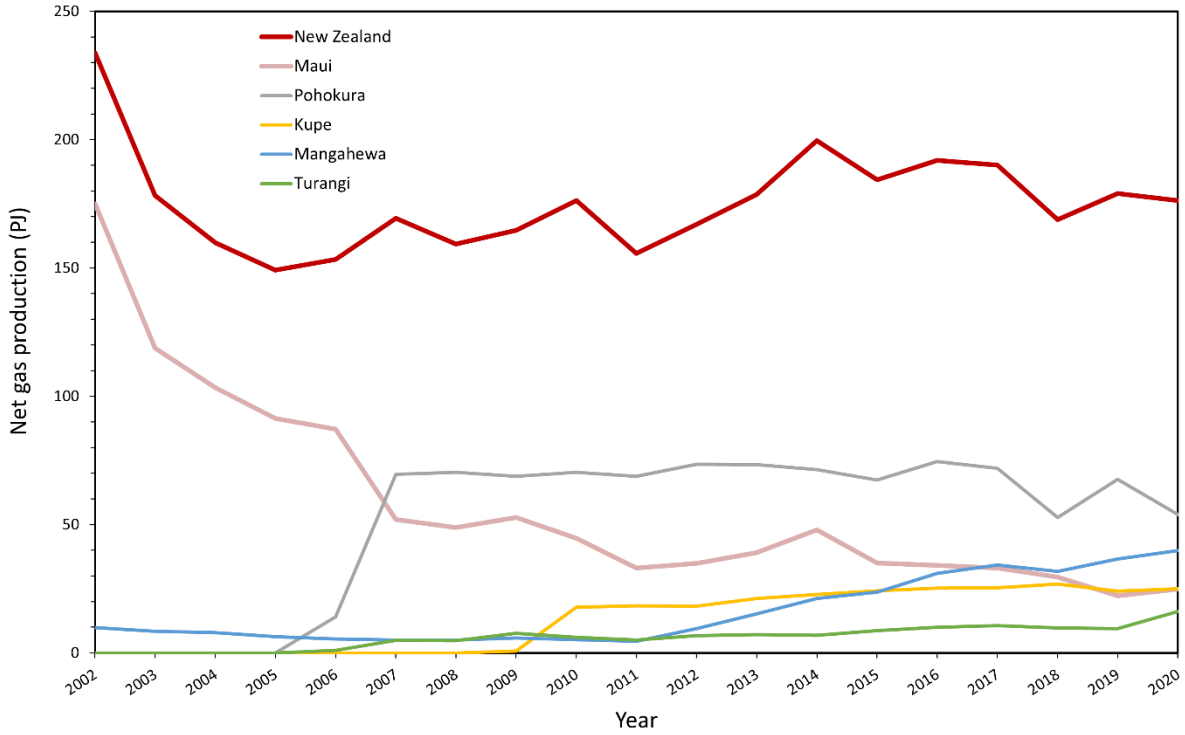

Figure 4: Following the abrupt reduction in natural gas output from the Maui field, the scale of Taranaki production was restored through the development of several offshore (Pohokura, Kupe) and onshore fields. Figure from MBIE (2021).

The Ahuroa gas storage project (2009) was a response to Contact Energy's desire to manage their gas-fueled power generation (at that time, combine-cycle turbine facilities at Stratford and Ōtāhuhu), and direct gas customer demand, including cogeneration at several industrial sites. With this storage facility, it became possible to extract gas from the offshore fields at a near-uniform rate, and deliver it to customers with fluctuating requirements, increasing supply flexibility beyond the linepack option.

Todd Energy also came to operate their Mangahewa/McKee field facilities with gas reinjection into the McKee reservoir serving as both a de facto gas storage project and enhancing oil recovery. The abrupt curtailment of gas, until new fields were developed to fill the gap, also saw coal used as fuel for the Rankine turbines at Huntly which have been required to a variable degree (largely governed by hydroelectric output as a function of precipitation in the catchments – dry year) to meet electricity demand.

Contact and Mercury Energy (then known as Mighty River Power, state-owned, and operating a combined cycle gas turbine facility in South Auckland), also invested heavily and successfully in developing new geothermal power generation in the central North Island during 2005 - 2015. That was also a period of significant expansion of wind generation, which grew from 39 GWh (0.1%) in 1999, to pass 2000 GWh (5%) by 2012.

In contrast to the previous era, the significant dislocation to New Zealand's energy system following the Maui field reserves redetermination was accommodated more by the strategies of existing corporate enterprises (some state-owned) than by government policy drivers.

Geothermal and wind generation (see Figure 5) was almost all implemented by the existing generators. New thermal generation since about 2006 has been limited to gas-fired peaking plants in Taranaki, but prior to that the government provided a guarantee for the financing of a 50MW combined cycle gas turbine to expand the Huntly power station, in 2004.

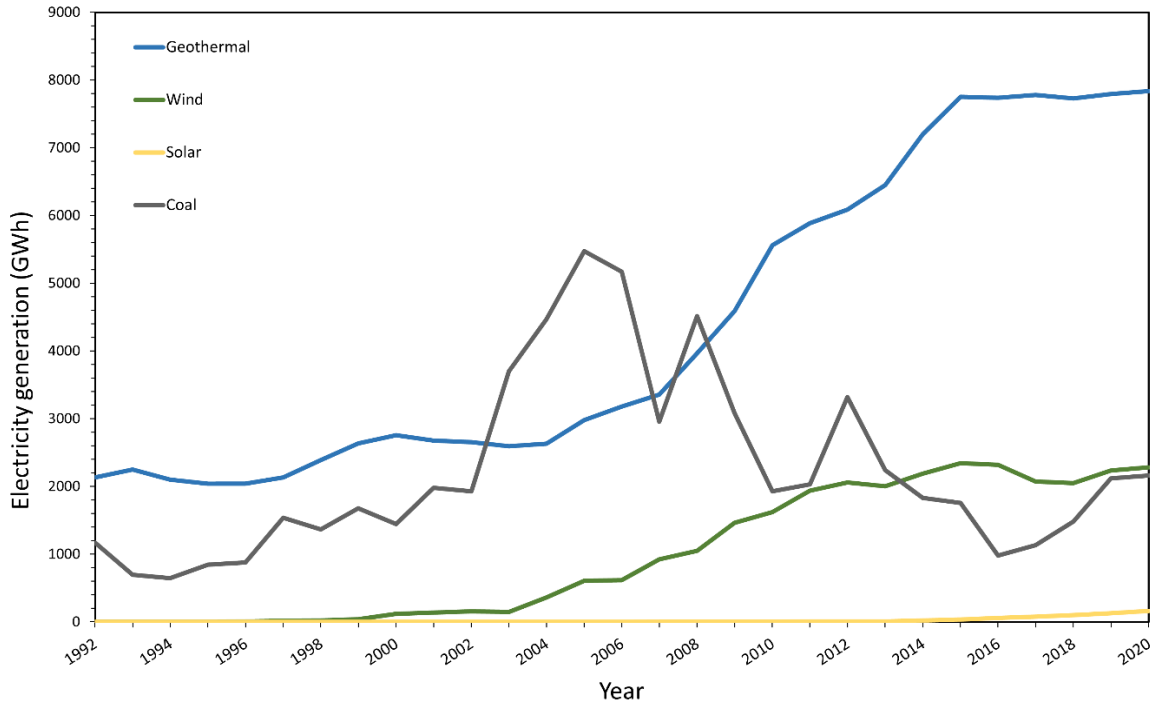

Figure 5: How electricity generation in New Zealand dealt with the curtailment of Maui gas output from 2002. Figure from MBIE (2021).

The decline in Maui gas production required a transition to alternate energy supplies to ensure continuity and security of supply, but with much less emphasis on minimizing greenhouse gas emissions than is presently the case. Energy prices rose and some industries (notably methanol) could not maintain their output for a period, until in combination, new gas fields and geothermal and wind generation developments supplanted a sharp increase in coal use as fuel.

2.2. The current transition

New Zealand is now at the start of a historic transition of its energy system to a future state, which is mainly being driven by Climate Change policy goals and a progressive depletion of Taranaki Basin gas and oil fields. In 2021, a combination of circumstances exposed the diminished capacity for these gas fields to meet market demand. This manifested in steep price increases and the inability of some gas customers to secure the supply of gas necessary to sustain their industrial output. Electricity output was sustained (except for one day in August 2019 when widespread blackouts occurred) in part by using coal to fire the Huntly Power Station imported from Indonesia (New Zealand Herald, 2021b). This exposed New Zealand consumers to high energy prices and in some industries, severe difficulty in securing energy. According to the Gas Industry Co (2021), “constrained gas supply, alongside a period of low hydro inflows … created a tension for industrial customers … seeking multi-year supply, and electricity generators seeking short term supply.”

The situation was partly alleviated by substitution of coal for gas by Genesis as fuel for the Rankine turbines at Huntly, and by Methanex (New Zealand's largest single gas customer), agreeing to forgo a substantial part of their contractual entitlement. In effect this was a brief reprise of the situation in the mid 2000's, described above, in the face of a longer-lived shortfall in gas availability. Substantial coal imports continued through 2021 and the current stockpile of coal at Huntly is understood to be at its largest since about 2015.

2.2.1. Emergence of hydrogen

With government stimulus and subsidization, Hiringa has achieved sanction for a few projects involving green hydrogen substitution for existing energy inputs: a wind farm at Kapuni, in conjunction with nitrogen fertilizer manufacturer Ballance Agri-Nutrients, and an initial North Island network of hydrogen fuel stations in conjunction with Waitomo. In addition, Obayashi in joint venture with Tūaropaki Trust has demonstrated the manufacture of green hydrogen from geothermal power.

The stage is set for a transformation on much the same scale as that of the 1970's and 1980's, in which green hydrogen's part will be dependent to a degree at least on underground storage (First Gas, 2021; MBIE, 2019). Corporate strategies are aligning with government policies, notably to give effect to commitments made under the Paris Agreement through the Climate Change Response (Zero Carbon) Act 2019 and, notwithstanding challenges to energy security and affordability, threats to the continuation of certain industries.

2.3. Possible future trajectories

2.3.1. Key recent studies

The Ministry of Business Innovation and Employment published an important "Green Paper" (MBIE, 2019) on hydrogen utilisation, and Hiringa Energy, a start-up company focused on facilitating and participating in development of hydrogen industries, produced a "Roadmap" document for Venture Taranaki (Tapuae Roa, 2019). More recently, Venture Taranaki has published a concept paper prepared for it by Sapere and Absolute Certainty, entitled "Power to X: Transforming renewable electricity into green products and services". These documents demonstrate the scope for green hydrogen to establish and grow niches in the future decarbonized New Zealand energy system.

FirstGas has analysed its situation and published a report undertaken by Aqua Consultants and Element Energy (2021). The core scenario "Integrated Energy System" (and the "High Hydrogen" scenario) estimates New Zealand's 2050 energy demand as 143 TWh (515 PJ), of which 28%, or 40 TWh (144 PJ) is derived from hydrogen. This is equivalent to 1.2 million tonnes of hydrogen, being generated from renewable electricity, mainly when electricity supply exceeds demand. This hydrogen would be dispatched to industrial users (including as feedstock for iron reduction and fertilizer manufacture), commercial and residential gas customers, and for peak power generation.

Major power companies Meridian Energy and Contact Energy have published "The New Zealand Hydrogen Opportunity" (Contact & Meridian, 2021), as background to their Southern Green Hydrogen initiative to supplant the Tiwai Point aluminium smelter with a hydrogen industry.

2.3.2. New Zealand UHS outlook

The business case for any UHS development will require the scale of hydrogen production (whether a single project, or a network system of several production and utilization projects), to exceed a level that can be managed efficiently with surface storage options (e.g., linepack or tanks).

New Zealand's advantage – plentiful renewable power

The existing preponderance of renewable electricity and its trajectory towards 100% of New Zealand's generation constitutes a competitive advantage for green hydrogen. In most other parts of the world, renewable electricity is rarely in surplus except locally. In Australia and other lower latitude, arid settings, increased renewable electricity will require extensive development of a large solar resource, which is generally inconveniently located relative to energy markets. The substantial existing hydro, geothermal, wind and emerging solar generation in New Zealand means that our reliance on future renewable-energy generation can be proportionally much lower than other countries.

Intermittency of wind and solar generation is likely to result in both short (daytime, and spells of favourable weather) to long (between dry spells in hydro catchments) periods of excess generation. This will be exacerbated by the degree of overbuild required to avoid regular reliance on thermal backup and/or more aggressive management of hydroelectric generation. Under these conditions, electricity surplus at low price will benefit green hydrogen, providing its production can be discontinuous. New Zealand has abundant resources of renewable electricity potential when classes such as offshore wind are considered (Tapuae Roa, 2019) 6).

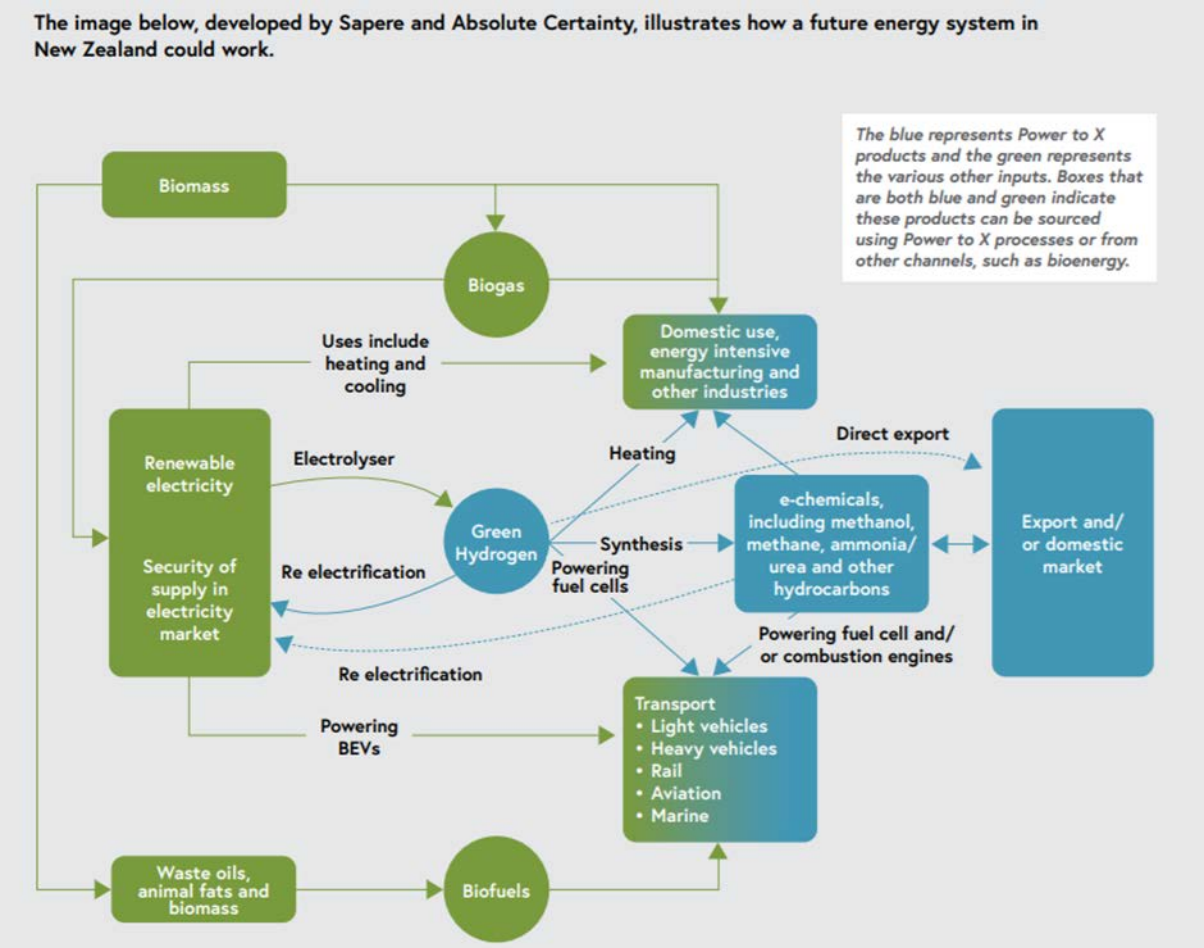

Figure 6: Schematic diagram showing how a hydrogen-based energy system could operate in New Zealand. Figure from (Venture Taranaki, 2021).

Transforming gas networks

FirstGas has presented a vision for substitution of current natural gas consumption with green gas including hydrogen and biogas, initially via blending. A substantial proportion of existing consumption is in industries that may not be viable for because, for example, they face competition with carbon-based products of at least equal utility and lower cost. Commercial and residential consumers should be able to move to electricity and would presumably do so unless green gas presented clear advantages.

The core scenario (as well as the "High Hydrogen" scenario) in FirstGas's New Zealand H_2 pipeline feasibility study (FirstGas, 2021) assumes that most domestic and industrial natural gas demand converts to hydrogen, the major exception being methanol. Methanol manufacture in New Zealand could discontinue when the available output of natural gas falls short of the minimum continuous requirements of any of the methanol facilities (about 30 PJ per year).

This would be a further dismantling of major infrastructure originating with the aggressive adaption of New Zealand's energy system in the 1970's-1980's, with much of the methanol plant having converted the synthetic gasoline plant at Motunui in 1996, and the recent discontinuation of oil refining at Marsden Point as other examples.

Ammonia and derivatives

Fertilizer manufacture, which currently consumes approximately 7 PJ of natural gas per year, appears more adaptable to hydrogen feedstock. Ballance Agri-Nutrients, the owner of the ammonia/urea plant at Kapuni, is already developing hydrogen production using a new 16 MW wind farm to be constructed at the site. Gas stock that is surplus to Ballance's own requirements may be directed to hydrogen for transport fuel (in conjunction with Hiringa Energy) as well as to ammonia manufacture, substituting for natural gas.

Ammonia presents considerable potential as a hydrogen-based commodity, which could in theory be produced intermittently in concert with surplus renewable electricity ("trough-harvesting"). It could be directed to a range of uses including nitrogen fertilizer, in New Zealand and exported. However, ammonia synthesis at scale cannot be managed intermittently, so green hydrogen would have to be aggregated to a volume large enough to carry its consumption through a period of low or zero output. This might be when renewable electricity is utilized for higher-value immediate uses, maintaining electricity supply when some of the renewable sources are constrained by weather and other factors.

In this respect, storage operates like bagpipes, maintaining the steady output required while input is cyclical and only partly manageable. Further modelling would be required to establish the optimal range of volume and rate of injection and extraction for a short-period storage facility to match low-cost renewable electricity with a hydrogen-based commodity such as ammonia.

Hydrogen export

International trade in hydrogen is at an early stage. Policies to address greenhouse gas emissions are providing a strong stimulus for growth of the hydrogen market in the Asia-Pacific region (especially Japan and South Korea) as well as Europe. Australia, with a strong basis in LNG exports, envisages being a major contributor of hydrogen for Asia. It is not inconceivable that New Zealand (whose methanol trade is also a precursor for energy commodity export), could be part of the same logistical chain. This would require aggregation of hydrogen, or a carrier fluid such as ammonia, at points of shipping. UHS as a compressed gas at these sites seems likely to be safer than cryogenic or carrier fluid storage at surface sites amongst concentrations of other critical infrastructure.

Electricity from hydrogen

The renewables-dominance of New Zealand's electricity system is favourable for interruptible green hydrogen manufacture. Furthermore, presuming adequate storage capacity, there is also an opportunity for using green hydrogen as fuel to meet electricity demand peaks, realizing high spot prices.

Hydrogen is an option under consideration in the government's "New Zealand Battery" project, which seeks an enduring and reliable solution to the "dry-year problem": the propensity for extended dry periods that severely curtail hydroelectric storage and hence output. The preferred solution appears to be pumped hydro as an extension to the Clutha system, and transmission system upgrades to ensure power from the lower South Island can be delivered to large loads in the upper North Island.

At a large scale, the Southern Green Hydrogen concept envisages an export hydrogen industry supplied by New Zealand's largest hydroelectric scheme (Manapōuri) which would be interruptible when electricity demand exceeded an agreed threshold, when the power would resume supply to the national grid.

Demand peaks and/or supply troughs much shorter than the "dry year" scenario could be addressed by incorporating bespoke storage with both renewable and thermal generation, where green hydrogen would be used as the fuel. Some open cycle turbines within the New Zealand generation portfolio already are understood to be able to operate with hydrogen (pure, or blended with natural gas) as fuel (A. Renton, personal communication, 2021).

Ammonia could also serve as the storage/green fuel element of such a system, but would require hydrogen storage unless the ammonia synthesis was continuous.

2.4. Summary

It is a widely held view that hydrogen may account for at least 10% of the global energy system by 2050 (e.g., Yergin, 2020) and with its disproportionately high share of renewable electricity, New Zealand is positioned to exceed the global average of hydrogen utilisation.

At 10% of present-day primary energy, hydrogen would amount to over 70PJ per year in New Zealand. This corresponds to almost 600,000 tonnes of hydrogen, some 800,000 tanker loads, over 2,000 per day. Cryogenic storage of such an annual volume of hydrogen would require about 800 tanks of the most advanced design, or more than 2,000 vertical shafts.

In-ground storage of these volumes would enable industry growth by accommodating fluctuations in hydrogen production and demand. For instance, green hydrogen production will presumably operate in the lowest cost settings, manufactured intermittently when there is surplus from rapidly growing renewables. On the other side, storage enables discontinuous demands to be met (e.g., peak electricity generation and export dispatch schedules).

It seems likely that UHS will contribute to feasibility and efficiency of such a system, and of the electricity system. A Taranaki UHS site is an element of infrastructure in FirstGas's core scenario, as is the possibility of hydrogen export, which would allow for a larger scale of hydrogen production than is projected for New Zealand demand alone.

The ideal UHS development would be of a scale that corresponded to the volumes to be stored. The rate of injection and extraction would be governed by the characteristics of the porous reservoir formation, unless based on a cavern or system of shafts, and if high rates are required (e.g., for peak electricity generation) then some formations may not be suitable.

At this embryonic stage, there is no requirement for UHS. Volumes are so small that conventional road tankers (standard capacity 730 kg) can easily store hydrogen from its point of manufacture to its point of consumption or export. However, as the substantial potential for hydrogen to assume numerous roles in New Zealand's energy system is progressively realized, the number of such tankers would not be able to support storage demand unless complemented by much larger volume subsurface storage.

3. Storage technologies

Storage of pure hydrogen is broadly divided into two categories: surficial storage and underground storage. Hydrogen can also be stored chemically (e.g., as ammonia or via absorption and adsorption), which is beyond the scope of this investigation.

The emergence of a hydrogen economy in New Zealand will require the widespread use of smaller, surficial storage options. Small producers and users will likely use medium–high pressure, or liquefied/cryogenic tanks to store hydrogen at the site of production or use. Emerging users include decentralised transport refuelling hubs and some on-site industrial heating and chemical industries.

Larger producers, users and exporters should consider UHS options for their increased energy storage capabilities and improved safety (Ennis-King et al., 2021; Tarkowski, 2019). This section presents benefits and challenges of key surface and UHS technologies, using best available data and research at the time of this report.

3.1. Above ground storage

Storage of hydrogen in containment vessels above ground is often the most suitable solution for small volumes (<10,000 m^3), especially at sites of lower production and/or usage. Surficial storage solutions often have no issues maintaining hydrogen purity, however may have increased risk of leakage.

3.1.1. Transmission network – linepack

Linepack refers to gas storage within a pipeline transmission network. Linepack storage can be increased through high pressure compression of gas in the network. The North Island transmission network comprises (1) the 300 km, large diameter (750mm) Maui pipeline operating at high pressure, and (2) a 2200 km smaller diameter (100–200 mm) pipe network, operating between 20 and 86 bar (FirstGas, 2020; WorleyParsons, 2014) (Figure 7).

The assessment here is based on published accounts of the management of network outages through linepack (FirstGas, 2018; WorleyParsons, 2014). Prior to planned outages, pressure was increased in the network to store more gas. During the outage, continued gas outtake from the network dropped pressure to a minimum value. Peak linepack energy content prior to outages was 260 and 300 TJ, and the minimum contingency linepack was 236 TJ.

Ennis-King et al. (2021) introduced a scaling factor as an approximate conversion between natural gas and hydrogen energy storage at equivalent pressure. The scaling factor reflects relative differences in energy content and densities of the two gases, and ranges between 0.22 and 0.27 depending on pressure. Applying this factor to reported linepack quantities (FirstGas, 2018; WorleyParsons, 2014), we estimate the transmission network could store between 57 to 81 TJ. However, it is not clear whether a hydrogen pipeline could operate at pressures used for natural gas. Hydrogen density scales approximately linearly with pressure at these conditions, therefore, a 75% reduction in operating pressures would reduce linepack storage to between 14 and 20 TJ.

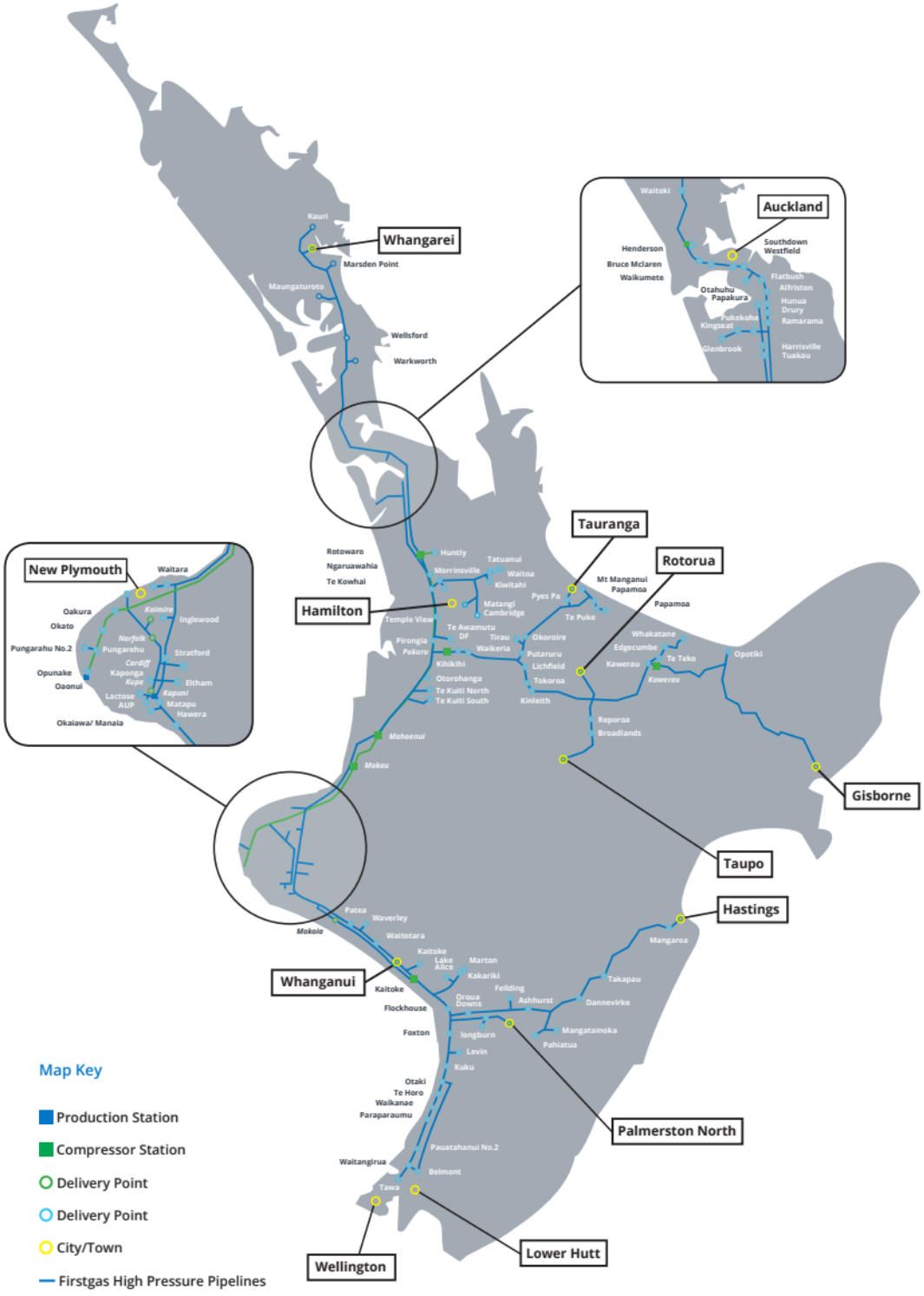

Figure 7: FirstGas gas transmission network in the North Island, New Zealand. Figure from FirstGas, (2020).

3.1.2. High-pressure tanks

Hydrogen can be stored in either high pressure or cryogenic surface tanks. A typical 300 L tank at 500 bar can store 10 kg (0.0012 TJ) of hydrogen. Hydrogen can also be stored as a liquid in cryogenic tanks. Liquid hydrogen has a density of about 70 kg/m^3, but tank insulation, cooling, and bleed off of boiled gas all contribute to increased cost. Spherical tank (Figure 8) volumes

can range from 2,500 m^3 to a new design of 10,000 m^3 with the latter holding up to 700 tonnes (84 TJ).

Figure 8: Hydrogen storage tanks. Left: 500 bar high-pressure storage. Right: spherical cryogenic tank.

3.2. Underground hydrogen storage

Four main technologies are widely considered in the literature for UHS: (1) salt caverns, (2) depleted oil or gas reservoirs (e.g., Figure 9), (3) saline aquifers, (4) excavated, hard-rock caverns (Figure 10). Each class of UHS has different geologic, infrastructure and economic requirements that must be met to be successfully implemented. This report will overview storage types and discuss storage options with respect to the geology and energy landscape of Taranaki, and New Zealand.

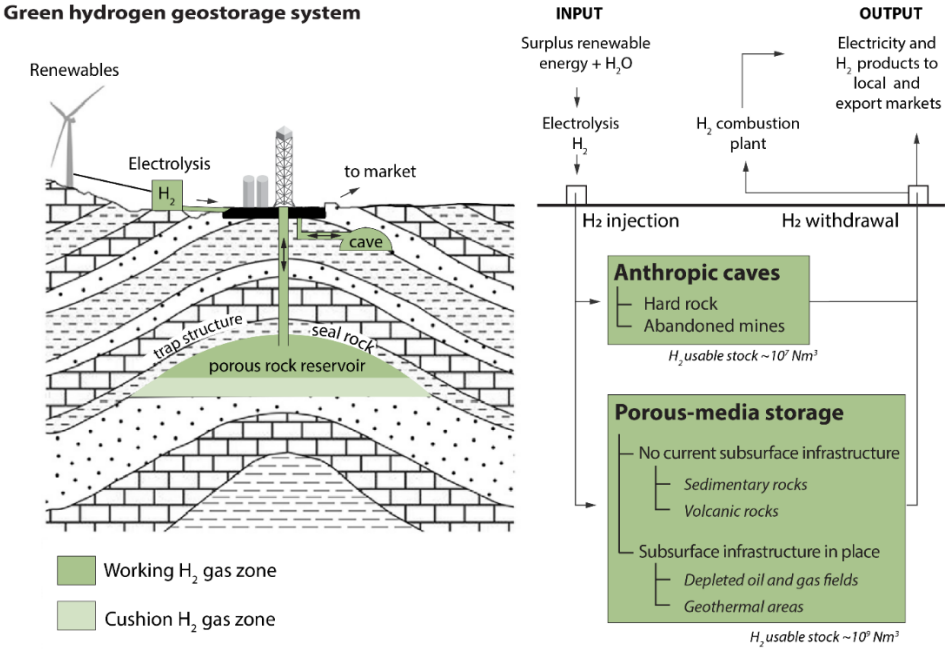

Figure 9: Green hydrogen storage schematic diagram showing potential UHS types adapted to a New Zealand setting. Figure from Bischoff et al. (2021).

3.2.1. Cavern storage

Cavernous storage options require creation of an open cavity that can store hydrogen or other economic fluids, utilising natural lithostatic pressure of overlying rock for containment. Caverns may be excavated for the purpose of UHS or pre-existing excavations (such as mines) could be retro-fitted. Depending on the geology at the excavation site, using a lining or a tank can help to minimise losses due to leakage and hydrogen–rock interactions (Gajda & Lutyński, 2021).

Salt caverns

Salt caverns are created by a process called dissolution mining where water is pumped into a salt rock formation. The salt is dissolved into a brine solution that is pumped to the surface, leaving a cavern behind. This is filled with economic fluids. Thus far salt formations have been the only active UHS reservoirs used to store hydrogen gas at >95% purity (Table 1).

Table 1: Known hydrogen storage and pilot sites. Table from Zivar et al. (2020).

Field/project name	Storage type	H_2 (%)	Working condition	Depth (m)	Volume (m^3)	Status
Teesside (UK)	Bedded salt	95	45 bar	365[a]	210,000	Operating
Clemens (USA)	Salt dome	95	70–137 bar	1,000[a]	580,000	Operating
Moss Bluff (USA)	Salt dome		55–152 bar	1,200[a]	566,000	Operating
Spindletop (USA)	Salt dome	95	68–202 bar	1,340[a]	906,000	Operating
Kiel (Germany)	Salt cavern	60	80–100 bar		32,000	Closed
Ketzin (Germany)	Aquifer	62	Not reported	200–250	Not reported	Operating with natural gas
Beynes (France)	Aquifer	50	Not reported	430	3.3×10^8	Operating with natural gas
Lobodice (Czech Republic)	Aquifer	50	90 bar/34 °C	430	Not reported	Operating
Diadema (Argentina)	Depleted gas reservoir	10	10 bar/50 °C	600	Not reported	Not reported
Underground Sun Storage (Austria)	Depleted gas reservoir	10	78 bar/40 °C	1000	Not reported	Operating

[a] Mean depth is reported for the salt caverns.

Salt caverns have so far been the status quo when considering UHS, so the occurrence of salt formations is addressed in most recent evaluations, for example, in Australia (Ennis-King et al., 2021; RISC, 2021). However, their limited geographic availability has prompted investigation of other UHS modes. No suitable salt formations are known in New Zealand, which lacked the geological conditions necessary for evaporite deposition throughout its geological history. Hence, this class of UHS is not available in New Zealand.

Excavated caverns

Shallow hard-rock caverns are a UHS option for intermediate volume storage (~1–100 TJ) that is readily scalable (Bischoff et al., 2021). This technology involves the excavation of a subsurface volume to depths of <300 m into which a high-pressure containment vessel is installed. For example, one untested method proposes drilling vertical shafts using the blind boring technique (Figure 10), with average shaft depths of 300 m and diameters of 5 m. For these dimensions, the corresponding volume is about 6000 m^3, which could hold between 18 to 32 TJ of hydrogen energy for storage pressures ranging between 350 and 700 bar. Scalability is achieved through the construction of multiple shafts. This technology is subject to the use of efficient lining materials that can effectively contain hydrogen stored at high pressures (Balasooriya et al., 2021) and may be expensive compared to other UHS alternatives

(Zivar et al., 2020). More research is required to test the utility of excavated caverns in general and vertical shafts specifically.

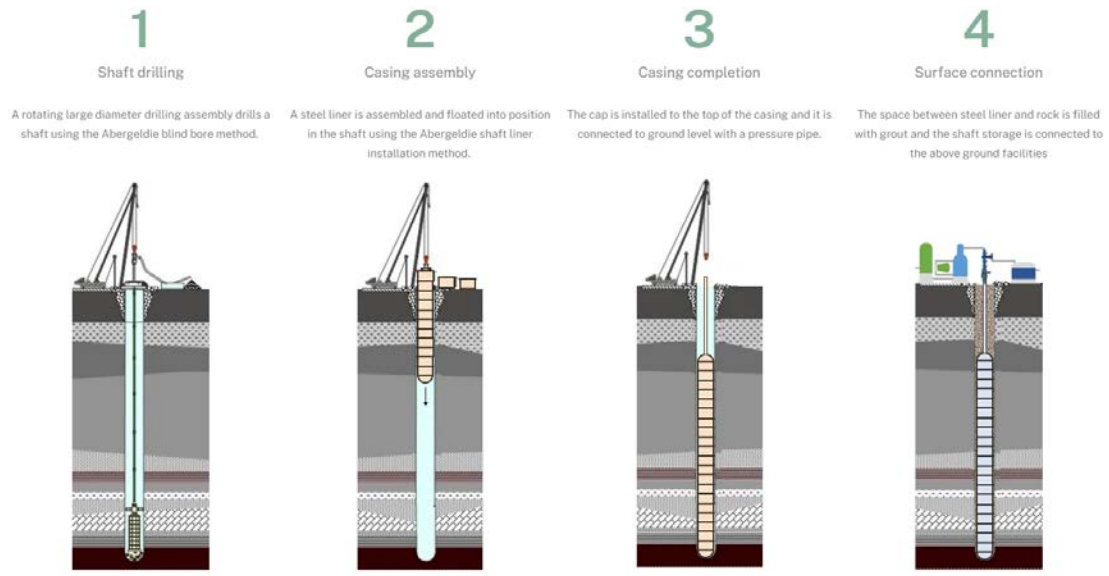

*Figure 10: Construction of underground storage shafts. Figure from (*Ardent Underground Storage*, 2022).*

Mines

Unused mine shafts may present UHS opportunities subject to further investigation and investment to ensure effective containment and address other risk factors (e.g., mine stability and fracture development due to high storage pressures). While this storage technology is presently immature, it is a topic of active research, including gas permeability, materials characterisation and preliminary modelling to improve understanding of potential reservoirs (Gajda & Lutyński, 2021; Saigustia & Robak, 2021; Wang et al., 2021).

The Huntly region, co-located with an important concentration of gas and electricity infrastructure, has had a considerable volume of coal removed from underground mines. Shafts here may be suitable to develop for energy storage. A similar strategy is being investigated in Poland where hydrogen storage in abandoned coal mines is deemed a promising but currently immature technology that requires further research and trials to overcome high costs, storage complications and leakage and safety concerns (Saigustia & Robak, 2021).

3.2.2. Porous media storage

Effective UHS in porous media requires that the geological system has a storage capacity befitting its desired use, sufficiently high injection/extraction rates and adequate containment. Storage capacity should be considered with respect to demand, the available pore volume must be large enough to adequately meet demand but small enough to not incur excessive capital expenditure (e.g., cushion gas). Reservoir permeability must be high enough to permit injection and withdrawal rates that meet peak production and demand. Injection and withdrawal rate modelling will be required to support facility design and maintain storage efficiency (Zivar et al., 2020). Containment ensures that the hydrogen remains in place and comprises two key elements; i) an effective cap rock, and ii) a suitable geological trap. A cap

rock is an impermeable material through which gas cannot effectively migrate on the timescale of facility operation and is located above the target reservoir rock. A geological trap must be shaped to prevent hydrogen migration around the cap rock. Traps may be either structural (e.g., anticlinal) or stratigraphic (e.g., reservoir pinching out, see section 4.1).

Underground gas storage (UGS) in porous-media is common worldwide, although porous media have not been used to store high purity (>95%) hydrogen (Zivar et al., 2020). Despite this, global optimism is high for both aquifers and depleted natural gas reservoirs with foundational research (Bischoff et al., 2021; Tarkowski, 2019; Tarkowski et al., 2021) and technical trials (Kittinger et al., 2017; Perez et al., 2016) showing promising results.

A recent discovery of large quantities of pure (98%) native hydrogen gas accumulated in sedimentary formations in Mali (Prinzhofer et al., 2018), is encouraging of the prospects of storing hydrogen in sedimentary reservoirs with minimal losses in purity. The native hydrogen was found across at least five reservoirs separated by dolorite sills up to a depth of 1800m. It is assumed groundwater has aided the effective containment of hydrogen over geologically significant time-scales due to low solubility with water at shallow depths.

Depleted oil and gas reservoirs

Depleted oil and gas reservoirs have commonly been utilised as UGS facilities globally, including the Ahuroa gas storage facility in Taranaki. Since these reservoirs previously held commercially-viable quantities of natural gas, they are assumed to have suitable containment for reinjected hydrocarbons. This assumes that reservoir pressures are operated such that hydrogen is not driven into and across the cap rock at unacceptable rates. Furthermore, if pressure exceeds the tensile strength of rock, a hydraulic fracture could propagate that negatively impacts containment.

Active, or previously active oil and gas reservoirs have generally undergone significant site-specific research during their lifetime. Established infrastructure and knowledge of depleted reservoirs facilitate their development to UGS. While site-specific research is still required before converting depleted reservoirs into UGS, it may require significantly less acquisition of new data than lesser developed reservoir types such as saline aquifers. In this way, UGS is analogous to UHS where site-specific subsurface information from seismic reflection data and wells (i.e., about the reservoir, cap rock, trap, chemistry and geology) may be used to inform decision making processes for UHS site selection and development.

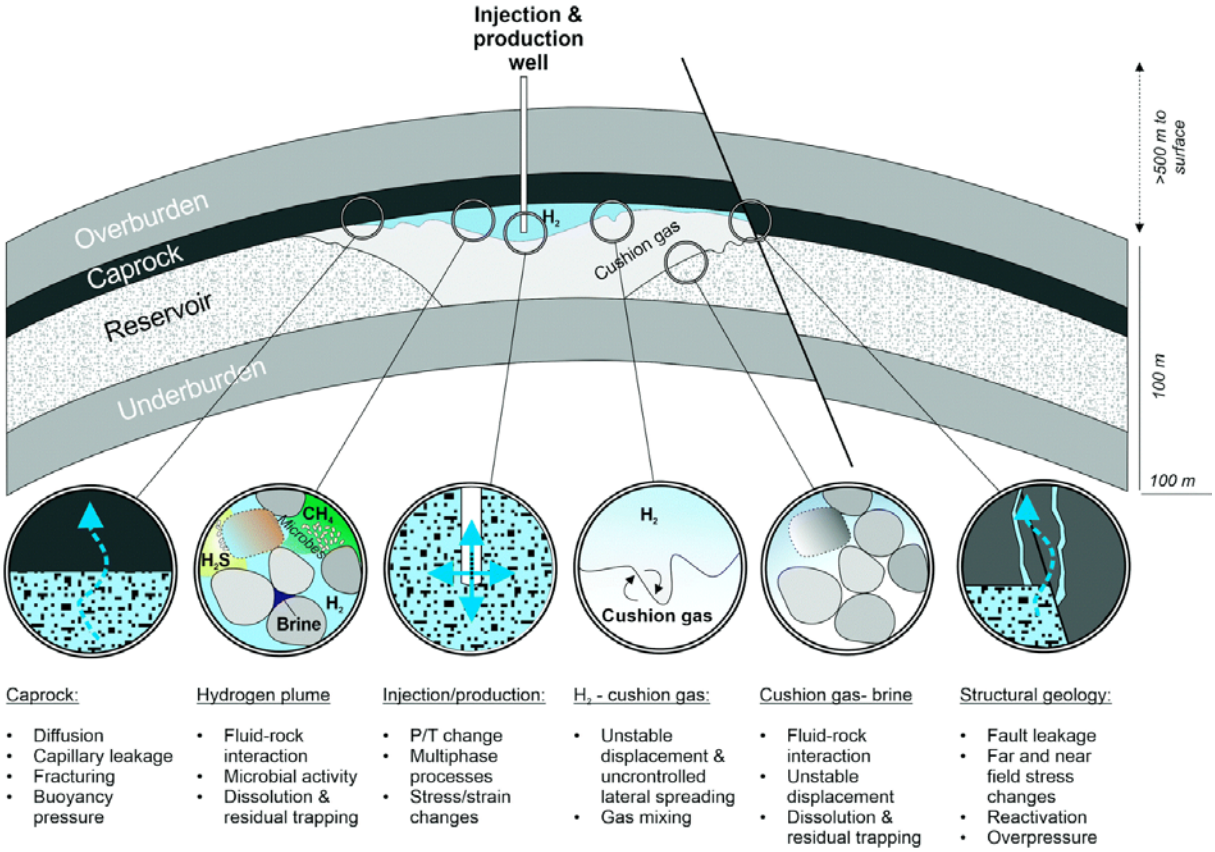

Figure 11: Diagrammatic representation of a depleted reservoir UHS facility with key aspects highlighted. Diagram from Heinemann et al. (2021).

Depending on the timeframe for project completion, it is often advantageous to select reservoirs that are at, or near, depletion. Occasionally reservoirs will have existing infrastructure that can be repurposed or upgraded, reducing the financial and time costs of becoming operational. Investigation of infrastructure should be undertaken to ascertain what infrastructure will be repurposed, upgraded or replaced on a site-by-site basis. Since H_2 is highly reactive, it may compromise the well casing – particularly steel wells due to hydrogen embrittlement (Dwivedi & Vishwakarma, 2018; Louthan et al., 1972).

Operational pressures are limited by geomechanical constraints including local and global stresses induced by pressure changes in the reservoir, in-situ stresses, and the mechanical properties of both the reservoir and overburden rocks (Bruno et al., 1998) (Figure 11). For a UHS reservoir to maintain operational pressures, cushion gas volumes between 15–75% of the total available pore volume are required (Namdar et al., 2020). Cushion gas could comprise cheaper inert gasses (e.g., nitrogen) or existing reservoir gasses to reduce cost. The required cushion to working gas ratio will vary between sites and is discussed further in Sections 5 & 6.

Hydrogen and natural gas have different density, viscosity, solubility and relative permeability characteristics and therefore their behaviour in the reservoir is different (Figure 11). However, their behaviour in relation to a water could be similar. Hydrogen is less dense than natural gas and requires larger storage volumes to achieve equivalent energy contents. Low viscosity and density of hydrogen should result in lower risk hydrogen loss and fluid mixing

caused by fluid coning during withdrawal, allowing higher extraction rates and longer withdrawal times (Thakur & Flores, 1974). Conversely, lower viscosity could cause unstable 'fingering' at the hydrogen-cushion gas interface during fluid displacement, and this could result in losses (Paterson, 1983). In practice, fingering effects may instead be dominated by heterogeneity. Hydrogen solubility is generally quite low in water, but could be appreciable in residual liquid hydrocarbons. Relative permeability of hydrogen will also depend on the nature of the wetting reservoir fluid and the tortuosity of the porous network. These issues should be considered on a site-by-site basis.

Saline aquifers

Saline aquifers are routinely used for UGS in the eastern USA, where well–established methods have been developed (Katz & Coats, 1968). They are a promising form of porous-media UHS and have been used to store gas mixtures up to 62% hydrogen (Table 1). There are two key differences between aquifers and depleted reservoirs. These are; (1) probable hydrostatic ambient fluid pressures which could lead to overpressures due to hydrogen injection and, (2) a relative lack of site-specific (including reservoir) knowledge and infrastructure. Suitable aquifers may be found at shallow depths (< 1 km), however, care may be required to ensure that UHS does not negatively impact potable water resources. In producing basins where reservoir-seal pairs have been well documented from petroleum exploration and saline aquifers may have similar structural or stratigraphic traps. Even in producing basins, there is more uncertainty about reservoir tightness for saline aquifers compared to depleted reservoirs, as the reservoir did not previously contained gas. Absence of pre-existing gas may also increase the cost of injecting cushion gas, however, hydrogen-hydrocarbon interaction modelling should not be required. Geomechanical, chemical and microbial interactions will require the same analysis on a site-by-site basis as depleted reservoirs. Geomechanical stability of the storage site would be promoted by first depleting the aquifer by pumping out water, although a treatment and disposal solution would need to be determined.

3.3. Comparisons of storage options

Each storage technology has different useable stock capacity and applications. Thus, technical considerations such as geological setting, pre-existing infrastructure and area footprint should be carefully examined to determine what solution best suits the proposed use. Technical readiness, storage volume (including operating pressure and cushion gas requirement), and site-specific requirements should also be considered.

It may be difficult to precisely estimate reservoir storage capacity due geological variations and uncertain in reservoir conditions including void space, pressure regime and cushion gas requirement, gas mixtures and wettability of the rock. Therefore, volume estimates in Table 2 and 3 are considered order of magnitude. Site-specific studies should be undertaken if more accurate estimates of storage volume are required. This report gives provisional volume estimates for four reservoirs in Section 6.

A brief summary of existing surface and underground options are presented in Tables 2 and 3. *Established* denotes that the hydrogen storage technology is currently operating at commercial capacity, *pilot* indicates the technology is operating in a trial mode, *conceptual*

refers to a likely feasible technology that has yet to move to pilot trials, and *analogues* refers to technologies that are established for gas storage (e.g., hydrogen blends, natural gas, CO_2), but have not been proven for storage of pure (>95%) hydrogen.

Table 2: Surface hydrogen storage technologies summary table. References in preceding text.

Surface storage technologies				
Type:	Storage (Nm^3)	Storage (TJ)	Technical readiness level	Comments
Cryogenic tank*	2.1 – 8.4 million	21 – 84	Established	Largest single tank surface storage option; **expensive to operate**; large area footprint, moderate scalability for large-scale storage.
High-pressure tanks	120	0.0012	Established	Small storage option; efficient for small scale producers and users; poor scalability for large scale-storage.
Linepack (NZ scenario)	1.4 – 8.1 million	14 – 81	Conceptual& Analogues	Required for domestic gas transmission network; unknown retrofit requirements; poor scalability.
* Liquified hydrogen				

Table 3: Underground hydrogen storage technologies summary table. Note that storage volumes are estimated from existing reservoirs storing hydrogen blends and is intended to give an order of magnitude. References within: [1] (Zivar et al., 2020); [2] (Tarkowski, 2019); [3] (Panfilov et al., 2006); [4] (Kruck et al., 2013); [5] (Amid et al., 2016); [6] (Kittinger et al., 2017).

Type	Storage (Nm^3)	Storage (TJ)	Technical readiness level	Comments
Salt Cavern	100,000 – 10 million [1-4]	1 – 100	Established [1]	**NZ geology not suitable.**
Depleted reservoirs	1 million - 1 billion [1,5]	10 – 10,000	Pilot [6] & Analogues	*Existing* site-specific knowledge and infrastructure; efficient hydrocarbon seal and trap; microbial and geochemical studies required.
Saline Aquifers	1 million – 1 billion [1,3]	10 – 10,000	Conceptual & Analogues	*Poor* site-specific knowledge and infrastructure; microbial, geomechanical and geochemical studies required.
Disused mines	150,000 – 7 million*	1.5 – 70	Conceptual	Efficient lining to prevent gas leakage is not commercially available yet; existing excavations likely reduce implementation time and costs.

Vertical shafts	1.8 – 3.2 million	18 – 32	Conceptual	Higher geographic availability; scalability to storage requirement.
* Void space based upon the Huntly coalfields using production data (Sherwood et al., 2019) and NZ coal densities (Gray & Macknight, 1986).				

4. Geological conditions

Safe and economic UHS in porous media requires that the geological conditions include a containing structure (i.e., trap), together with an effective reservoir and cap rock. Assessment of reservoir pore volume and connectivity is essential to evaluate potential hydrogen storage volume, and injection and recovery rates, while an assessment of the integrity of the cap rock is vital to ensure that hydrogen migration from the container is at acceptable levels.

New Zealand and its offshore exclusive economic zone are underlain by a number of sedimentary basins which contain sedimentary strata up to ~10 km thick and ~100 million years in age (King & Thrasher, 1996). The Taranaki Basin is the only sedimentary basin in New Zealand that is a commercial petroleum province. As a consequence, a wealth of subsurface geological information (e.g., wells and seismic reflection data) is available which can be used to constrain the properties and structure of reservoir-cap rock pairs. These subsurface datasets demonstrate the occurrence and broad distribution of sandstone formations which might be utilised for UHS, where effective containment (top seal, and lateral structural and/or stratigraphic confinement) can be demonstrated. Geological information supports the possibility of UHS outside of Taranaki (e.g., Arcadia, Kate anticlines in North Canterbury – see Beggs & Nicol, 2020), however, significant work is required at most of these sites to test their suitability, with lower data availability than in Taranaki gas and oil fields.

Reservoir and cap rocks can be evaluated using conventional techniques, although may require modification to account for injection of hydrogen. For example, geochemical reactions may occur between injected hydrogen, original pore fluid, and the reservoir and/or cap rocks, potentially impacting reservoir quality, cap rock integrity, and/or in some circumstances resulting in hydrogen loss (cf. Carden & Paterson, 1979). Although studies on hydrogen-rock reactivity are sparse, several have been undertaken in recent years to evaluate the significance of these issues, and a brief summary of current understanding is presented in the next section. This summary is followed by an overview of the mineralogy and rock properties for reservoir and cap rock intervals across the area of interest, and of the potential for chemical interactions that result from hydrogen storage to increase or decrease reservoir/cap rock performance. We also consider the geological structures that may promote or reduce the prospects for safe hydrogen storage.

4.1. Trap structure

The majority of potential UHS sites in the Taranaki region can be classified in geological terms as stratigraphic or structural traps. Anticlinal folds forming dome-shaped closures or structural culminations are a common type of structural trap for oil and gas fields (both depleted and operating) in the Taranaki Basin (e.g., Kapuni, Waihapa, McKee, Kupe fields; see

Figure 2) (e.g., see also Figure 17). Hydrocarbons generally accumulate in the top of these anticlinal culminations, where they are typically accessed via crestal drillholes.

The Ahuroa gas storage facility is located in the crest of an anticline immediately adjacent to the Tarata Thrust Fault (GSNZ SPV1, 2020)(Figure 2). This reservoir is one example of anticlines that occur throughout the onshore Taranaki Basin, mainly formed in response to reverse faulting and tectonic shortening of sedimentary strata during the Early to Middle Miocene time interval (e.g., 11–24 million years ago) (King & Thrasher, 1996; Reilly et al., 2015; Stagpoole & Nicol, 2008).

Fault-seal traps have also been documented or postulated for some oil and gas fields in Taranaki (e.g., McKee, Maui, Rimu, Kaimiro fields; Reilly et al., 2016; Figure 2). In these fields, hydrocarbons are trapped against low permeability fault rock. The precise role of fault rock in the formation of hydrocarbon accumulations is often poorly resolved and may be geologically complicated, adding a degree of uncertainty beyond what is usually encountered for anticlinal culminations.

4.1.1. Containment

Storing hydrogen in existing or depleted oil and gas reservoirs using anticline structures or fault-seal traps has a number of advantages over green-fields sites. These advantages include; i) the availability of existing subsurface data for geological evaluation and capacity estimates, ii) proximity of the storage site to existing infrastructure (e.g., wells and pipelines) and, iii) demonstrated containment of gas on geological timescales (e.g., millions of years) (Ennis-King et al., 2021). Despite the advantages of utilising depleted reservoirs, additional investigations will be required at these sites to characterise the response of the reservoir and cap rock to repeated injection and withdrawal of hydrogen (Sections 4.4, 4.5, & 6). In particular, subsurface storage of hydrogen requires testing to ensure that the storage reservoir can accommodate economically viable gas volumes, the reservoir has adequate deliverability (so that hydrogen can be injected and extracted at the desired rates from the available wells), and the geological reservoir is capable of safe containment with acceptably low losses.

The containment of potential cap rocks may be aided by the short life expectancy of hydrogen storage facilities compared to geological timescales (e.g., tens of years vs millions of years). However, further work may be required to demonstrate adequate gas containment by these structures. Global investigations suggest that losses due to imperfect sealing of cap rocks may be in the range of 0.1–2% (Amid et al., 2016; Carden & Paterson, 1979; Ennis-King et al., 2021). These estimates vary between sites and do not specifically address UHS with fractured or faulted cap rock, as is often the case in the hinges of anticline structures (Watkins et al., 2015).

In onshore Taranaki and offshore in the southern Taranaki Basin normal faults that formed in the last five million years and cut through cap rocks can locally promote the migration of gas to the surface (Ilg et al., 2012; Massiot et al., 2019). Migration of hydrogen along faults and formation of new fractures in the cap rock could be promoted by overpressures in the reservoir due to hydrogen injection. (Darby, 2002) have shown that levels of fluid overpressure in the onshore Taranaki Basin are significantly lower than the measured minimum stress in the region, and so overpressure-driven cap rock failure is unlikely.

Overpressures have been effectively managed at many water, CO_2 and gas injection sites, and will be a key element of monitoring hydrogen-storage sites (see Section 7).

4.2. Reservoir rocks

Reservoir rocks form the 'container' into which hydrogen is injected and from which it is later withdrawn. These rocks are typically sandstones comprising interconnected pores that allow fluids to pass through the rock formation. Reservoir sandstones are generally characterised by porosities of at least 10% and permeabilities of 10s to 100s of mD. Here we provide brief descriptions of some of the main reservoir rocks in the Taranaki region. These include the Tariki Sandstone Member, McKee Formation, Moki Formation and the Mt Messenger/Urenui formations. These summaries are based on a large number of petrographic and core analysis data, with details on the mineralogical and petrophysical variability provided in Appendix A2.1.

4.2.1. Tariki Sandstone Member

The Tariki Sandstone Member occurs in the lower part of the Oligocene Otaraoa Formation along the eastern side of the Taranaki peninsula, where it reaches thicknesses of 250–320 m. The reservoir is best developed in the Ahuroa and Tariki fields, where it has a gross thickness of about 200 m and high net:gross (~70% sandstone). Sand content and thickness diminish north of Tariki/Ahuroa and the member is represented by a few thin pebble and calcareous sandstone bands north of Toetoe (De Bock et al., 1990). The Rimu/Kauri wells in the south peninsula region penetrated the Tariki Member of <50 m to ~100 m in thickness, which produced hydrocarbons from different fault-bound blocks. The Tariki is deepest at Waihapa-1 (>3600 m) and shallowest in the Tariki Field (>2400 m). The Tariki Member is divided into three groups, which are described in Appendix A2.1.1

Our review of the Tariki Member in Appendix A2.1.1 shows that the best reservoir quality sands for hydrogen storage and recovery occur in the main Tariki-Ahuroa producing field area (Figure 2). These sands at Tariki-Ahuroa are coarser grained and have much lower labile and clay composition than in the southern Rimu-Kauri fields. Although all silicates are expected to be relatively inert in the presence of hydrogen over the timeframe for underground storage (see Section 4.4), the high clay and labile content of sands in the Rimu-Kauri field has a higher risk of fines mobilisation. Together with the finer grain size at Rimu/Kauri, any fines mobilisation could result in a significant reduction in permeability and hence affect hydrogen injection/recovery rates. It is also notable that the Tariki Member in the main Tariki-Ahuroa fields is at a shallower depth compared to the southern Rimu-Kauri fields, which would be favourable for UHS.

The available data indicate that the overthrust McKee Formation might be a better option for hydrogen storage than the in-situ McKee (i.e., below the thrust fault; see Figure 17 and Appendix A.2.1.2). The significantly shallower depth of the reservoir in the overthrust favours UHS, while the better reservoir properties in the overthrust (compared to the McKee beneath the fault) will result in higher total pore volume The available mineralogical data show that carbonate, and in particular calcite, is locally a significant component of the Tariki Member. Skeletal carbonate has been identified in most petrographic samples, and it is possible that this forms the main source of calcite cements. Overall, calcite is least abundant in the main

Tariki-Ahuroa field area (Appendix Table A2.1-3), however, in all cases it is recommended that the potential impact of hydrogen-rock reactions on calcite-rich beds is assessed during site evaluation for hydrogen storage. The presence of locally significant pyrite in the Tariki reservoir interval at Rimu-Kauri (Appendix Tables A2.1-3) should also be considered in any site investigation.

4.2.2. McKee Formation

The Late Eocene McKee Formation has been penetrated in many onshore wells (e.g., McKee, Tuhua, Toetoe, Stratford-1) and forms a significant hydrocarbon producing reservoir from the overthrust blocks adjacent to the Taranaki Fault. The McKee Formation ranges in thickness between ~60–170 m, and typically occurs at depths >2100 m. The formation is locally characterised by high net:gross (e.g., Toetoe wells; see Figure 17), and is commonly heterogeneous due to the presence of interbedded sandstone, mudstone and better deliverability and recovery rates. The quartz-feldspathic mineralogy of all McKee sands is likely to be relatively inert to hydrogen-water-rock reactions and it is thought that the typically fine- to medium grain-size and high rigid: labile composition will help prevent significant petrophysical changes resulting from repeated hydrogen storage cycles. However, there is a risk of clay migration and of dislodgement of fractured grain particles in the overthrust reservoir, both of which pose a risk of permeability reduction with time.

Based on available mineralogical data the McKee reservoir sands contain only very minor carbonate (Appendix Table A2.1), mostly dolomite and siderite. However, cuttings record locally abundant calcite (Appendix Table A2.2), suggesting that calcite-rich bands occur within the reservoir interval. These carbonate-rich horizons have the potential to react over a hydrogen storage timeframe and it is recommended that site-specific assessments are undertaken during site evaluation (e.g., abundance and stratigraphic position, and geochemical modelling to investigate impact).

Pyrite has been recorded in only minor amounts of most McKee samples, with locally higher contents in samples from below the fault, potentially favouring the overthrust for hydrogen storage (Appendix Table A2.1 & A2.2). However, studies on hydrogen-rock reactivity suggest that even small amounts of pyrite can react to form H_2S gas (see Section 4.4) and the impact of this on hydrogen purity and operational health and safety requires further experimental and modelling studies. The greatest potential for reactivity may be at the contact with cap rocks and baffles, and it is recommended that these areas are targeted for mineralogical evaluation.

4.2.3. Moki Formation

The southern and central offshore Taranaki Basin is the type area for the Moki Formation, where the sand-dominated sequence is ~250–350 m thick and comprises massive, thick-bedded or amalgamated channel and sheet sands. A generally lower net: gross correlative of the mid-Miocene Moki Formation occurs across the Taranaki peninsula, with some blocky sands interbedded with overall more thickly developed interbedded argillaceous siltstone and mudstone.

The presence of Moki reservoir in the onshore Taranaki region, while less well developed than the offshore, may still provide an option for hydrogen storage. The shallow burial depth (<2 km) is favourable, and the thick intervals of interbedded mudstone potentially would provide good cap rock (see Section 4.3). Although the sands are mineralogically complex (see Appendix A2.1.3), the main rock forming minerals (quartz-feldspar-clays) are expected to be relatively inert in the presence of hydrogen over the timeframe for underground storage (see Section 4.4). However, a high clay and other labile content together with the fine grain size of these sands creates a risk of fines migration, which may impact both injection and recovery rates. Presence of smectite in the formation may also cause formation damage and drilling difficulties if water-based drilling fluids are used (cf. Palmer, 2021). Additionally, common calcite rich beds may undergo reaction and result in dissolution and reprecipitation that could alter the heterogeneity and flow of the reservoir. Small volumes of pyrite may react to form pyrrhotite and H_2S (see Section 4.4).

4.2.4. Mt Messenger/ Urenui formations

Mount Messenger reservoir sandstones have been intersected in numerous onshore and offshore Taranaki wells. Net: gross is generally high within the formation as a whole, with sands commonly occurring within fining- and thinning-upward cyclic packages (King & Thrasher, 1996). Potential Mount Messenger reservoir strata comprise major channel systems that are typically between 30 and 60 m thick. Much of the overlying Urenui Formation is non-reservoir, composed of heavily bioturbated siltstones and mudstones.

The shallow (<2 km) Late Miocene sands provide some potential for hydrogen storage, with the presence of several small onshore fields demonstrating evidence of hydrocarbon containment (e.g., Ngatoro and Kaimiro, Figure 2)). These Late Miocene sands are compositionally similar to the Mid-Miocene sands (see Appendix A.2.1.4) and hydrogen-rock reactivity will mostly be limited to local reaction of carbonate horizons and pyrite zones. However, the very fine grain size of these sands, together with the high labile and clay content and the presence of smectite, increases risk of fines migration/formation damage, along with capped injection and withdrawal rates.

4.2.5. Matemateaonga Formation; Manutahi Sands

The Manutahi Sands are a Late Miocene to Pliocene-aged reservoir that may provide a shallow (<1.5 km) option for H_2 storage. In the Kauri PMP, on the southeastern side of Taranaki peninsula, this reservoir comprises ~140 m thick interbedded sandstone and shale with minor conglomerate and coal. This formation in the Kauri PMP has a net sand of ~60 m (Core Lab, 2003) and a gross oil column height of 40 m.

The shallow burial and high pore volumes of this reservoir are favourable for hydrogen storage (see Appendix Table A2.4). Containment is only locally recorded (i.e., the Manutahi oil field within the Kauri PMP), however, there may be options for storage in possible fault block traps (see Section 4.1). Based on available data the composition of the Manutahi Sands is similar to other Miocene sands (see Appendix A.2.1.5), and they may therefore behave in a similar manner during storage. There is very little quantitative data for the Manutahi Sands and more work is required for reservoir characterisation.

4.3. Cap rocks

Hydrogen is the smallest and lightest of all the elements, and it diffuses rapidly in air and other materials. It can be reactive in rocks and when it combines with oxygen, either in the air or bonded to minerals, forms water (Zgonnik, 2020). Based on these attributes, it is anticipated that hydrogen may not be retained in geological traps for long periods of time (e.g., thousands of years or more). However, hydrogen has a very low solubility (cf. Ennis-King et al., 2021) and given that the cap rock (top seal) in UHS will be water saturated, the potential loss of hydrogen via solution or diffusion into the cap rock at typical reservoir temperature and pressure is likely to be low (cf. Ennis-King et al., 2021). Notably, Paterson (1983) and Ennis-King (2021) both suggested that existing data indicates that the diffusion process may only lead to 1–2% of hydrogen loss over typical project lifetimes. This preliminary evaluation therefore assumes that the cap rock will be effective in containing hydrogen if it has been proven to contain hydrocarbon gases.

Studies suggest that the main lithological factors producing good quality cap rocks include fine grain size, fabric (e.g., lamination, aligned carbonaceous material and mica), and presence of carbonate or other cement. Additionally, depositional variation is considered a more important risk to cap rock effectiveness than depth of burial. Proven cap rocks in the Taranaki Basin include the Eocene Turi Formation (including the Omata Member or D shale), the Oligocene Otaraoa and Tikorangi formations where unfractured, and Miocene-Pliocene mudstones in the Manganui, Urenui and Tangahoe formations (King & Thrasher, 1996). In addition, inter-bedded mudstones within reservoir intervals can act as intra-formational baffles and barriers. Across the Taranaki peninsula these sealing rocks are widespread and there are no areas where absence of cap rock is identified within Eocene or Early-Late Miocene intervals.

There is relatively limited petrographic and capillary seal capacity data for Taranaki cap rocks, partly due to a paucity of mudstone samples except as cuttings, which are not generally suitable for relevant analyses such as MICP. Results for onshore Taranaki are available in previous compilation studies (Field et al., 2011; Higgs et al., 2005); these data illustrate the range of sealing capacities and local occurrence of carbonate and pyrite, which potentially could react with injected hydrogen (see section 4.4). However, more data is required for a detailed understanding of cap rock capacity, variability and for prediction of maximum hydrogen column heights. Seal capacity of cap rocks and/or failure needs to be evaluated on individual prospect basis for UHS and should include an assessment of the lateral and vertical variability in mineralogy and rock properties. Below three potential cap rocks in onshore Taranaki are summarised, with more detailed information on the provided in Appendix 2.2.

Turi Formation: the Eocene Turi Formation, together with the Oligocene Otaraoa Formation, specifically its basal Matapo member, forms the cap rock for the McKee Formation reservoir. The uppermost Late Eocene Turi Formation is thickest on the western side of the peninsula (>50 m thick), but thins to <25 m along the eastern basin margin. The quality of the cap rock is good offshore, but it is expected that overall quality may be poorer onshore due to a more proximal palaeoenvironment. However, very good seal quality does locally occur onshore, in places associated with a high carbonate content.

Otaraoa Formation: the Oligocene Otaraoa Formation forms the cap rock for the Tariki Member and is part of the seal interval for the late Eocene McKee Formation. It is more than 100 m thick along the eastern regions of the Taranaki Basin, reaching a maximum thickness of 1000–1200 m in the Waihapa Field, thinning in the western Taranaki Basin to less than 100 m thickness where it becomes more calcareous. Quality of the cap rock will be variable and dependent upon the proportion of sand/silty grains, clay and carbonate minerals; very good sealing potential has locally been demonstrated onshore (Appendix 2.2.2).

Manganui Formation: the Miocene Manganui Formation is widespread and thick across the Taranaki peninsula, providing effective top and lateral seals for the Moki, Mount Messenger, and Urenui reservoirs. Manganui mudstones are generally characterised by good sealing quality, which reflects the basin-floor fan depositional setting with mudstones likely to have relatively high clay percentages compared to more proximal basin-floor fan, slope and shelfal settings. However, slope mudstones (Urenui equivalent) may form the cap rock to the Mount Messenger reservoir, with more variable sealing quality, and lithofacies ranging from mudstone, interbedded siltstone and sandstone, through to localised sandstone-filled slope channels (Urenui Formation). Petrographic and capillary seal capacity data demonstrate the mineralogical variation and range of properties associated with these Late Miocene lithologies (Appendix A.2.2.3).

4.4. Geochemistry

In the absence of experience with hydrogen storage in porous formations of New Zealand, uncertainties regarding containment and purity must be addressed in the first instance by theoretical and experimental approaches.

4.4.1. Geochemical models

There is little published work on geochemical modelling of hydrogen-brine-rock systems, and the kinetics of hydrogen gas dissolution remain poorly understood. Models for quartz-rich sandstones suggest that minor quartz and K-feldspar may dissolve in hydrogen solution over long time periods (>10 years) (Bo et al., 2021; Yekta et al., 2018), although (Yekta et al., 2018) suggest that the reactions might need the presence of iron in the aqueous phase. Other minerals, in particular carbonates, sulphates and pyrite, are predicted to react more quickly with hydrogen in aqueous solution, potentially resulting in significant mineral dissolution, which may locally enhance porosity and permeability (Amid et al., 2016; Bo et al., 2021; Hassannayebi et al., 2019; Henkel et al., 2014; Shi et al., 2020). Pyrrhotite precipitation and redistribution of carbonate cement would also be a consequence of these reactions with resulting local changes in porosity. Notably, modelling results from (Hemme & Van Berk, 2018) also predict complete reaction of sulphates (barite and anhydrite) and goethite over a 30 year storage time, some dissolution of quartz, calcite and illite, and precipitation of feldspar, kaolinite and dolomite in the reservoir rock; this precipitation led to a small decrease in pore volume. The modelled porosity loss was greater at higher temperature and pressure (161 atm and 80 °C compared to 40 atm and 40 °C) associated with greater dissolution and precipitation (Hemme & Van Berk, 2018).

A major uncertainty with chemical modelling studies is the timeframe for reactions. Hassannayebi et al. (2019) modelled clay and carbonate-rich sandstones that contain

significant carbonate (calcite, dolomite, siderite) and minor pyrite (35% and 1%, respectively). Equilibrium batch models (where the equilibrium of the aqueous phase is maintained with the injected H_2) predict the potential for redox reactions resulting in dissolution of carbonate, sulphate, sulphide, and clay minerals associated with an increase in pH and ion concentration of the brine. This predicts the expected results over a long time period. Kinetic models from (Hassannayebi et al., 2019) also show a minor early increase in pH, with slow dissolution of primary minerals (dolomite, ankerite, muscovite, pyrite) over a shorter, 12-month period, but without the formation of secondary minerals. Notably, different kinetic conditions (where reactions of pyrite and pyrrhotite are at equilibrium) result in much faster reaction rates and a higher increase in pH (Figure 12).

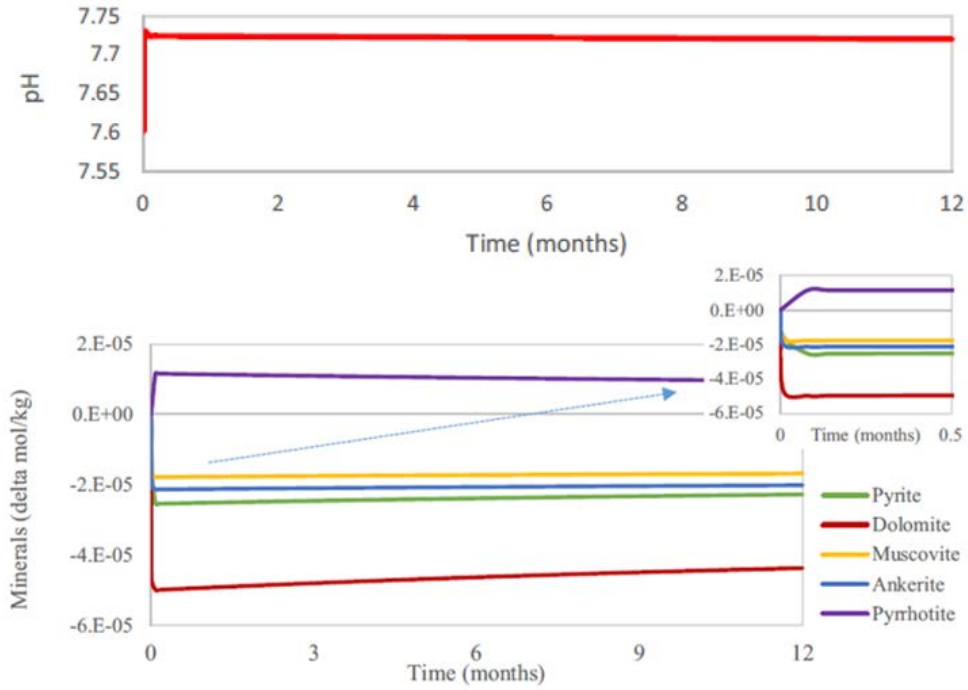

Figure 2: Evolution of pH and mineral abundance changes obtained from the final kinetic model of Hassannayebi et al. (2019). Hydrogen injection over a period of 12 months showing fast reaction resulting in an increase in pH associated with dolomite dissolution and pyrite reaction to form pyrrhotite.

In a recent study by Bo et al. (2021) the degree of hydrogen loss associated with dissolution and fluid-rock interactions was modelled for quartzose sandstones from two commercial gas storage reservoirs at different temperatures and pressures. It was shown that an increase in temperature and pressure will only slightly increase hydrogen solubility in brines (in the absence of mineral phases), while increasing the salinity slightly decreases the solubility (Bo et al., 2021).These results suggest that the risk of loss of free hydrogen gas due to solution into formation brine during UHS would be very low. However, preliminary results from an experimental study by De Lucia et al. (2015) show greater hydrogen solubility than the values predicted by theoretical models (see Figure 15a), demonstrating the need for further work.

The geochemical models by Bo et al. (2021) show very little reaction between the hydrogen-saturated aqueous solution and silicate and clay minerals. However, the presence of

carbonate minerals (av. 3% in the models) triggers up to 9.5% hydrogen loss due to mineral dissolution-induced hydrogen dissociation processes (Bo et al., 2021). Bo et al. (2021) conclude that deep carbonate-free reservoir with carbonate-free cap rock is optimal for hydrogen underground storage.

It is clear from these studies that rock reactivity will be heavily dependent upon reservoir and cap rock mineralogy as well as reservoir conditions (e.g., temperature, pH, pressure, fluid chemistry). Much of the modelling work to date suggests that silicates (quartz, feldspars, clay minerals) are not likely to undergo significant alteration over a typical hydrogen storage cycle (say, several months). However, small amounts of sulphate, carbonate and pyrite in either the reservoir or cap rock may be reactive over that timeframe. Significant differences were observed in geochemical results depending on input data, highlighting the need for better kinetic data, constrained by experiments, to reduce uncertainties (see further work section 8.2.2).

4.4.2. Experimental studies

A number of experimental studies have been undertaken over recent years investigating the effect of hydrogen injection into reservoir sandstones (De Lucia et al., 2015; Flesch et al., 2018; Henkel et al., 2014; Shi et al., 2020; Yekta, Manceau, et al., 2018; Yekta, Pichavant, et al., 2018) and claystones (Truche et al., 2013). Most of these are batch experiments run over short time frames (weeks to few months), under reservoir-specific pressure, temperature and salinity conditions (Appendix Table A2.7).

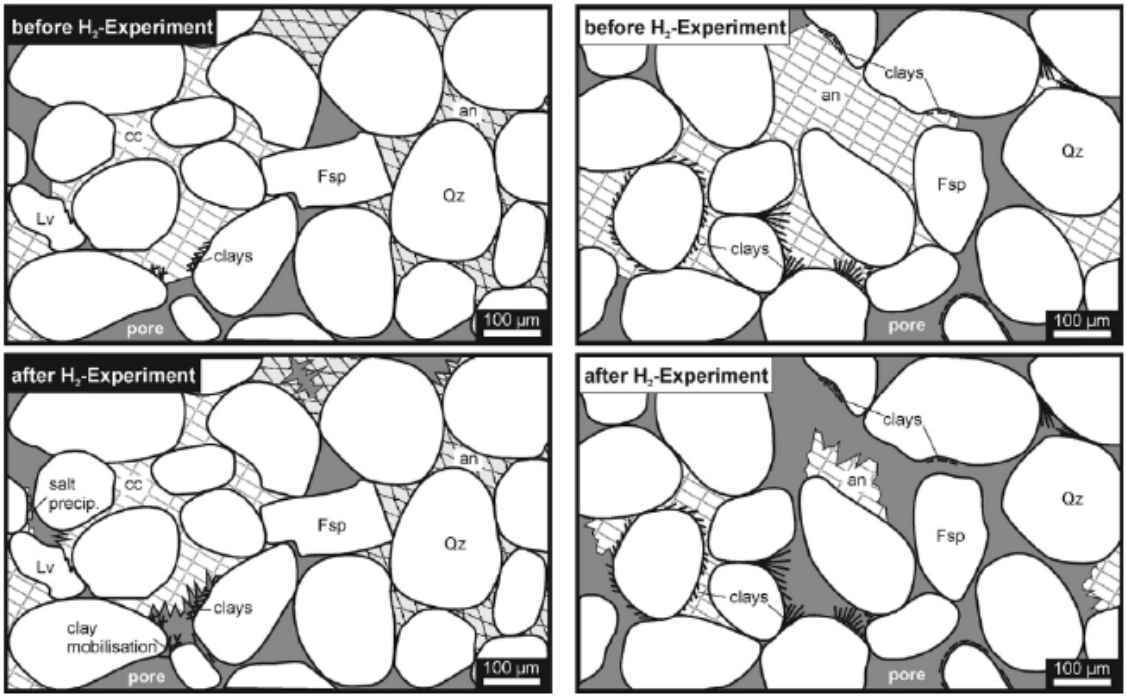

Figure 13: Schematic illustration showing the before-after experiment comparison of cement reaction with hydrogen, from Flesch et al. (2018). Note the increase in porosity and pore connectivity (permeability) associated with anhydrite (salt) dissolution (RHS).

Experimental results are consistent with the geochemical models that predict both carbonate and sulphate reaction with hydrogen-saturated aqueous pore fluid (e.g., Figure 13). However, Flesch et al. (2018) show that the partial and total dissolution of pore-filling anhydrite and carbonate cements (detected by thin section and u-CT) only occurs where those minerals are directly exposed to open, connected pores. These authors suggested that the reactions occur in a zone where highly saline formation fluid, reactive minerals, and injected hydrogen can interact and that this zone will change during the course of a storage project as H_2 is injected and removed (Figure 14).

The initial water saturation of the reservoir will be variable depending on the type of storage system (e.g., aquifer or depleted reservoir) and during the first injection cycle it might be expected that residual formation fluid in contact with hydrogen will become saturated, and geochemical reactions may occur. However, during subsequent cycles, and depending upon site-specific conditions (e.g., intraformational baffles and barriers), there may be little remaining residual water; pores will be filled with H_2, underlain by cushion gas and the main zone of hydrogen reaction may therefore be at the reservoir-cap rock boundary.

In general, the experimental work shows very little reaction of the main clastic sedimentary rock forming minerals (quartz, feldspar, clays) with hydrogen. However, results suggest that where carbonates and sulphates (anhydrite) are present in the rock there can be locally significant dissolution (e.g., Henkel et al., 2014; Shi et al., 2020). Anhydrite is more reactive than carbonate, and Flesch et al. (2018) suggest that anhydrite dissolution could result in a significant permeability enhancement compared to the relatively minimal dissolution of carbonate, which may result in an increase in porosity but not a corresponding large increase in permeability (Figure 13). It should be noted that carbonates, in particular calcite, are locally significant in both reservoir and cap rock units in Taranaki. However, sulphate minerals are generally absent.

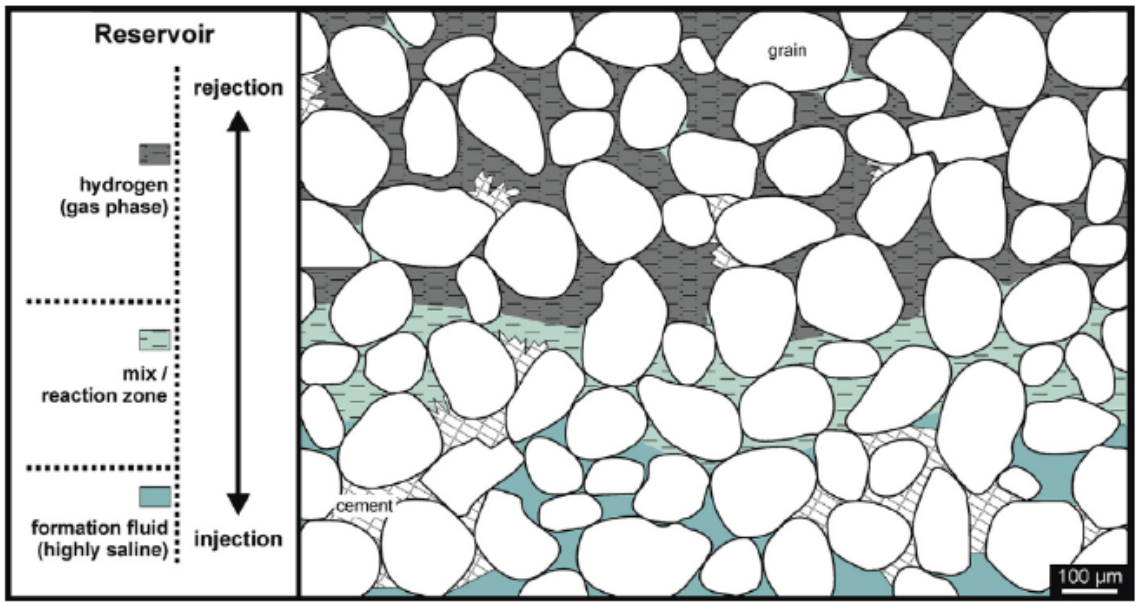

Figure 3: Schematic illustration showing a mix zone between pores filled with formation fluid (below) and hydrogen (above), from Flesch et al. (2018).

Experimental results from Truche et al. (2010) indicate that most possible redox reactions induced by hydrogen, even carbonate and sulphate reduction, remain insignificant at low temperatures (<100°C), provided no catalyst (bacteria, mineral surfaces or engineered material) is present. A later study looking at the geochemical impact of hydrogen in a clay-rich rock (i.e., minerals present) shows that silicate and carbonate minerals have not reacted over a five-month experiment period (Truche et al., 2013). However, those authors also demonstrate that pyrite reduction could be significant, with pyrite solubility controlling the sulphide concentration at reservoir conditions (T<150 °C, pressure <6 bar), and with alkaline conditions promoting pyrrhotite precipitation. This reaction involves H_2S production that can modify the redox potential and pH of the porewaters (Truche et al., 2013), and thus may drive other reactions. Given that reaction can occur with very small concentrations of pyrite, Truche et al. (2013) suggest that reservoirs with acidic pore fluid may be most suitable for hydrogen storage to prevent pyrite reduction. Pyrite is relatively widespread in New Zealand reservoir and cap rock formations.

4.4.3. Implications of geochemical reactions

Geochemical and experimental work to date predicts there to be some geochemical reactions within the hydrogen-brine-rock system. Uptake of hydrogen into aqueous solution may trigger these reactions (Berta et al., 2018; De Lucia et al., 2015), with implications for UHS operations.

Dissolution of carbonates and sulphates has been modelled and observed in experiments, and this could result in local increases in porosity and/or permeability. Precipitation of other mineral phases may also occur and could result in porosity losses (e.g., Hemme and van Berk, 2018). These changes in petrophysical properties need to be investigated for site-specific reservoir and cap rocks in order to determine possible changes in pore volume and reservoir heterogeneity that could affect hydrogen injection and recovery. Hydrogen reactions within carbonate and/or sulphate rich cap rocks may locally result in a reduction of seal capacity, and this needs to be evaluated on a case-by-case basis. Additionally, Bo et al. (2021) suggest that the modelled calcite dissolution associated with hydrogen storage in calcite-rich rocks may trigger wellbore integrity issues in the long term (Boersheim et al., 2019).

Another consideration is the potential reduction of pyrite to pyrrhotite, which has been shown to be significant at low temperature conditions in the presence of hydrogen (Hassannayebi et al., 2019; Truche et al., 2013). This reaction would lead to reservoir souring, where the reservoir starts to produce sour fluids (with H_2S) – a toxic and corrosive species that could affect hydrogen purity and present risks to health and the environment. However, geochemical models of brine-rock interactions by Li et al. (2020) suggest that rock composition is an important constraint on the degree of mineral souring, with sour gas being a problem in rocks containing carbonates and sulphates (calcite/dolomite/anhydrite); conversely, sour gas may not be a problem in rocks containing pyrite and goethite where Fe can absorb the sulphide through precipitation of iron sulphide minerals (pyrite and pyrrhotite; Hemme and van Berk, 2018). Further studies are recommended to better quantify the likelihood for H_2S production from minor pyrite within hydrogen storage time cycles.

The type and severity of geochemical reactions will be dependent on a number of factors including reservoir / cap rock mineralogy, formation fluid composition, temperature and pressure. In particular:

- Presence of carbonates and sulphates in the reservoir interval may lead to change in porosity/permeability: assumed minor effect in UHS due to low residual formation fluid (partly dependent on reservoir heterogeneity).
- Presence of carbonates and sulphates in cap rocks may lead to reduction in seal capacity: assumed to be a local effect at the reservoir-cap rock boundary where cap rock minerals would be in contact with H_2-saturated pore fluid.
- Presence of pyrite in reservoir or cap rock may lead to H_2S synthesis and an undesirable contamination of subsequently produced gas.
- More mineral reactions are expected at higher hydrogen solubilities;
    - The experimental work by De Lucia et al. (2015) suggests that hydrogen solubility increases in very saline fluids (Figure 15a); however, these salinities (up to halite concentration) have not been reported in Taranaki or other New Zealand basins. Additionally, the experimental results are inconsistent with geochemical models, which leads to uncertainties with respect to the effect of salinity on hydrogen solubility.
    - Geochemical modelling results indicate that hydrogen loss will increase with lowering of the temperature in a hydrogen-brine-calcite system due to calcite dissolution (Bo et al., 2021, Figure 15b); this needs to be considered for the calcite-bearing Taranaki formations.

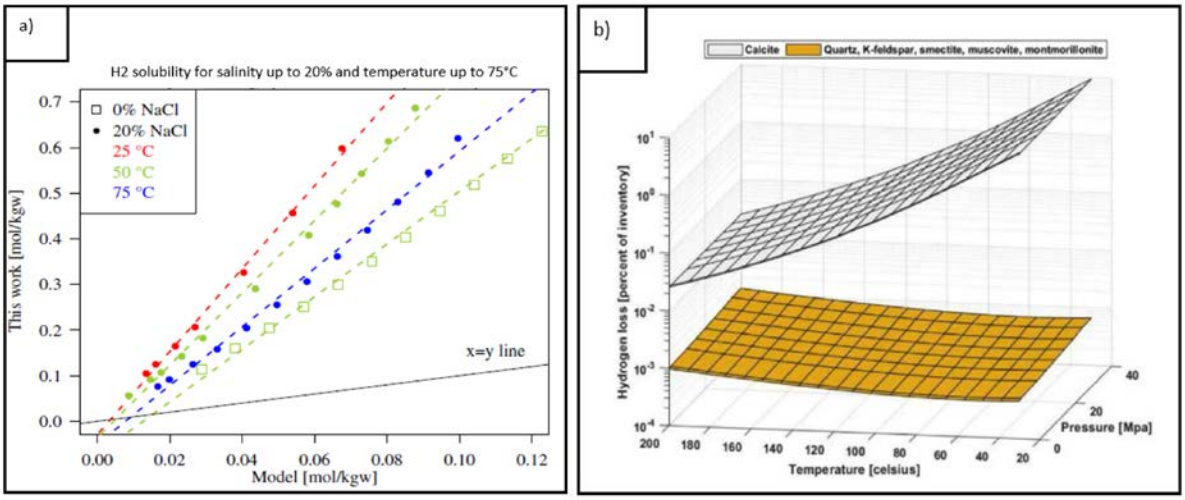

Figure 15: a) Experimental results showing hydrogen solubility at different salinities (0 and 20% NaCl) and temperatures (25, 50, 75 degree C), and highlighting the discrepancy with geochemical models. From (De Lucia et al., 2015). B) Geochemical modelling results showing the difference in hydrogen loss at different temperatures for a calcite-brine-hydrogen system and siliciclastic-brine-hydrogen system. From Bo et al., 2021.

4.5. Microbiology

Hydrogen is known to have microbial interactions when emplaced in rock reservoirs. These interactions are a potential concern because: (i) a significant proportion (>10%) of the emplaced gas could be consumed by microbes and/or converted to methane; (ii) sour gases,

such as H_2S, may be produced as a by-product of microbial activity; and (iii) large accumulations of microbes can create biofilms that negatively impact porosity or permeability, inhibiting gas flow and reduce reservoir performance

Microbial communities can convert hydrogen to methane where there is an available source of carbon (e.g., CO_2). For example, methanogenesis has been observed in the field associated with the storage of town gas (a H_2-CH_4-CO mixture), presumably due to abundant carbon (Buzek et al., 1994). Methane production could impact gas purity and necessitate hydrogen 'cleaning' on extraction. H_2S gas produced by microbes that reduce sulphate ions (using hydrogen as an electron donor) can be toxic to humans and corrosive to steel infrastructure. However, the presence of available sulphate, for example in formation water, appears to be necessary for gas production (Ivanova et al., 2007; Tarasov et al., 2011). Microbial production of H_2S and methane are enhanced at low temperatures (~40° C) and may be of reduced significance for deeper, hotter and more saline reservoirs (Groenenberg et al., 2020).

Microbial interactions should be factored into assessment of reservoir dynamics on a site-by-site basis. Recent studies have shown how their impacts can be incorporated into dynamic reservoir simulations (Heinemann et al., 2021). A list of potential microbial reactions is summarised in Table 4. Little is known about the significance of in-situ microbial interactions in New Zealand and further research on this topic may be required (see Hemme and van Berk, 2018 and Section 8.2.3).

Table 4: Microbial reactions that consume hydrogen and the conditions in which the reactions may take place in porous reservoirs. Table from *Heinemann et al. (2021)* and compiled from *Thaysen et al. (2020)*.

Class of microorganism	Main storage impact	Hydrogen consumption (nM hour^{-1})	Temperature (°C)	Salinity (g L^{-1})	pH
Methanogens	H_2 loss by CH_4 production, clogging	Laboratorial[a]:[92–95] 0.008–5.8 × 10^5	Optimum[b]: 30–40	Optimum[b]: <60	Optimum[b]: 6.0–7.5
		Oil and gas fields:[96,97] 0–1185 Wells:[97] up to 4533	Critical[b]: 122	Critical[b]: 200	Critical[b]: 4.5–9
Sulfate reducers	H_2 loss by H_2S production, corrosion, clogging	Laboratorial[a]:[68,92,98,99] 0.005–130 × 10^5	Optimum[b]: 20–30	Optimum[b]: <100	Optimum[b]: 6.0–7.5
		Oil and gas fields:[96,97] 0.05–351 Wells:[97] up to 2544	Critical[b]: 113	Critical[b]: 240	Critical[b]: 0.8–11.5
Homoacetogens	H_2 loss by CH_3COOH production, clogging	Laboratorial[a]:[68,98,100,101] 0.2–5.0 × 10^5	Optimum[b]: 20–30	Optimum[b]: <40	Optimum[b]: 6.0–7.5
			Critical[b]: 72	Critical[b]: 300	Critical[b]: 3.6–10.7
Iron(III) reducing bacteria	H_2 loss by Fe(II) Production, clogging	Laboratorial[a]:[68,102–106] 0.005–2.2 × 10^5	Optimum: 0–30 Critical: 90	Optimum: <40 Critical: 200	Optimum: 6–7.5 Critical: 1.6–>9

5. UHS opportunities

Taranaki is well positioned to emerge as a major hydrogen hub for New Zealand. Although there are potential UHS options throughout the North Island (Appendix Figure A3. 1), regions with existing petroleum infrastructure together with future hydrogen production and export will likely be most favourable. Furthermore, in Taranaki, there is existing hydrocarbon infrastructure and knowledge. This is matched by the presence of depleted (and depleting) reservoirs, and growing renewable electricity resources (e.g., Waipipi wind farm, significant offshore wind resource). All of these factors have been recognised by both government and

private sectors (Green Paper, Taranaki Roadmap, Hiringa, Kapuni Ballance Agri-nutrients) (MBIE, 2019; Tapuae Roa, 2019). UHS will help realise the full potential of a Taranaki hydrogen economy.

This section describes key UHS opportunities in Taranaki. The locations presented below are considered the most prospective porous-media UHS options given the available data.

5.1. Depleted reservoirs

FirstGas conducted an initial screening using 2018 production data for 18 fields (including some composite fields, for example, Tariki/Ahuroa). This screening study was used to assess the suitability of these fields for their post-depletion redevelopment as gas storage reservoirs, including hydrogen storage. Of the 18 fields, five offshore reservoirs were dismissed due to their relative inaccessibility. A potential exception is the offshore Pohokura reservoir, which was partially developed from onshore. The remaining sites were screened based on the following criteria:

1) field size (match with storage requirements preferred),
2) peak production rate (more prolific preferred),
3) reservoir quality (higher porosity and permeability preferred),
4) reservoir formation (younger/ shallower formations preferred),
5) reservoir depth,
6) well numbers,
7) well cost.

The presence of oil is some reservoirs may be an additional challenge for UHS, due to the possibility of hydrogen dissolving in the oil and increasing the potential for hydrogen contaminants on withdrawal. We have not considered this factor in our screening here.

The Surrey, Copper Moki, Ngatoro and Supplejack fields were all deemed to have reservoirs too small for anticipated UHS requirements. The Mangahewa, Turangi, and Kowhai and Radnor fields produce from deep and relatively tight (low permeability) reservoirs, which would make UHS challenging. Gas losses, water flood (Sidewinder, Cheal and Cheal E) and reservoir geochemistry (Waihapa/ Ngaere) were deemed as critical factors preventing or hindering UHS for some fields. FirstGas's provisional ranking of the Taranaki fields graded WestSide's Rimu/Kauri complex most promising, with Todd's McKee and Kapuni fields, and NZEC's Tariki field also potentially of interest. In the sections below, we have developed these prospects further. For the locations of the fields refer to Figure 2.

Of current operators of depleted and late-life producing oil and gas fields in Taranaki, WestSide, together with Tamarind, are distinguished in being purely producers. Todd and Greymouth (treating NZEC as a controlled offshoot of Greymouth) also sell gas and, in Todd's case through their Nova subsidiary, generate and sell electricity. Commercial arrangements with purely producer outfits, such as Westside and Tamarind, might be considered more straightforward than collaboration with partners that have vested interests in electricity generation and retailing gas.

5.1.1. Rimu/ Kauri/ Manutahi fields

Rimu/Kauri/Manutahi fields (Figure 2) are conveniently situated close to the Kapuni to Wellington gas pipeline, within adjacent petroleum mining permits (PMP) held by WestSide subsequent to their acquisition from Origin Energy in 2016. The Kauri field produced from numerous wells drilled across the shoreline into a poorly performing muddy sandstone reservoir. The Manutahi oil field in the Kauri PMP produces from higher quality Miocene sandstones at a depth of about 1100 m. Although there is a considerable quantity of oil in place not yet produced (see table in Section 6.3.1), production of the highly viscous oil is limited to low rates. Thus, the Rimu Field is expected to provide the highest quality UHS reservoir of the Westside fields.

The Rimu field, with about 10 wells, produces from Tariki Sandstone in a complex structural setting. Production from the Rimu field has been steadily decreasing from its peak at almost 7 PJ (167 million m^3 in 2005, with a subsidiary peak of around 1 PJ in 2015 (Figure 16; further discussion in Section 6.3.1). Remaining reserves in Rimu as of 1st January 2021 were reported as between 0.02 (90% probability of exceedance) and 9.04 PJ (10% probability of exceedance) and a P50 ("most likely") of 3.99 PJ. Kauri and Manutahi fields are treated separately in the Reserves tabulation although apparently combined with Rimu in the Production tabulation.

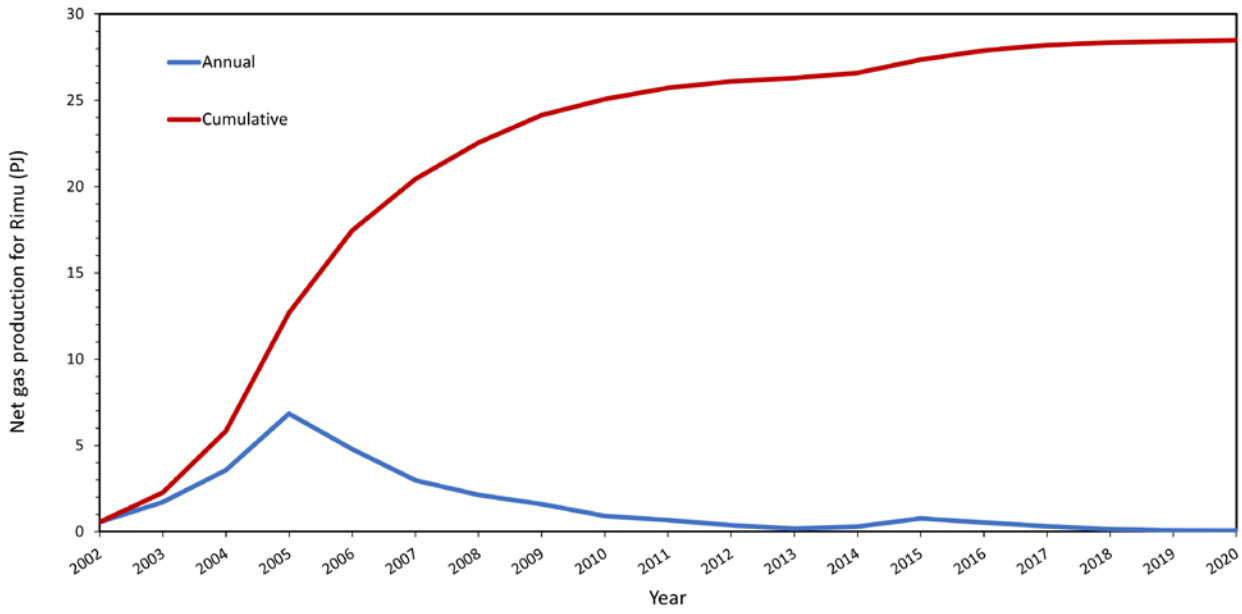

Figure 4: Cumulative and annual gas production from Rimu field, which has declined in recent years. Data from MBIE (2021).

5.1.2. Kapuni Field

In the latest statistics, the Kapuni field is ascribed remaining reserves of 100 – 273 PJ, and a considerable volume, over 700 PJ, of contingent gas resources. This is thought to be dominated by deeper, less permeable reservoirs yet to be fully appraised, which will be necessary in advance of development. Considering the depth of the depleted reservoirs, gas or hydrogen injection for storage would be expensive both for drilling new wells and for compression. However, existing wells may suffice: gas injection wells operated for several years while production strategy focused on condensate recovery.

Moki sands (refer to Section 4.2.3), at a depth of 2000–2400m, above the Kapuni gas reservoirs, may be worth evaluating as a UHS prospect, considering the proven anticlinal structure and amount of well and 3D seismic data in existence.

5.1.3. McKee Field

The McKee field in north-east Taranaki is owned and operated by Todd Energy subsidiaries and is the largest producing onshore oil field (MBIE, 2021). The McKee field was described in a conference presentation prior to its sale to Todd Energy, following the acquisition of original operator Fletcher Challenge (Rickard, 2000). Rickard (2000) describes various inter-well communication and states, “There are local pressure variations across the field, but it is doubtful that any portion of the field is totally isolated from the other areas”.

The McKee Formation reservoir sandstone is shown in Figure 17, bound by a steep thrust fault to the west and dipping steeply on its eastern flank. The crest of the structure is at about 1720 m below sea level (Rickard, 2000). The initial gas-oil contact occurred at about 1930 m, and the initial oil-water contact at about 2170 m. A 3D seismic was undertaken in 2016, covering approximately 85 km^2 over both the McKee and Mangahewa fields, which should have resulted in improved imaging of the complex structure.

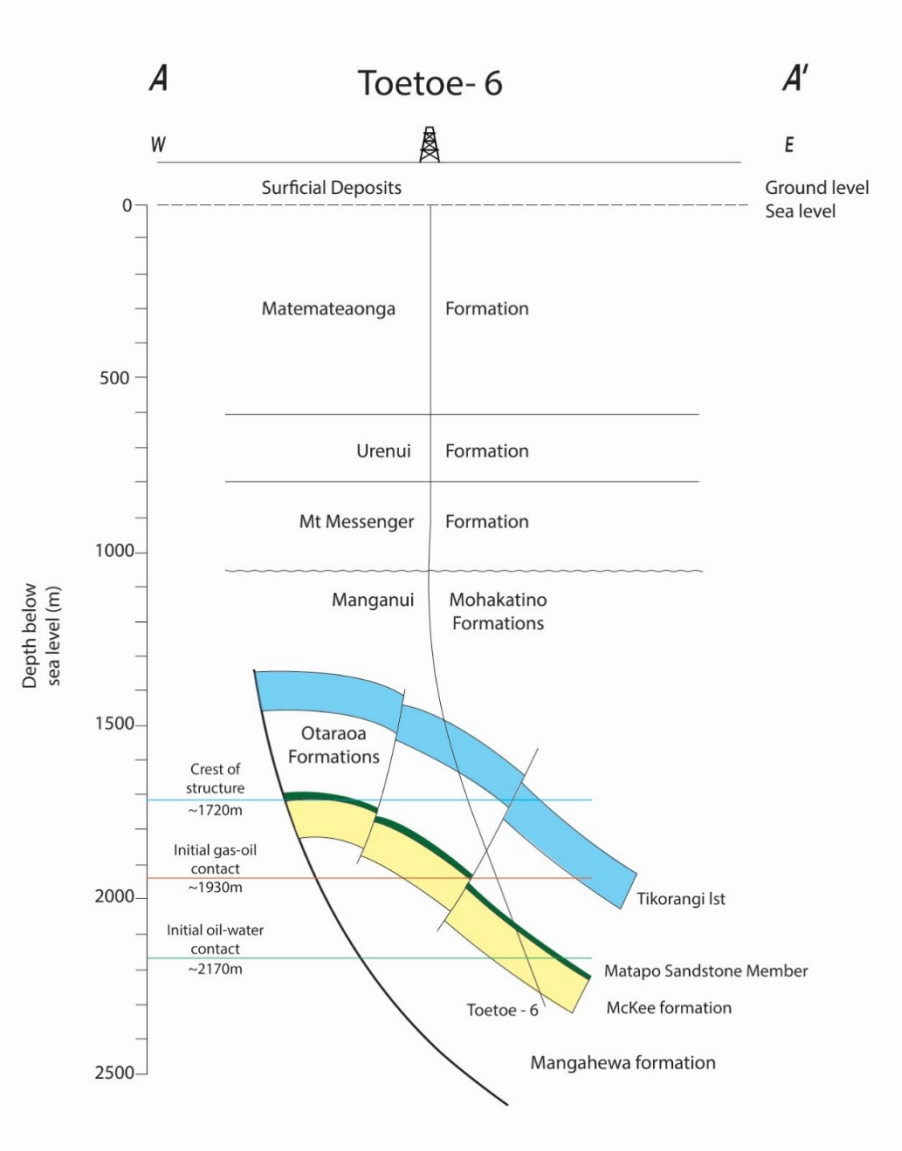

Figure 17: Simplified cross section of the McKee Field structure. Black line represents the well path into the reservoir (yellow) and overlying cap rock in green white. Figure adapted from Rickard (2000).

The most recent MBIE (2021) reserves data indicate that the McKee field has produced 47.3 million barrels of oil and 19.61 PJ of gas up until the end of 2020, giving some indication of the potential storage capacity, although a full assessment would need to consider aquifer influx. A scenario based on this constraint is developed in 6.3.3. Remaining reserves at the beginning of 2021 were up to 50 PJ of gas and 220,000 barrels of oil. Contingent resources in the field amount to 33 million barrels of oil. Peak oil production for McKee was in 1989, producing 23.45 PJ with peak gas production in 2009, producing 10.64 PJ (MBIE, 2021).

In general, publically available information is insufficient to allow for a detailed scoping of a project to convert depleted gas reservoirs and facilities to UHS. However, Crown Minerals (Petroleum) Regulations 2007 require mining permit operators to provide MBIE with reports on field operations and production twice each year, and versions with information considered commercially sensitive can be obtained after 5 years. The 2011 report on Mangahewa and McKee fields reveals that four McKee field wells have been used for reinjection of produced

gas, McKee-3A was the only gas injection well remaining in service in the second half of 2011 (Table 5**).**

Table 5: Gas injection wells in the McKee field, note that in the second half of 2011 the McKee-3A well was the only operating injection well.

Well	**Fluid type**	**Total cumulative injected volume** (m^3)	**Monthly gas injection days for 2011**					
			Jul	Aug	Sep	Oct	Nov	Dec
McKee-3A	Produced Gas	314,645,243	29.6	30.2	28	29.6	7.3	27.2
McKee-10	Produced Gas	45,688	0	0	0	0	0	0
McKee-12	Produced Gas	8,831,006	0	0	0	0	0	0
McKee-15	Produced Gas	71,257,151	0	0	0	0	0	0

The McKee-3A well had a 25m interval perforated in 2007, 2130-2154m along-hole depth (1894–1917.7m true vertical depth below sea level), in the McKee A1 sand. McKee-3A had produced 14,016 m^3 of oil and 28,484,293 m^3 of gas before being converted for gas injection (to provide pressure support for oil production from the field).

Initial field pressure was 3415 psia, by 2000 it had been drawn down to about 2000 psia (Rickard, 2000), reducing productivity of the field. As of 2011, oil and gas were being produced from 5 McKee field wells, the most prolific being McKee-9A which was producing 213,931 m^3 of gas per day and 21.82 m^3 of oil as well as 10m^3 of formation water. Productivity is likely due to reinjection into the McKee-3A well increasing pressure in the field.

5.1.4. NZEC fields

As noted above, Tariki is understood to be under evaluation for gas storage – new 3D seismic coverage was acquired in 2021. The field has produced 64.38PJ of gas, the last production being in 2009 (MBIE, 2021).

The Waihapa/Ngaere oil reservoir is not well understood and, being fractured limestone, would be challenging to model and to be assured of recovering injected fluids. As noted in section 4.4**,** hydrogen may also react with abundant carbonates in limestone reservoirs. For similar reasons, GNS excluded the Tikorangi limestone reservoir in Waihapa/Ngaere from consideration for CO_2 sequestration (King et al., 2009).

5.1.5. Smaller fields

In onshore Taranaki, Mount Messenger and subsidiary Urenui sand bodies serve as oil and gas reservoirs in several small fields. Production information for these fields, which gives a general indication of the pore volume available for UHS, is presented in Table 6.

Table 6: Productions and depletions statistics for several small onshore fields within the Mount Messenger and Urenui reservoir sands. Data tabulated from *(MBIE, 2021)*.

Field	Produced		% of 1P depleted		2020 production	
	Gas (PJ)	Oil (mmbbls)	Gas (PJ)	Oil (mmbbls)	Gas (PJ)	Oil (mmbbls)
Ngatoro	48.1	10.2	85	94	0.99	0.1
Cheal	7.65	4.34	83	82	9.25	0.37
Copper Moki	2.39	0.54	94	81	0.49	0.03
Surrey	0.32	0.18	95	76	.001	0

Notes:

1. *"Ngatoro" includes all pools in the Ngatoro Petroleum Mining License (PML), including a gas pool in Kapuni sandstone, Kaimiro-1*
2. *"Cheal" includes Cheal East, also some reserves assigned to the deeper and older (Kapuni) Cardiff reservoir*
3. *Tamarind's Supplejack and Sidewinder fields not included.*

5.2. Aquifers

Requirements for aquifers are similar to depleted reservoirs and require a trapping structure and appropriate reservoir and cap rocks. The same formations which serve as reservoirs and cap rocks in Taranaki oil and gas fields also present aquifer UHS opportunities where petroleum charge may have been lacking. However, containment may exist due to structural, stratigraphic, or a combination of configurations, including anticlinal and fault-seal traps common to Taranaki. As with oil and gas reservoirs, anticlinal structures adjacent to the Tarata Thrust Fault might provide the best prospective aquifer structures in the region (Section 4.1).

Aquifers are generally lacking the extensive subsurface data that is available for producing oil and gas fields. Initial site observations may require interpolation of distant data points. The distribution of groundwater bores into volcanic and sedimentary aquifers across Taranaki are shown in Figure 18.

Specific target aquifers include volcanic units in the Taranaki ringplain, Matemateaonga Formation (Section 4.2.5), Whenuakura Group and marine terraces. Of course, groundwater resources accessed for potable, agricultural or industrial water need to be managed sustainably, and UHS, which might interfere with water quality, would likely face resource consent issues if targeting freshwater aquifers. These same units have saline pore water where they are present deeper in the subsurface, in some cases, and could be considered for UHS.

With lack of other contingent site-specific data on aquifers in Taranaki, we have provisionally evaluated the hydrogen storage capacity and dynamics of a single shallow aquifer. The reservoir is a thin (7 m) sandstone within the Urenui Formation at about 820 m below sea level in the Ahuroa permit zone. This is the basis for a UHS scenario developed in Section 6.3.2.

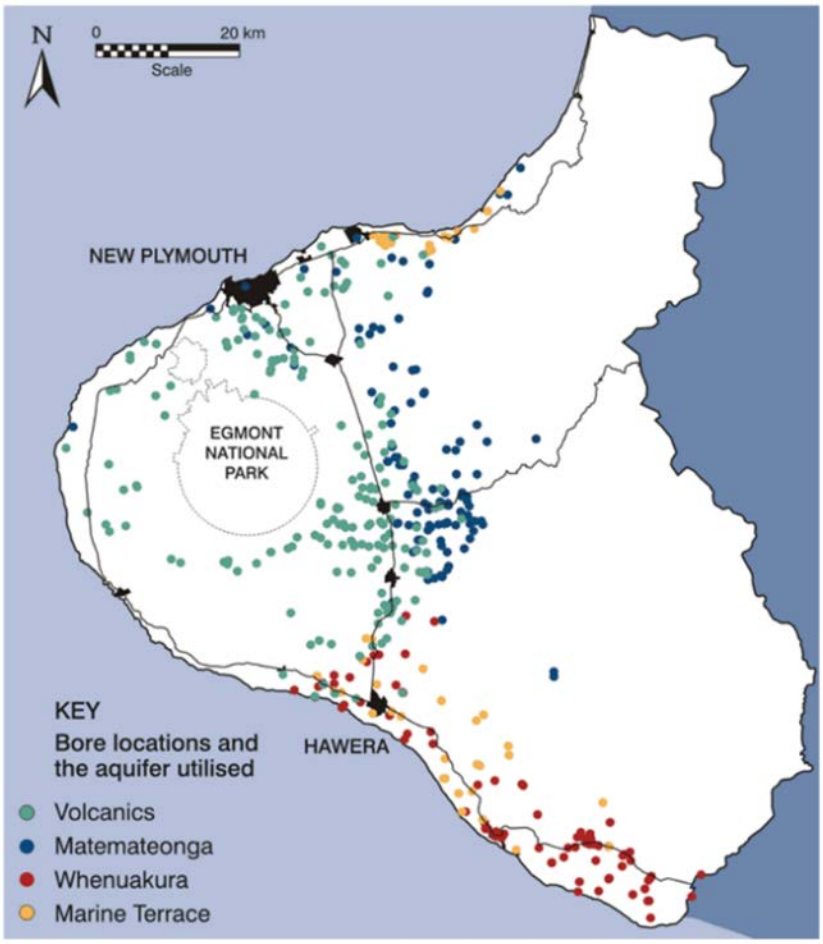

Figure 18: Groundwater bore distribution and lithologies of penetrated aquifers in Taranaki. Figure from King et al. (2009).

6. Reservoir engineering

This section presents a preliminary assessment of UHS at specific sites in Taranaki, focusing on depleted gas reservoir and saline aquifers. This is not an exhaustive study of all prospects and should therefore not be interpreted as a total inventory of available UHS. Rather, we have selected illustrative sites with favourable conditions and evaluated these for storage potential and performance. The evaluation is made with the best available data and stated assumptions. Any deviation from these due to future investigations could materially change the estimated storage capacity and performance.

6.1. Principles of hydrogen storage modelling in porous media

This section introduces physical concepts necessary to understand the scale and performance of UHS in depleted reservoirs for the sites discussed in this report. It is not a comprehensive review of UHS reservoir dynamics and implementation, details of which can be found in other studies (Ennis-King et al., 2021; Heinemann, Alcalde, et al., 2021; Zivar et al., 2020).

Two approaches are applied here to evaluate UHS in Taranaki: estimation of in-place volumetric gas storage, and numerical reservoir modelling. The former approach was used by Ennis-King et al. (2021) to estimate UHS potential at sites across Australia. The latter, reservoir modelling, is routinely used when assessing prospective resources (groundwater, geothermal,

hydrocarbon, CCS), to predict a project's performance, and to inform decision-making at all stages. Regardless of approach, all such models embed a degree of uncertainty and inaccuracy due to: absent or approximate constraints by data; numerical approximations; and simplifying assumptions about the reservoir geometry or fluid physics. The acceptable level of uncertainty depends on the manner in which the model is to be used (SKM, 2012) and the resources that can be devoted to its development.

The models presented here are intended for pre-feasibility assessment. Their purpose is to provide order-of-magnitude storage volumes, injection and recovery rates, and cushion/working gas ratios. Further development of the models would be needed for feasibility assessment at specific sites. This could include undertaking sensitivity and uncertainty analysis, identifying data gaps, developing site-specific multi-phase equations of state, and optimizing well infrastructure.

6.2. Modelling approaches

Static

A volumetric (or static) model is an assessment of the required or available pore volume for UHS. Hydrogen is to be stored within this volume, and the total amount of hydrogen contained will depend on its density at reservoir pressure and temperature.

A volumetric model does not account for the rate at which hydrogen can be injected or extracted into the reservoir, the cushion gas requirements, or other losses of the gas: these can be addressed by a reservoir (or dynamic) model. Nevertheless, volumetric models are useful for early screening of prospects on their storage potential.

In a depleted reservoir, the available pore volume for hydrogen storage can be approximated by the volume of extracted hydrocarbons given in historic production records (Ennis-King et al., 2021). Ordinarily, this requires a density rescaling of the recorded production volumes, which are generally given at standard conditions.

Further details about the static modelling methodology are given in Appendix A4.1.1.

Dynamic

A reservoir (dynamic) model is a numerical representation of the amounts and movements of fluids in an underground porous rock volume. A reservoir model of UHS quantifies the amount of hydrogen gas in storage, where it is located in relation to other fluid phases (water, natural gas, oil), and the rate at which it is moving away from (or toward) the injection well.

There are a range of commercial and research simulators that can perform reservoir modelling, and these use different numerical techniques and representations of rock and fluid physics. As UHS is relatively novel, there are fewer simulators available with the necessary hydrogen equation of state (e.g., DuMu^x, and Petrel - (Feldmann et al., 2016) and (Heinemann, Scafidi, et al., 2021), respectively). The approach used here has been to adapt a research simulator for CO_2-water injection studies (Dempsey et al., 2014), called FEHM, and replace CO_2 gas properties with equivalent H_2 values. This has the advantage of leveraging an existing simulator that meets United States Department of Energy standards for

benchmarking and quality assurance (Dash et al., 2015; Zyvoloski, 2007; Zyvoloski et al., 1997).

Further details about the dynamic modelling methodology are given in Appendix A4.1.2.

6.2.1. Hydrogen properties

Density

Hydrogen is in its gas phase for all temperature and pressure conditions relevant to UHS. Density determines what mass of hydrogen that can occupy a certain reservoir pore volume. In this study, we have used the polynomial model of Zheng et al. (2016), which agrees with NIST density data to within 0.01% in temperature and pressure ranges of interest (Figure A4. 1). At standard conditions (15°C temperature and 1 atm pressure), the density of hydrogen is 0.084 kg/m^3. For comparison, the density of natural gas (methane) is 0.67 kg/m^3 at the same conditions.

Viscosity

Viscosity quantifies a fluid's resistance to flow through a porous medium. The range of hydrogen viscosity at UHS conditions (9-11 µPa s) is comparable to other gases (CO_2, 0.05-77; natural gas, 11-27 µPa s), and low compared to water (300-900 µPa s). To calculate viscosity in reservoir simulations, we used the correlation of Muzny et al. (2013), which was obtained from regression to a large experimental dataset. This model overpredicts viscosity by a few percent in the reservoir conditions of interest (Figure A4.1).

Energy density

The Lower Heating Value of hydrogen is the readily available energy liberated during combustion and is 120 MJ/kg. The LHV for methane is 50 MJ/kg. Depending on the blend of natural gas, its LHV is slightly lower than that of methane (the main constituent). For simplicity, we have used the value for methane.

At fixed pressure and temperature conditions, the relative energy content of a volume filled with natural gas versus hydrogen depends on: (1) the ratio of their mass densities and, (2) the ratio of their LHV. The ratio of mass densities depends on pressure is between 8 and 9.5 over ranges of interest. Combined with the LHV numbers quoted above, Ennis-King et al. (2021) recommend using a conversion factor of 0.22-0.27. This conversion factor is helpful for approximate conversions in unknown conditions, as may be the case for an undrilled reservoir, or in a pipe network with varying pressure.

Solubility

Solubility of hydrogen in water is considered low compared to other gases and is generally neglected in UHS simulation studies (Heinemann, Scafidi, et al., 2021). Ennis-King et al. (2021) have argued that solubility losses are likely to be less than 1% over UHS commercial time-scales. Therefore, solubility has been neglected in this analysis. For an expanded discussion on solubility effects, refer to Appendix A4.1.3.

Relative permeability

The relative movement of co-existing hydrogen and water phases under a pressure gradient depends on how gas and water interact. In a reservoir model, this is captured by relative

permeability curves, which rebalances the individual hydrogen and water flow rates to account for the saturation of each. We have used exponential curves fitted to the data of Yekta et al. (2018), who measured relative permeability of hydrogen-water mixtures in sandstone rocks. Further details are given in Appendix A4.1.3.

6.2.2. Model elements

Wellbore representation

Injection of a fluid phase into the subsurface – either in the field or a model – occurs at either a specified rate or pressure. For the latter, pressure is specified either at the wellhead (WHP) or at a depth in the well where fluid enters the formation (downhole pressure, DHP). In this analysis, we have opted to specify operating injection pressures that remain within reservoir performance criteria. For saline aquifers, injection pressure should not exceed 90% of the fracture gradient. For depleted reservoirs, it is desirable that injection pressure should not exceed predevelopment formation pressure. Further details about the wellbore model are given in Appendix A4.1.4

Domain and grid

Because of its low density, hydrogen is buoyant in the subsurface and will migrate upward unless trapped, structurally or stratigraphically. It is for this reason that depleted reservoirs are favoured prospects for UHS, because a structural trap is generally a prerequisite for a reservoir to have accumulated at these locations. Anticlines are a common geometry for UHS simulation (Feldmann et al., 2016; Heinemann et al., 2021b). This study uses the anticline geometry with a dip angle of 3°, similar to Feldmann et al. (2016).

The models used here consider an azimuthally symmetric anticline with a single injection and production well penetrating its central crest across the entire reservoir thickness. The domain has a 2000 m radial extent with a logarithmically increasing grid spacing toward the boundary that enables full resolution of near wellbore processes. Reservoir thickness is variable depending on location. All boundaries are closed to flow and the cap rock is assigned very low permeability (0.01 mD). The model grid and reservoir geometry are shown in Figure 19.

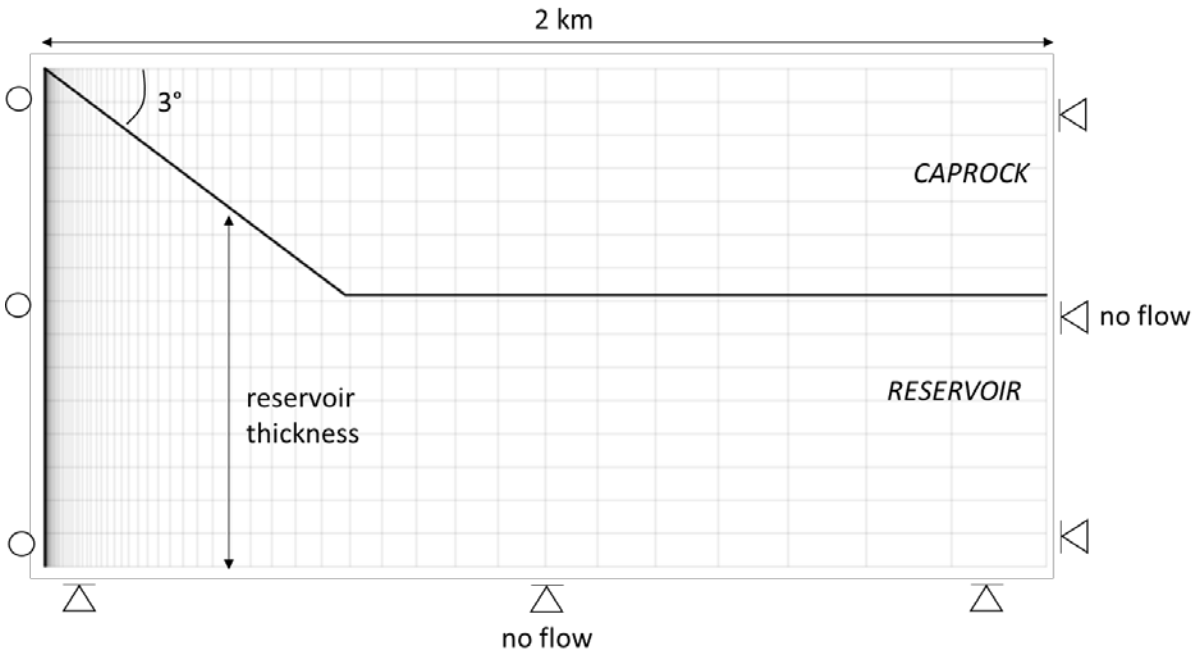

Figure 19: Simplified anticline reservoir geometry and simulation grid. Open circles denote fixed pressure boundary conditions. Terminated triangles denote directions closed to flow. The grid has azimuthal symmetry.

Cushion gas and cycle representation

UHS projects distinguish between cushion and working gas. Cushion gas is generally emplaced during an initial injection phase, which creates a compressible gas plume in the reservoir by displacing some of the liquid present (oil, water). Then, subsequent cycles of working gas injection and production achieve storage through pressure-driven compression and decompression of the plume, and less by lateral growth of the plume itself.

In underground natural gas storage, cushion gas can occupy between 15 and 75% of the total storage, depending on the suitability of the reservoir and the optimization of its operations (Namdar et al., 2020). Emplacement of cushion gas is a substantial cost for UHS. This can potentially be offset by pre-injection of a low-cost cushion gas (N_2 or CO_2), or by using pre-existing natural gas in a depleted reservoir. However, mixing of the hydrogen and cushion gas, and the impacts on produced gas purity, would need to be considered.

This study considers multiple yearly cycles of injection and production of hydrogen, wherein cushion gas is accumulated steadily with each cycle. The cushion gas is the difference between injection and production volumes in a single cycle, with the proportion of cushion gas declining over subsequent cycles.

Each cycle comprises: (1) an initial four months of hydrogen injection at a fixed pressure above the pressure midpoint, (2) four months of shut-in, (3) four months of hydrogen production at a fixed pressure below the pressure midpoint. Back produced water is presumed to be discarded, treated, or otherwise disposed of. A total of ten cycles were modelled.

The dynamic storage volume was quantified by the amount of produced hydrogen during the withdrawal phase of the final cycle. This is different to the static storage, which uses static modelling to estimate available pore volume.

Geomechanical and microbial considerations

Concerns have been raised about hydrogen interaction with reservoir or cap rock and aqueous pore fluids, or consumption and conversion by in-situ microbial communities. The main concerns are (1) consumption of hydrogen, a storage loss, (2) generation of harmful gases, e.g., H_2S, (3) dissolution, precipitation or formation of biofilms that negatively impact reservoir or cap rock performance (porosity and permeability). Our current understanding of these processes, based on laboratory, field and modelling studies, is described in Sections 4.4 & 4.5.

In principle, these processes can be described and incorporated into a reservoir model. However, the associated model parameters (rates, reaction coefficients) are likely to be highly site-specific and require a degree of individual characterization that exceeds the scope of this study.

6.3. Taranaki UHS scenarios

Below, we develop four UHS scenarios at three sites in Taranaki. These were selected on the basis of available characterization, proximity to existing infrastructure, and to provide an indicative service range for UHS (static/dynamic storage and transfer rates).

6.3.1. Rimu depleted reservoir

Background of the Rimu field scenario is introduced in Section 5.1.1.

The cumulative historic production from Rimu of 30.39 PJ of gas (685.1 m3 net 759.6 m3 gross) gives an indication of the capacity of the reservoir pore volume within its original pressure regime. Petroleum reserves statistics do not discriminate between Rimu and Kauri (and which presumably includes Manutahi oil field). The Rimu field volumes can be derived approximately from the 2021 data (Table 7).

Table 7: Rimu 1P reserves at the end of 2020 (MBIE, 2021). Gas volume at reservoir conditions is calculated by applying a scale factor based on the relative methane density between standard (0.67 kg/m^3) and reservoir conditions (166 kg/m^3 at 36 MPa and 120°C, see Table 1). LPG density calculated as a 60:40 propane-butane mix. Std = standard conditions, res = reservoir conditions.

Rimu 1P reserves	Oil		Gas			LPG		
	10^3 bbl	10^6 m^3	PJ	10^6 m^3 (std)	10^6 m^3 (res)	PJ	10^6 kg	10^6 m^3 (res)
Ultimate	864	0.137	3.36	81.6	0.328	0.44	9.18	0.018
Remaining	84	0.013	0.02	0.5	0.002	0.0	0.013	0.
Produced (difference)	780	0.124	3.34	81.1	0.326	0.44	9.17	0.018

An advantage of the Rimu field is that it is only 20 km from the Waipipi wind farm, which is a potential source of renewable energy spill. The Waipipi windfarm is expected to generate 455 GWh/year. Assuming hydrogen is only created during off-peak times, energy generation is constant and off-peak hours make up 16 hours of the day, then approximately 300GWh/year could be available for hydrogen electrolysis. Assuming current production of 1 kg of hydrogen uses 43.1-55.4 kWh of green electricity (Holm et al., 2021), and 1kg H_2 is equivalent to 11.13 Nm^3 (Mehmeti et al., 2018), then 60 to 77 million Nm^3 of hydrogen could be produced in a year, approximately 600 – 770 TJ.

Review of site-specific conditions

The reservoir unit at the Rimu-A1 site is the Tariki Sandstone (Harris et al., 1999). This unit is approximately 55 m thick at a target depth of 3.6 km. The estimated temperature and pressure conditions at this depth are 120°C and 36 MPa. Various fluid densities at reservoir conditions are given in Table 8. The relatively high temperature is likely to inhibit some microbiological reactions.

Table 8: Rimu reservoir/Tariki sandstone conditions. LPG density calculated assuming a 60:40 mix of propane and butane.

Depth (km)	T (°c)	P (MPa)	H_2 density (kg/m^3)	Methane density (kg/m^3)	Propane density (kg/m^3)	Butane density (kg/m^3)	LPG density (kg/m^3)
3.6	120	36	19.4	166	467	540	496.

Porosity-permeability data for the reservoir unit are summarized in Appendix Figure A2.1 and Appendix Table A.2.4. Reservoir simulations used a porosity of 15%, and a permeability range of 10 to 50 mD. All models assume a constant, homogeneous permeability, which does not account for structural or stratigraphic variability in the field. These effects would be important to explore in follow-up modelling to support a pilot study.

Media reports (OGJ, 2000) at the time noted that:

> *"The well flowed 1,525 b/d of 44° gravity [806 kg/m^3] oil and 4.8 MMcfd of gas from Upper Tariki at–11,831-962 ft. A 10-day pressure drawdown and build-up test of Upper Tariki in December indicated that the oil reservoir has initial reservoir pressure of 5,223 psi [36 MPa]"*

Corresponding oil and gas component flow rates are 2.26 and 1.05 kg/s. At this density, oil compressibility is between 4.5 and 23×10^{-10} MPa (PetroWiki, 2015a), which is up to five times higher than water (5×10^{-10} MPa). At the reservoir temperature of 120°C, oil viscosity is approximately 0.002 Pa s (PetroWiki, 2015b), which is about eight times higher than water at the same temperature and pressure (0.00024 Pa s).

Static storage assessment

Rimu proven reserves (1P), ultimate and remaining, are summarized in Table 7, subdivided into Oil, Gas and LPG components. Using in-situ densities (Table 7), the corresponding pore volumes at reservoir conditions are 0.124, 0.326 and 0.018 million m^3, respectively (28, 68, and 4% by volume).

By 2020, gas production had declined and the remaining volume fractions of Oil, Gas and LPG were 86, 14 and <1%, respectively (Table 8) and the total produced volume of hydrocarbons under reservoir conditions was 0.468 million m^3. This pore volume could store 9.1 kT of hydrogen at a reservoir density of 19.4 kg/m^3. The corresponding energy content is 1.1 PJ.

Dynamic storage and transfer assessment

Transfer rates of hydrogen into and out of storage, as well as cushion gas requirements, are assessed using a numerical reservoir (dynamic) model. The assumed geometry is a 3° dipping anticline with azimuthal symmetry. The reservoir unit has a maximum thickness of 55 m at the crest of the anticline. The crest is fully penetrated by the injection/production well, assumed to have a radius of 0.1 m at the reservoir depth (7" casing). The operating pressure range for injection and production is ±3 MPa.

The principal uncertainty in characterizing an injection/production cycle model of Rimu UHS is the reservoir permeability. Therefore, low and high models were developed based on a 10 to 50 mD range (Figure 20).

We have assumed that the dominant phase prior to injection is liquid (oil), and this must be first be displaced by the injection of a cushion gas. It is not clear whether there is significant remaining gas in the reservoir in a separate accumulation, which could act as a pre-existing cushion for the injected hydrogen. If this were the case, the cushion gas requirements would be less than modelled here.

After 10 years, working gas injection and production into the reservoir ranges between 50 and 300 TJ (0.45 and 2.4 kt) over the 4-month extraction phase, depending on permeability. Corresponding daily average flow rates are 0.45 to 2.4 TJ/d (3.7 to 20 t/d). The cushion gas percentage is high in the first cycle (60-70%) but drops rapidly with subsequent cycles. A higher operating pressure range could be expected to achieve higher gas storage rates.

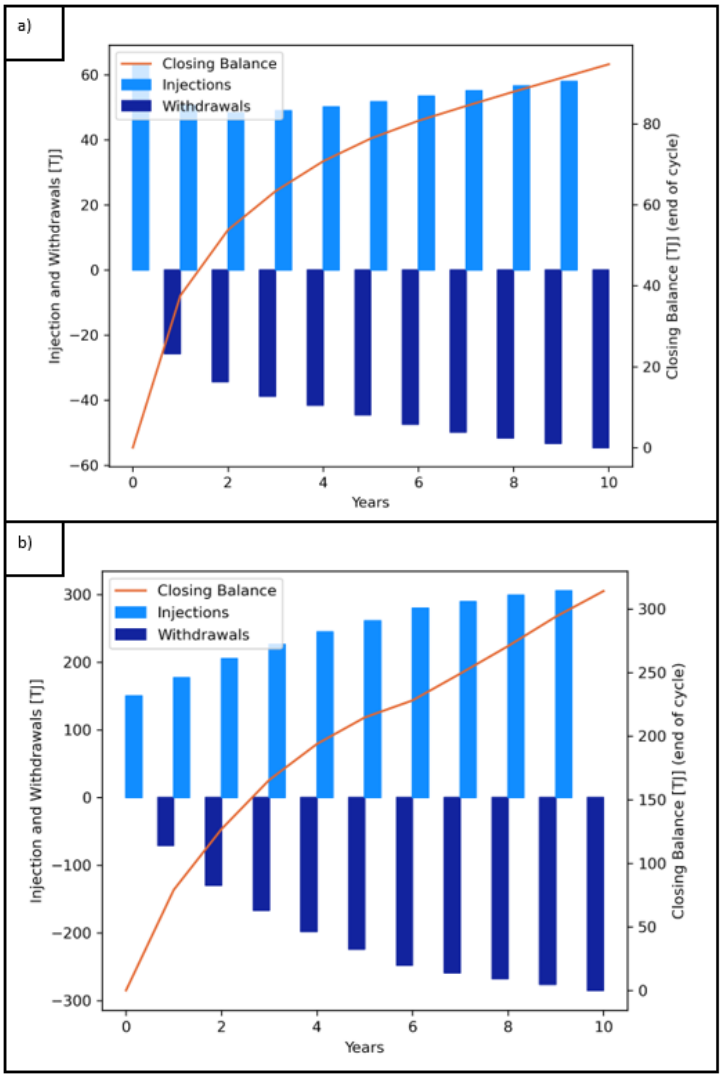

Figure 5: Injection and withdrawal volumes for Rimu depleted reservoir. End-member a) low and b) high permeability simulations, 10 and 50 mD, respectively. Orange line tracks total gas in the reservoir.

6.3.2. Ahuroa: shallow aquifer and deep reservoir

Ahuroa is a depleted gas reservoir that was converted for storage in 2009. Gas storage occurs in the Tariki sandstone at 2.3 km depth. Reported storage potential is 18 PJ of natural gas, with injection and production rates of 65 TJ/d, although this aggregates the output of several wells. Recent injections and withdrawals from the reservoir are shown in Figure 21.

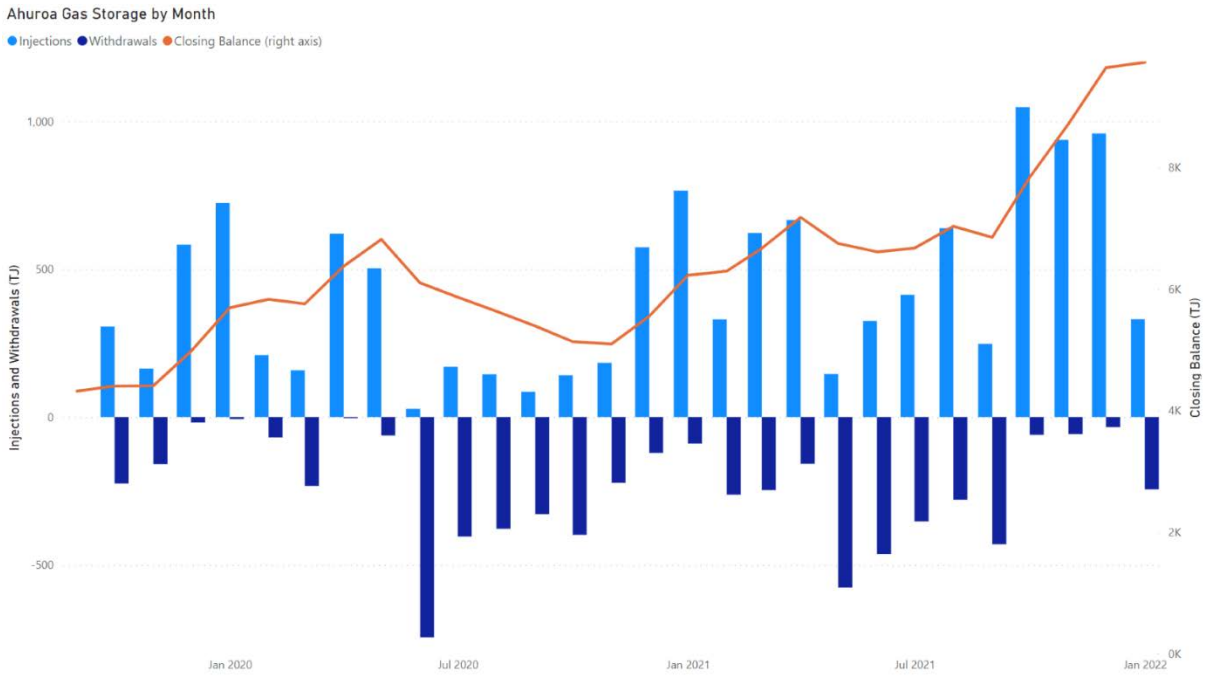

Figure 6: Monthly injections and withdrawals from Ahuroa gas storage in the two years to Jan 2022.

Ahuroa wells also intersect shallower aquifers (e.g., U20 sand, within the Urenui Formation). Saline aquifers have several favourable properties for UHS. Hydrogen has low solubility in water, and therefore dissolution losses are expected to be low. Saline aquifers are geographically more widespread than oil and gas fields.

There are drawbacks to the shallower aquifers. In the absence of a hydrocarbon accumulation, there is no clear demonstration of long-term structural trapping. Seismic surveys are likely necessary to prove capping structure and geometry, accompanied by exploratory drilling to confirm formation characteristics. The lack of prior characterization makes modelling of these sites uncertain.

This section evaluates two prospects: (1) the equivalent storage and transfer of the Tariki sandstone reservoir if converted from natural gas to hydrogen, and (2) the shallower U20 sand. The latter prospect is a saline aquifer and is intersected by the Ahuroa-3 and other wells.

Static storage assessment in Tariki Sandstone

Applying the Ennis-King et al. (2021) volumetric conversion factor (0.27), the corresponding storage and transfer rates of hydrogen are 4.9 PJ and 18 TJ/d. However, at assumed reservoir conditions for 2.3 km depth (23 MPa and 82°C), hydrogen has about half the viscosity of methane (10 vs 19 µPa s). Therefore, hydrogen transfer rates could be nearly a factor of two higher for the same operating pressure range, about 33 TJ/d.

Dynamic storage assessment in U20 sand: site-specific conditions

The U20 sand is a reasonably clean unit about 7 m thick at approximately 1 km depth. Pressure and temperature conditions at this depth are assumed to be 10 MPa and 44°C. For screening purposes, the properties of this unit are inferred from Mount Messenger/Urenui reservoirs

in other Taranaki fields (Figure A4. 1). Porosity of 20% and permeability in the range 10 to 100 mD (see Appendix Figure A2.4, Appendix Table A.2.4).

For a saline aquifer, injection pressure limits are based on remaining below the fracture pressure. For an assumed extensional tectonic setting and typical friction properties, this is estimated to yield an operating pressure range of ±1.7 MPa. Further details of this calculation are given in Appendix A4.1.2 & A4.2.

Even injecting at this pressure, care should be taken during seismic characterization that there are no faults in overlying strata that could be activated under small pressure changes. Reactivated faults can enhance permeability locally and thereby compromise the integrity of cap rock formations. The risk can be partly managed through close microseismic monitoring, particularly during the initial injection of cushion gas (Jiang et al., 2021).

Dynamic storage and transfer assessment

Transfer rates of hydrogen into and out of storage, cushion gas requirements, and total storage volume, are assessed using a numerical reservoir model. Similar to the Rimu model, the assumed geometry is a 3° dipping anticline with azimuthal symmetry. The reservoir unit has a maximum thickness of 7 m at the crest of the anticline. The crest is fully penetrated by the injection/production well (Figure 21), assumed to have a radius of 0.1 m at the reservoir depth. The operating pressure range for injection and production is ±1.7 MPa.

The principal unknown in characterizing an injection/production cycle model of the U20 sand is the reservoir permeability. Therefore, low and high models were developed based on a 10 to 100 mD range (Figure 22).

After 10 years, working gas injection and production into the reservoir ranges between 0.9 and 9 TJ (7.5 and 75 tonnes) over the 4-month extraction phase, depending on permeability. Corresponding daily average flow rates are 61 to 610 kg/d (7.4×10^{-3} to 7.4×10^{-2} TJ/d). These relatively low amounts compared to the Rimu field reflect the combined effect of: (1) reduced reservoir thickness (7 vs. 55 m), (2) reduced hydrogen density at storage depths (8 vs. 20 kg/m^3, at 1 and 3.6 km, respectively); and (3) the lower operating pressure range (±1.7 vs. 3.0 MPa). Cushion gas requirements drop rapidly after the first couple of cycles.

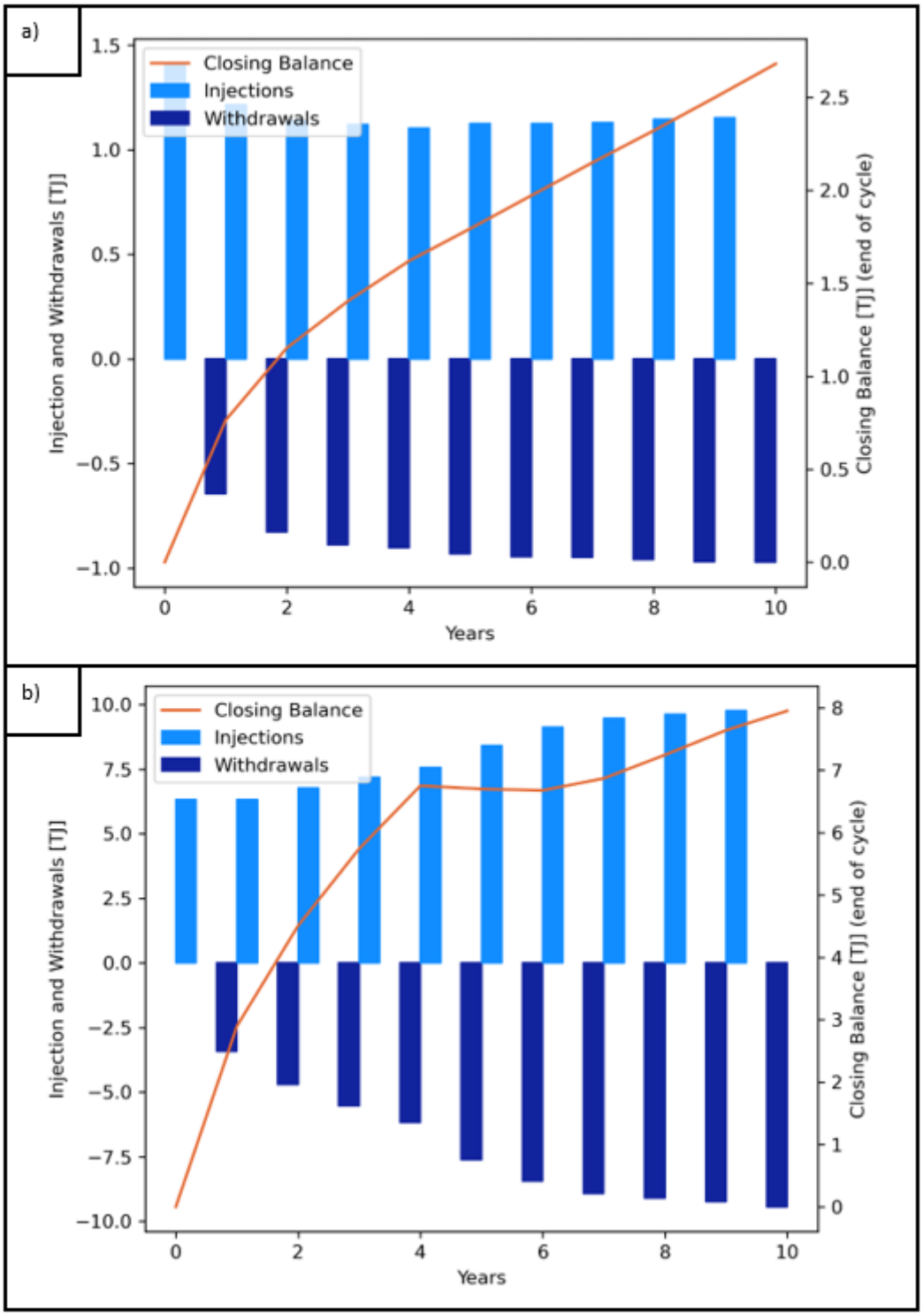

Figure 7: Injection and withdrawal volumes for Ahuroa saline aquifer. End-member a) low and b) high permeability simulations, 10 and 100 mD, respectively. Orange line tracks total gas in the reservoir.

6.3.3. McKee: depleted reservoir

The McKee Field is the largest producing onshore oil field in New Zealand and is reaching depletion having produced over 47 million barrels of oil and 19 PJ of gas. The field is known to have repurposed the McKee-3A well for reinjection of produced gas, reinjecting over 314 million Nm^3 (31.4 TJ) of natural gas by the end of 2011. The McKee-3A well has an along-hole

depth of approximately 1900m below sea level and penetrates the McKee A1 sand – further details can be found in Sections 4.2.2 & 5.1.3.

Review of site-specific conditions

We have used the McKee-3A well (Palmer & Beardman, 1983) as an example to develop a hypothetical storage scenario. This well has perforations over a 50 m interval within a 90 m gross formation. Compiled porosity data for this formation (Appendix Table A.2. 4, Appendix Figure A.2) suggest a mid-range value of ~17%. As with previous scenarios, an indicative permeability range is used to bound the principal uncertainty, in this case 50 to 300 mD (Figure 23).

Rickard (2000) report that, by 2000, reservoir pressure had declined from an initial value of 23.6 MPa to 13.8 MPa. In situ temperatures are reported to be about 80°C.

Dynamic storage and transfer assessment

Transfer rates of hydrogen into and out of storage, cushion gas requirements, and total storage volume, are assessed using a numerical reservoir (dynamic) model. Similar to the scenarios above, the assumed geometry is a 3° dipping anticline with azimuthal symmetry. The reservoir unit has a maximum thickness of 50 m at the crest of the anticline. The crest is fully penetrated by the injection/production well assumed to have a radius of 0.1 m at the reservoir depth. Based on reported values in Rickard (2000), we have taken the midpoint operating pressure as half the historic field decline at 2000 (18.7 MPa) and assumed a swing pressure of ±5 MPa.

After 10 years, working gas injection and production into the reservoir ranges between 300 and 850 TJ (2.5 and 7.1 kt) over the 4-month extraction phase, depending on permeability. Corresponding daily average flow rates are 2.5 to 7.0 TJ/d (21 to 58 t/d). The cushion gas percentage is low (50%) compared to other scenarios and drops with subsequent cycles.

The hydrogen plume extends up to 500 m away from the injection well after 10 years (Figure 23). It is well contained by the structural trap and is efficiently extracted during withdrawal except for a residual hydrogen fraction that remains trapped.

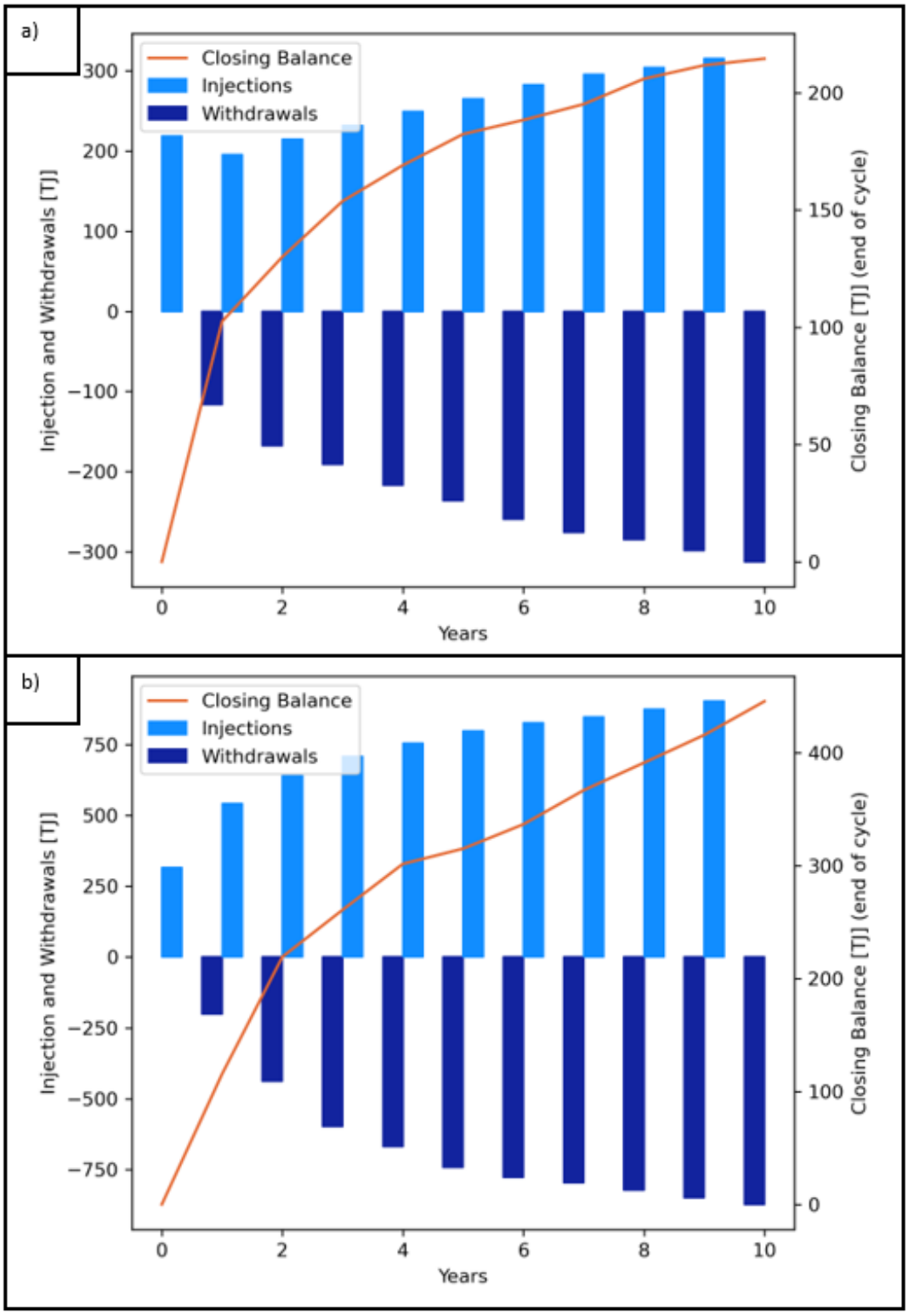

Figure 8: Injection and withdrawal volumes for McKee formation. End-member a) low and b) high permeability simulations, 50 and 300 mD, respectively. Orange line tracks total gas in the reservoir.

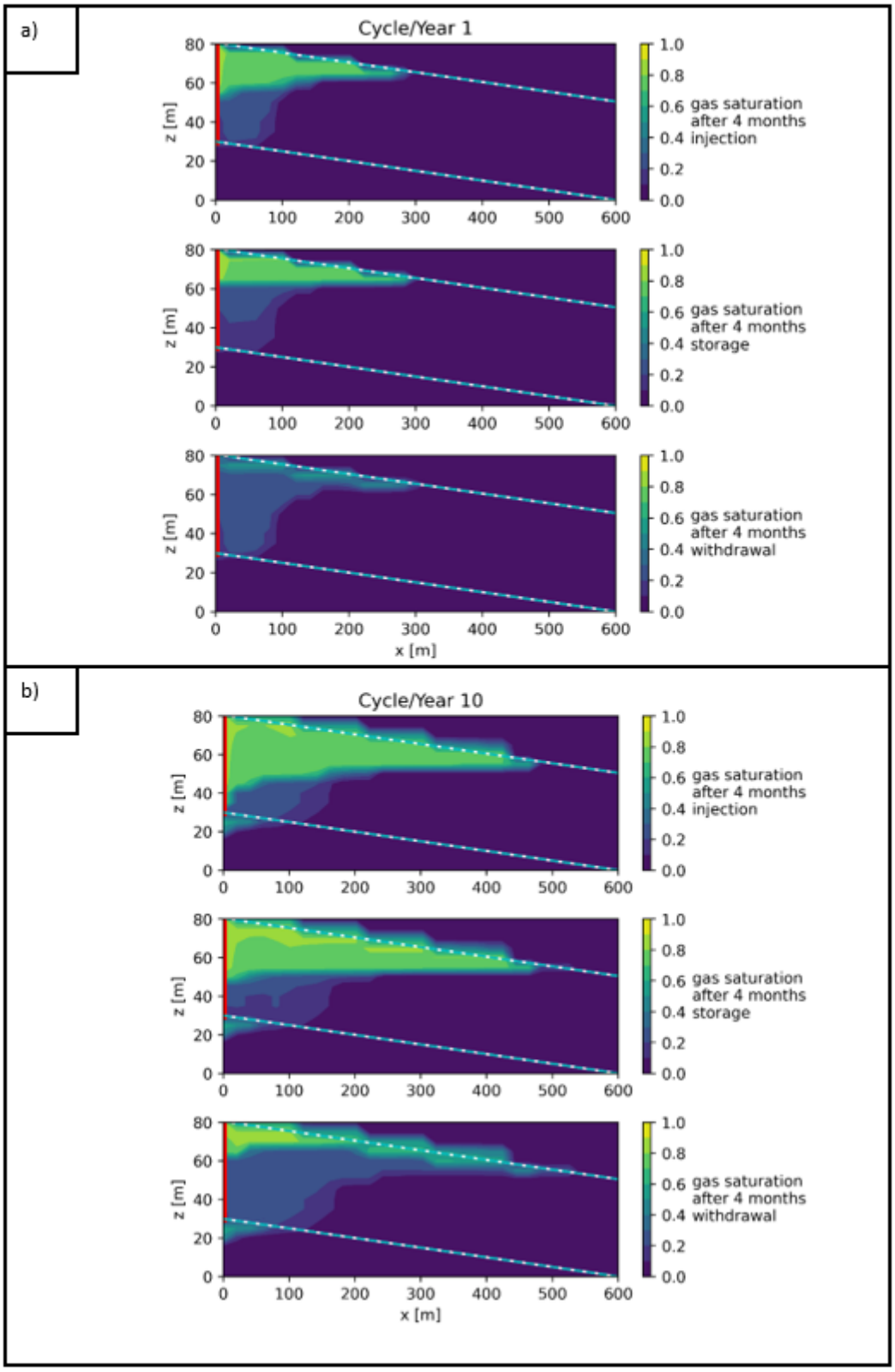

Figure 9: Simulated plume development during (top) first and (bottom) final year/cycle for McKee high storage scenario. Three stacked plots show gas saturation at the end of injection, storage and withdrawal. Dashed line shows position of anticline, red line shows injection well.

6.4. Summary of prospects

Of the three scenarios for which a dynamic modelling assessment has been performed, the McKee and Rimu scenarios indicated storage in the 100's of TJ range for individual wells (Table 9). Fields developed with multiple wells would have larger capacity. The McKee scenario was rated highest for storage due to its relatively higher permeability and ability to operate at a higher pressure range. These volumes are equivalent to hundreds of thousands of surface tanks, and comfortably exceed other surface storage options (Table 10).

It is worth noting that dynamic (annual) storage on the order of 100's of TJ is similar to the ~600-770 TJ of hydrogen that could potentially be generated by a Waipipi windspill scenario detailed in 6.3.1.

Static modelling assessments for Ahuroa and Rimu (Tariki formation) suggest storage in the 1000's of TJ range. This is tens of times larger than advanced surface (cryogenic) and cavern storage options (Table 10). Burial depth and mineralogy are both more favourable for UHS for the Ahuroa site than the Rimu site.

Rimu and McKee hydrogen transfer rates range between 0.45 and 7.0 TJ/d. This is considerably below an equivalent hydrogen transfer rate estimated for Ahuroa gas storage (18 to 33 TJ/d), which itself is less than the current estimated performance with natural gas (65 TJ/d).

The Ahuroa U20 sand has unremarkable performance compared to the other sites, owing to its narrow width, shallow depth (low pressure and density) and limited pressure operating range. Storage volumes of 0.9 to 9 are comparable or lower than existing surface technology (cryogenic storage, artificial caverns, linepack; Table 2; Table 10). The low temperatures may also be problematic with regard with microbial interactions. Cap rock integrity is untested.

With these hypothetical modelling exercises, there is always some uncertainty due to assumed homogeneity. We have estimated some of the uncertainty by assigning high and low estimates of permeability and developing models accordingly. Similarly, there is uncertainty about the effective thickness of reservoir units away from where they are intersected by the borehole. For this parameter, a first-order correction to the model results presented in Table 9 can be obtained through rescaling by a thickness ratio. For example, if the effective thickness at Rimu-A1 was actually 40 m, 73% of the modelled value (55 m), then the associated storage volume and transfer rates would also be approximately half (40 to 210 TJ, and 0.33 to 1.7 TJ/d).

Table 9: Summary of static and dynamic storage assessments of four sites in Taranaki.

Scenario	Depth [km]	Temp. [°C]	Thick. [m]	Poro. [%]	Perm. [mD]	Pressure [MPa]	Storage volume [TJ]	Transfer rate [TJ/d]
Rimu-A1	3.6	120	55	15	10 to 50	±3.0	1100* 55 to 290†	0.45 to 2.4
Ahuroa Tariki	2.3	82	-	-	-	-	4900*	18 to 33
Ahuroa U20 Sand	1.0	44	7	20	10 to 100	±1.7	0.9 to 9†	0.007 to 0.07
McKee	2.3	80	50	17	50 to 300	±4.9	300 to 850†	2.5 to 7.0
*Static model. †Dynamic model, production volume in cycle 10.								

Table 10: Comparison of UHS scenarios with surface and cavern technology. Equivalent counts for alternate storage technologies use high estimates given in Table 2.

Scenario	Storage [TJ]	Equivalent count of surface storage technology			
		High-pressure tank (0.0012 TJ)	Cryogenic tank (84 TJ)	Linepack (81 TJ)	Vertical Shafts (32 TJ)
Rimu (static)	1100	920 000	13	14	34
Rimu (dyn.)	290	240 000	3.5	4	9
Ahuroa Tariki	4900	4 000 000	58	60	150
Ahuroa U20 Sand	9	7500	0.11	0.11	0.28
McKee	850	710 000	10	10	27

7. Monitoring and hazards

Monitoring is highly recommended to support the effective management of hydrogen stored in the subsurface (Ennis-King et al., 2021; Gombert et al., 2021; Zivar et al., 2020). Monitoring ensures that; i) engineering infrastructure (e.g., wells and pipelines) and reservoir performance are within specifications, ii) injected hydrogen remains within the storage container, iii) extracted hydrogen gas is not contaminated and, iv) the injected hydrogen does not adversely modify the rocks, adjacent water aquifers or surface environments (Deng et al., 2017). The scope and methods for monitoring hydrogen stored in the subsurface will be set

by operators and regulators based on operational requirements and the acceptable levels of risk. The challenge is to develop a monitoring framework that is practical, with a balance maintained between data acquisition (and the stakeholder assurance that arises from these data) and cost. Not all of the monitoring techniques discussed here are to be employed at each site. Which technique(s) should be used will depend on economics, viability (e.g., offshore sites) and risks, driven by regulations and the type of information that is required when monitoring storage.

To-date there are no regulations on how UHS should be monitored. Nonetheless, there is extensive literature for monitoring UGS (Moratto et al., 2019; Priolo et al., 2015), oil and gas depletion and carbon dioxide (CO_2) geosequestration. Compared to methane and CO_2, hydrogen has a low density, is relatively mobile and in some cases may produce organic and inorganic reactions in rocks. Hydrogen stored in the subsurface could be monitored via; i) atmospheric emissions, ii) monitoring wells or iii) indirect geophysical methods. The next sections (7.1, 7.2 & 7.3) discuss each of these monitoring techniques. There is a particular focus on wells which are the most widely used technique for monitoring sub-surface gases. We also briefly discuss volcanic and seismic hazards that could impact hydrogen storage sites in Taranaki (section 7.4).

7.1. Atmospheric monitoring

Atmospheric emission of hydrogen could be monitored at scales of metres (e.g., wells) to several kilometres (Leuning et al., 2008). Still, atmospheric monitoring techniques require more research as it is unknown how hydrogen reacts with mineral and microbes and how the end products of these reactions contribute to natural leakage from a reservoir (Leuning et al., 2008). Hydrogen may be rapidly consumed by subsurface microbes resulting in only a portion of the hydrogen leakage being released to the atmosphere. Lastly, leaked H_2 has short-term residence times in the atmosphere and can mix or interact with atmospheric gasses, complicating atmospheric monitoring (Zgonnik, 2020). Moreover, atmospheric monitoring developments are based on geosequestration of CO_2 and it is unknown how applicable it is to hydrogen. Therefore, monitoring of atmospheric hydrogen is not presently considered a practical means of assessing surface leakage of hydrogen from the underground storage container. However, it may have a role to play in detecting leaks from surface pipelines and facilities.

7.2. Well monitoring

Monitoring wells have particular relevance for onshore sites and are presently the preferred method for monitoring UGS operations (Figure 25). The standard in UGS is to use wells to monitor and history match reservoir pressure performance, and to use down-dip wells to observe gas movement to ensure that it does not approach the spill point (Deng et al., 2017; Ennis-King et al., 2021). Wells are also routinely used to record subsurface changes in properties such as temperature and chemistry in UGS, oil and gas depletion and carbon dioxide (CO_2) geosequestration (Deng et al., 2017; Freifeld et al., 2009; Furre et al., 2017). Repurposed or new monitoring wells enable collection of both direct sampling of the reservoir and indirect characterisation of the subsurface using geophysical techniques. Monitoring of well performance is considered part of the engineering operations and is not addressed here.

The primary purpose of wells in UHS would be to; i) verify the location of the stored hydrogen and associated 'cushion gas' (Nogues et al., 2011; Zivar et al., 2020), ii) confirm that hydrogen is not migrating from the reservoir into overlying aquifers and, iii) test that the chemistry of the reservoir and overlying aquifers does not change beyond pre-defined bounds due to the presence of hydrogen. Tracers (i.e., chemical compounds) injected into the reservoir with the hydrogen could be used to identify leakage, as they are in CO_2 pilot projects and gas storage facilities (Erol et al., 2022). Such quantitative chemical data on the location of stored hydrogen is commonly supported by mass balance calculations and numerical reservoir modelling.

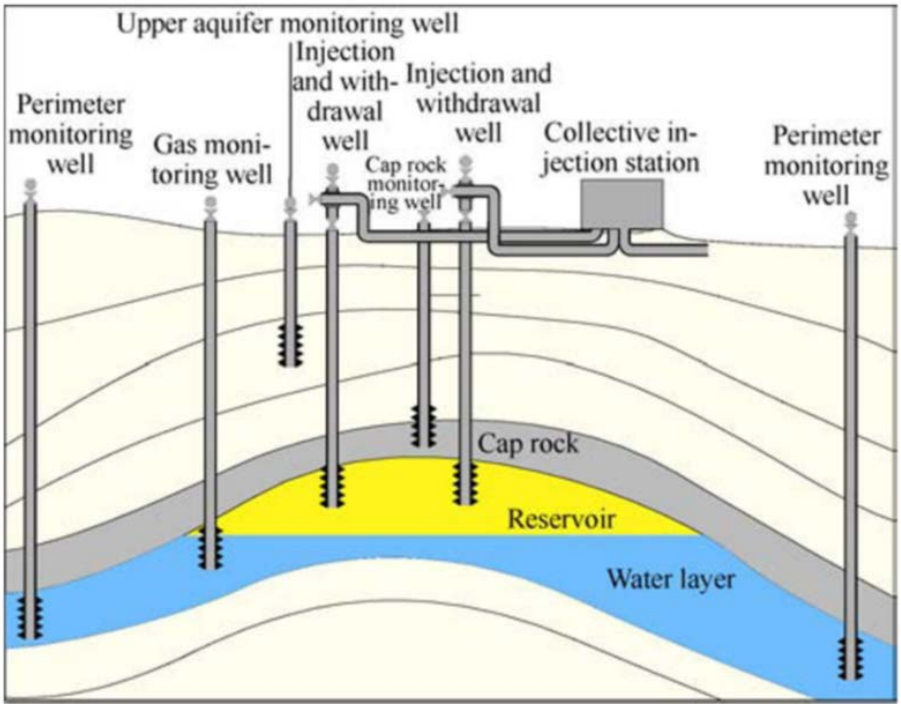

Figure 25: Schematic diagram showing potential monitoring wells for a cap rock and reservoir system at the crest of an anticline. The diagram shows both injection/withdrawal and monitoring wells. Refer to the text for further discussion of perimeter monitoring wells. Figure from Deng et al. (2017).

Monitoring wells also provide information about the chemistry of the fluids in the reservoir and their potential contamination. For the most promising Taranaki sandstones (described in Sections 4.4 & 4.5), hydrogen-rock chemical interactions are not expected to produce significant contamination of injected hydrogen (see Section 4.4). This is still untested but can be confirmed via laboratory experiments or by testing the chemistry of reservoir fluids prior to, during, and after hydrogen withdrawal. For reservoirs in depleted reservoirs, contamination of injected hydrogen with residual hydrocarbons could be discounted with in-well sampling and chemical analysis (Lord et al., 2014; Tarkowski, 2019). Microbial activity is unknown and should be tested with experimental data and in-situ sampling of fluids and microbes (Zgonnik, 2020; Zivar et al., 2020). Understanding the levels of possible hydrogen contamination will inform the processing requirements for withdrawn hydrogen.

Key to avoiding unexpected containment issues will be maintaining cap rock integrity (Figure 26), which could be compromised if reservoir and cap rock pressures are permitted to exceed the tensile strength of these rocks, resulting in the formation of fractures. Downhole pressure

and temperature gauges in wells provide real-time data that can be used to maintain acceptable reservoir pressures and temperatures, as well as input for calibrating predictive reservoir models (Teatini et al., 2011; Tenthorey et al., 2011).

7.3. Geophysical monitoring

Geophysical techniques offer indirect measurements of the stored hydrogen and are less invasive than drilling wells, although some geophysics requires downhole deployment of geophysical tools. These tools are developed and have been used for decades. Therefore they are ready to be deployed under a hydrogen geostorage scenario, provided some initial feasibility studies (numerical studies) to design their deployment and imaging resolution. They can be used to locate and track the movement of stored hydrogen, as well as changes in pressure in the storage unit. Figure 28 and Appendix Table A5.1 summarize well- and surface-based geophysics, although it is important to understand that a method(s) is selected from this list, no all methods are deployed to monitor a site.

Any fracturing of the reservoir and cap rocks can be monitored using downhole seismometers, which enable the locations and magnitudes of small earthquakes (M_w<2) to be determined. Microseismicity is a common response to fluid injection into wells and has been widely documented since the 1980s, without causing operational issues (Allis et al., 1985; Jiang et al., 2021). Microseismic activity is caused by rapid changes of stress during fluid injection and withdrawal cycles, providing a basis for assessing the risk of cap rock failure and for changing injection or withdrawal rates to avoid ongoing seismicity, including larger earthquakes (e.g., M_w>3) that could trigger public alarm (Grigoli et al., 2017; Hsieh & Bredehoeft, 1981; Nicol et al., 2011). Subsurface rock deformation can also be modelled using uplift or subsidence of the ground surface at the storage site recorded by a range of satellite-based techniques, including InSAR (Yang et al., 2015) and permanent GPS stations.

Hydrogen injected into a rock saturated with brine or petroleum (reservoir) changes the physical properties of the fluids (e.g., density), which in turn changes the geophysical properties of the rock (e.g., acoustic wave speed, electrical conductivity). The ability to detect these changes with geophysical methods depends on the contrast of the physical and geophysical properties in the original rocks (before injection) to those after injection of hydrogen. In addition, changes in the *in-situ* pressure and temperature due to injection can influence the geophysical properties. Given the requirement that injected hydrogen change rock properties to be routinely detected using geophysical techniques, these methods are likely to be of most value in aquifers during the first cycles of hydrogen injection. Present understanding and regulations suggests that geophysical techniques may be of less value when storing hydrogen in depleted gas reservoirs.

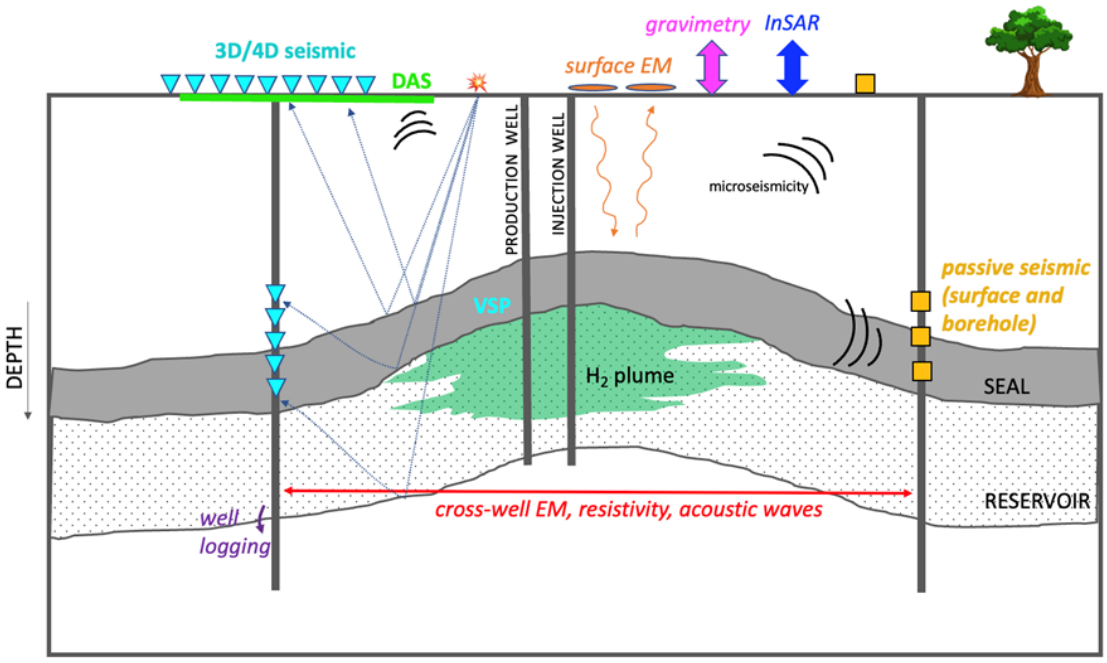

Figure 10: Schematic summarizing geophysical borehole and surface methods able to monitor the hydrogen plume. For details on the methods please refer to Table A5.1.

Taranaki sandstones are saturated with water and injecting hydrogen would result is significant differences in the physical and geophysical properties of these rocks before and after injection. Because hydrogen has lower density, acoustic wave speed and higher resistivity than that of water, all methods shown in Figure 26 and Table A5.1 would be sensitive to imaging the hydrogen plume and its movement. Deciding on which method to use would depend on; i) levels of risk when injecting, ii) desired vertical and lateral resolution, iii) cost and, iv) access to boreholes or surface deployment. Cost-effective methods are borehole or DAS sensors to monitor microseismicity. However, neither of these techniques will provide a clear image of the plume. For plume imaging over time, 4D seismic reflection surveys on the surface or VSP are ideal. Before deciding on a geophysical method, a feasibility study to understand the sensitivity of the method to imaging the hydrogen plume is recommended. This commonly involves numerical modelling of the acquisition parameters, geology and physical/geophysical properties (Sim & Adam, 2016).

7.4. Geological hazards

The monitoring methods outlined above mainly focus on mitigating potential risks in the reservoir or primary container. Risks and hazards from outside the storage container could also disrupt hydrogen storage projects, including a wide range of economic, social, political and engineering issues. For example, in many countries, including New Zealand, past experiences of large engineering projects suggest that gaining public support and navigating through legislative processes are likely to be important for UHS implementation in Taranaki. In addition to these factors a number of geological hazards should be considered. In Taranaki, volcanic eruptions from Mt Taranaki and the central North Island and earthquakes could disrupt hydrogen storage operations.

Volcanic hazards are higher in Taranaki than in other parts of New Zealand due to the presence of Mount Taranaki (Turner et al., 2008). This volcano has not experienced a significant eruption since written historical written records began in 1840. The impact of future volcanic eruptions on hydrogen storage projects is likely to be dominated by volcanic ash, however, lahars are also possible. The volume of ash and associated volcanic hazards are likely to be dependent on a range of factors including, the size and duration of the eruption, proximity of the storage facility to the volcanic cone, wind direction and the magnitude of earthquakes that accompany the eruption.

Seismic hazards are low in Taranaki compared to the central, eastern and southern North Island of New Zealand (Stirling et al., 2012). Although there have been no known large-magnitude earthquakes ($M_w > 6$) in the Taranaki region since 1840, the prehistoric record indicates that many such events have occurred in the last 10,000 years (e.g., Townsend et al., 2010). Large magnitude earthquakes are likely to affect most parts of New Zealand (including Taranaki) in the next 50-100 years (i.e., the time interval typically considered relevant for seismic hazard analysis of infrastructure projects in New Zealand). The potential impact of these earthquakes on hydrogen storage will depend on the individual storage site and its proximity to the earthquake epicentre. Migration of fluids to the ground surface following historical large magnitude earthquakes has been observed in many parts of the world (Noir et al., 1997; Yamamoto & Koide, 2006). By contrast, a M_w 6.8 earthquake in Japan located within 20 km of a Carbon Capture and Storage pilot project created no detectable damage to, or leakage from, the storage reservoir (Shimada, 2006).

Given the available data, improved understanding of earthquake and volcanic hazards at hydrogen storage sites in Taranaki would be prudent. In addition to 'natural' earthquakes fluid-injection could induce earthquakes large enough to cause damage (Majer et al., 2007; Nicol et al., 2011). The maximum size of these earthquakes appears to be associated with the volume of fluid injected (McGarr, 2014), while the rates of seismicity often increase with rising reservoir pressure (e.g., Dempsey & Riffault, 2019). There may be value in establishing plans for managing reservoir conditions to avoid triggering earthquakes during hydrogen injection or withdrawal. Hydrogen storage in depleted reservoirs is less likely (than green fields sites) to induce seismicity as fluid extraction often reduces pressures in the reservoir.

8. Future work

8.1. Appraisal methodology

Future commercial decisions to develop UHS must understand uncertainties to determine the suitability of prospective candidate sites and to constrain risks within acceptable ranges. Depleted reservoirs have the advantage of proven containment, existing characterization of reservoir properties that control storage volume and transfer rates, and knowledge of pressure conditions within which the facility can be safely operated. However, no more than a handful of Taranaki's variably-depleted fields are likely to be compelling candidates for conversion to storage (natural gas, hydrogen, or blends). UHS prospects in contained aquifer formations may rank more favourably for such reasons as synergy of location with hydrogen infrastructure as a whole – renewable electricity generation, the gas pipeline network, major

industrial users of hydrogen as either feedstock or energy, or peaking electricity generation with green hydrogen as thermal fuel.

Exploration and appraisal of UHS prospects in contained aquifers will require substantial investment to prove their viability, case by case. Drawing on the workflows and technologies that are applied to exploration and appraisal for oil and gas, the appraisal of such prospects will need to address:

- Target reservoir formation
    - Depth range
    - Thickness range
    - Characteristics affecting fluid distribution, e.g., fabric (internal bedding and lamination, heterogeneity etc.)
    - Porosity and permeability range
    - Mineralogy
    - Pore fluid(s), e.g., salinity, hydrocarbon and CO_2
- Cap rock
    - Capillary entry pressure
    - Mineralogy
    - Lateral continuity and homogeneity
    - Possible defects, e.g., local absence within the area of closure
- Containment
    - Structure at the top of the reservoir level
    - Spill points
    - Fault offsets
    - Intraformational barriers (stratigraphic containment)
    - Compartmentalisation
- Other risks requiring assurance
    - Microbial processes
    - Geochemical – mineral reactions, fluid mixing
    - Geomechanical, e.g., induced seismicity, ground subsidence/inflation.

These factors would be assessed in the first instance by desktop study to compile existing regional and local knowledge, from which key gaps specific to any prospect case would be identified. Further investigation might involve geophysical surveys, such as seismic lines or 3D seismic to map inferred structural closure in the required detail.

Ultimately, it is likely that an exploratory well would be required to establish unequivocally the presence and key characteristics of the target reservoir and cap rock, and to provide for detailed in-situ evaluation. In some situations, more than one well may be necessary to most effectively appraise a prospect. Ennis-King et al. (2021) adapt a proposed management system for CO_2 storage (itself adapted from the Petroleum Resource Management System of the Society of Petroleum Engineers) to UHS (Figure 27).

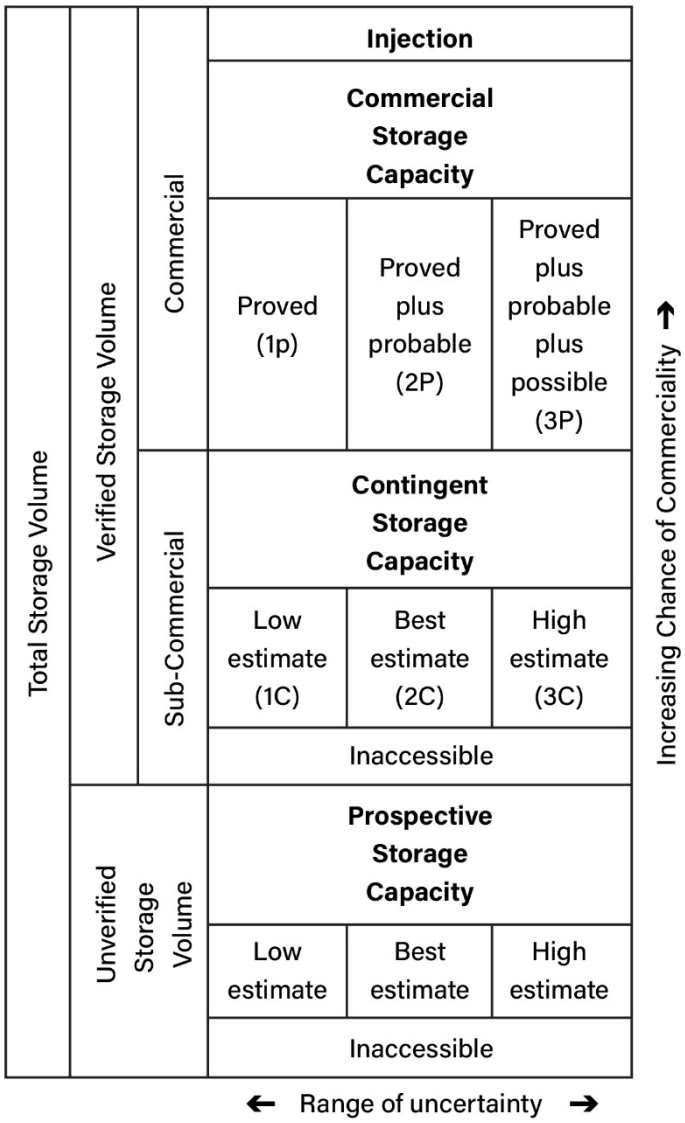

Figure 11: UHS Resource Management System, from Michael et al. (2021), adapted from SPE Petroleum Resource Management System and Allinson et al. (2014).

The purpose of appraisal investment is to allow an opportunity to be moved from the "Prospective" category towards commerciality.

8.2. Research directions

As a technology, UHS in depleted reservoirs and aquifers is at an early stage. Research to date has considered the storage concept (Heinemann, Alcalde, et al., 2021; Zivar et al., 2020), site inventories (e.g., Ennis-King et al., 2021; Scafidi et al., 2021), numerical modelling (e.g., Feldmann et al., 2016; Heinemann et al., 2021), geochemical (e.g., Hassannayebi et al., 2019; Yekta et al., 2018) and microbiological impacts (e.g., Eddaoui et al., 2021).

A common theme amongst these studies is the need for case-by-case evaluation and research tailored to a region or reservoir's particular characteristics. This conclusion applies in New Zealand, where geological and socio-economic conditions differ from other regions of the world. Here, we briefly discuss the geological, geochemical, microbiological, geophysical and

reservoir performance research that will be required to support the implementation of UHS in New Zealand. We do not consider the facilities engineering, social, economic or legislative/ regulatory work required before UHS can proceed.

8.2.1. Underground hydrogen storage prospectivity

UHS prospectivity is required to identify, characterise, model and evaluate the most promising sites for UHS in Taranaki and New Zealand. Future studies should include geological characterisation and preliminary reservoir modelling to support assessment of site prospectivity and decisions about collection of additional data.

Geological characterisation via the collation of existing geological information for some specific sites has commenced with the FirstGas screening study, the site prospectivity study of Yates et al. (2021) and this report. Further work may be required using a multiscale site analysis approach integrating information and reinterpretation from seismic reflection lines, drillhole data, outcrop description, petrography, electronic microscopy (SEM), petrophysics (porosity, permeability, density) and analytical geochemistry (XRF, EDS, cathodoluminescence) to quantify the parameters that determine the quality of reservoirs, cap rocks and structures for target sites. The primary purpose of this work is to construct improved 3D geological models, which define the geometries, lithofacies and interconnectivity of reservoir and cap rocks. These models are essential to inform detailed numerical reservoir modelling and improve estimates of storage system performance.

Surrogate Reservoir Modelling is key for providing estimates of volumes of H_2 storage, injection-discharge rates and optimal field design (e.g., well design and spacing). More detailed 3D reservoir models than presented in this report, will provide the opportunity to refine the quantification of storage system performance presented in this study and provide estimates of reservoir performance from additional sites of interest. In addition, stochastic reservoir modelling could be employed to maximise operational performance by considering existing and proposed well locations for injection and production.

8.2.2. Fluid-Rock chemical interactions

Chemical interactions between reservoir/cap rocks and stored hydrogen have the potential to impact storage operations. The preliminary conclusions of this report are that these reactions may not be significant for most New Zealand rocks over the timeframes for UHS, however, prospect-specific studies would be required to confirm this. In particular, laboratory experiments can be performed to determine reactions between H_2, H_2 gas mixes (e.g., CH_4+CO_2), and their physical-chemical impacts (e.g., contamination of H_2, losses, and changes to reservoir-cap rock porosity-permeability) on rock targets. Experiments should consider a range of temperatures and pressures (e.g., 10-100°C and 10-350 bar), as well as incorporating unsaturated versus fluid-saturated, static versus gas-flow, anaerobic versus aerobic, and organic versus inorganic material to determine reactions under diverse environmental conditions. These studies will help improve understanding of the rates of chemical reactions, which is essential for reducing the uncertainties of chemical models that are expected to inform reservoir selection.

Chemical reactions could also impact the cap rock integrity. Modelling of chemical impacts of H_2 in shallow groundwater can be used to track pH and dissolved H_2 concentrations of plumes in generic groundwater aquifer models, similar to studies performed for carbon sequestration security. These models will provide a means of assessing hydrogen containment efficiency, tracking leaks, and devising mitigation. However, these types of models depend, in some part, on the site-specific relative permeability and capillarity relations. These, too, should be determined through laboratory experiments on target rocks.

Ultimately, this research should focus on evaluating the chemistry so-as-to fully understand the potential behaviour of hydrogen in the sub-surface. Of particular interest will be using the chemistry to inform degradation of injection-storage-withdrawal performance as well as operational losses due to adverse impacts on gas mobility or consumption by chemical reactions.

8.2.3. Microbial activity

The precise impact of microbiota on stored hydrogen remains uncertain. Experimentation and modelling may be required to determine the physicochemical parameters that support microbial communities to grow in target H_2 storage conditions. It may be necessary to determine the rates of these biogeochemical reactions between rock substrates, microorganisms and H_2. These H_2 utilisation rates and interactions with rock substrates can be characterised using hydrogenotrophic strains/consortia from international microbial culture collections (methanogens, SO_4^{2-} reducers, others) or in-situ samples at target sites. The main focus of this work would be to evaluate and minimise operational losses due to in-situ bio-methanation during long-term storage and to minimise decreases in reservoir performance due to microbiological activity.

8.2.4. Monitoring and hazards

The regulatory and operational requirements for monitoring of stored hydrogen have not been addressed in this report and the extent to which safe storage should be demonstrated prior to commercial operations commencing remains uncertain. To this end, consideration could be given to incorporating tests of well and geophysical monitoring methodologies. For, example at present, it is not clear what value geophysical techniques will add to standard well monitoring techniques. In addition, the anticipated low rates of induced seismicity for H_2 storage at depleted reservoirs sites could be demonstrated by a pilot seismic network at the operational natural gas injection/production Ahuroa Gas Storage site.

9. References

Allinson, W. G., Cinar, Y., Neal, P. R., Kaldi, J., & Paterson, L. (2014). CO2-Storage Capacity—Combining Geology, Engineering and Economics. *SPE Economics & Management*, *6*(01), 15–27.

Allis, R. G., Currie, S. A., Leaver, J. D., & Sherburn, S. (1985). Results of injection testing at Wairakei geothermal field, New Zealand. *Trans. GRC*, 289–294.

Amid, A., Mignard, D., & Wilkinson, M. (2016). Seasonal storage of hydrogen in a depleted natural gas reservoir—ScienceDirect. *International Journal of Hydrogen Energy*, *41*(12), 5549–5558.

Andersson, J., & Grönkvist, S. (2019). Large-scale storage of hydrogen. *International Journal of Hydrogen Energy*, *44*(23), 11901–11919.

Ardent underground storage. (n.d.). Ardent Underground. Retrieved 1 February 2022, from https://ardentunderground.com/

Armstrong, P. A., Chapman, D. S., Funnell, R. H., Allis, R. G., & Kamp, P. J. (1996). Thermal modeling and hydrocarbon generation in an active-margin basin: Taranaki Basin, New Zealand. *AAPG Bulletin*, *80*(8), 1216–1241.

Balasooriya, W., Clute, C., Schrittesser, B., & Pinter, G. (2021). A review on applicability, limitations, and improvements of polymeric materials in high-pressure hydrogen gas atmospheres. *Polymer Reviews*, 1–36.

Beggs, M., & Nicol, A. (2020). Petroleum Exploration and Production in North Canterbury. *Geoscience Society of New Zealand Post-Conference Field Trip Guide*, 22.

Berta, M., Dethlefsen, F., Ebert, M., Schäfer, D., & Dahmke, A. (2018). Geochemical effects of millimolar hydrogen concentrations in groundwater: An experimental study in the context of subsurface hydrogen storage. *Environmental Science & Technology*, *52*(8), 4937–4949.

Bischoff, A., Adam, L., Dempsey, D., Nicol, A., Beggs, M., Rowe, M. C., Bromfield, K., Stott, M., & Villeneuve, M. (2021, April 19). Underground hydrogen storage in sedimentary and volcanic rock reservoirs: Foundational research and future challenges for New Zealand. *EGU General Assembly 2021*. EGU21, online. https://doi.org/10.5194/egusphere-egu21-3496

Bo, Z., Zeng, L., Chen, Y., & Xie, Q. (2021). Geochemical reactions-induced hydrogen loss during underground hydrogen storage in sandstone reservoirs. *International Journal of Hydrogen Energy*, *46*(38), 19998–20009.

Boersheim, E. C., Reitenbach, V., Albrecht, D., Pudlo, D., & Ganzer, L. (2019). Experimental investigation of integrity issues of UGS containing Hydrogen. *SPE Europec Featured at 81st EAGE Conference and Exhibition*.

Bruno, M. S., Dusseault, M. B., Balaa, T. T., & Barrera, J. A. (1998). Geomechanical analysis of pressure limits for gas storage reservoirs. *International Journal of Rock Mechanics and Mining Sciences*, *35*(4–5), 569–571.

Buzek, F., Onderka, V., Vančura, P., & Wolf, I. (1994). Carbon isotope study of methane production in a town gas storage reservoir. *Fuel*, *73*(5), 747–752.

Carden, P. O., & Paterson, Ljij. (1979). Physical, chemical and energy aspects of underground hydrogen storage. *International Journal of Hydrogen Energy*, *4*(6), 559–569.

CCC. (2021). *Nāia tonu nei: A low emissions future for Aotearoa.* He Pou a Rangi: Climate Change Comission.

Concept. (2019a). *Hydrogen in New Zealand Report 1—Summary*. Concept Consulting Group Ltd.

Concept. (2019b). *Hydrogen in New Zealand Report 2—Analysis*. Concept Consulting Group Ltd.

Concept. (2019c). *Hydrogen in New Zealand Report 3—Research*. Concept Consulting Group Ltd.

Contact, & Meridian. (2021). *The New Zealand hydrogen opportunity*. https://www.datocms-assets.com/49051/1626295071-the-nz-hydrogen-opportunity.pdf

Core Lab. (2003). *Reservoir performance assessment of the Tariki, Kauri, and Manutahi Sandstones, Rimu-Kauri Field, New Zealand* [NZP&M Petroleum Report 2787].

Darby, D. (2002). Seal properties, overpressure and stress in the Taranaki and East Coast Basins, New Zealand. *2002 New Zealand Petroleum Conference Proceedings*, 24–27.

Dash, Z. V., Robinson, B. A., Pawar, R. J., & Chu, S. (2015). *Software Validation Report for the FEHM Application Version 3.1-3*. Citeseer. https://www.lanl.gov/orgs/ees/fehm/docs/FEHM_VERIFICATION_V3.3.0.pdf

De Bock, J. F., Palmer, J. A., & Lock, R. G. (1990). Tariki Sandstone-early Oligocene hydrocarbon reservoir, eastern Taranaki, New Zealand. *1989 New Zealand Oil Conference Proceedings*, 214–224.

De Lucia, M., Pilz, P., Liebscher, A., & Kühn, M. (2015). Measurements of H2 solubility in saline solutions under reservoir conditions: Preliminary results from project H2STORE. *Energy Procedia*, *76*, 487–494.

Dempsey, D., Kelkar, S., Pawar, R., Keating, E., & Coblentz, D. (2014). Modeling caprock bending stresses and their potential for induced seismicity during CO2 injection. *International Journal of Greenhouse Gas Control*, *22*, 223–236.

Dempsey, D., & Riffault, J. (2019). Response of induced seismicity to injection rate reduction: Models of delay, decay, quiescence, recovery, and Oklahoma. *Water Resources Research*, *55*(1), 656–681.

Deng, H., Bielicki, J. M., Oppenheimer, M., Fitts, J. P., & Peters, C. A. (2017). Leakage risks of geologic CO2 storage and the impacts on the global energy system and climate change mitigation. *Climatic Change*, *144*(2), 151–163.

Dwivedi, S. K., & Vishwakarma, M. (2018). Hydrogen embrittlement in different materials: A review. *International Journal of Hydrogen Energy*, *43*(46), 21603–21616.

Eddaoui, N., Panfilov, M., Ganzer, L., & Hagemann, B. (2021). Impact of Pore Clogging by Bacteria on Underground Hydrogen Storage. *Transport in Porous Media*, *139*(1), 89–108.

Ennis-King, J., Michael, K., Strand, J., Sander, R., & Green, C. (2021). *Underground storage of hydrogen: Mapping out the options for Australia* (No. RP1-1.04). Future Fuels CRC.

Erol, S., Bayer, P., Akın, T., & Akın, S. (2022). Advanced workflow for multi-well tracer test analysis in a geothermal reservoir. *Geothermics*, *101*, 102375.

Feldmann, F., Hagemann, B., Ganzer, L., & Panfilov, M. (2016). Numerical simulation of hydrodynamic and gas mixing processes in underground hydrogen storages. *Environmental Earth Sciences*, *75*(16), 1–15.

Field, B., Lawrence, M., Berthelson, T., Kroeger, K., & Daniel, R. (2011). *Seal Rock Properties, Taranaki Basin.* (GNS Data Series 10a).

First Gas. (2021). *Bringing Zero Carbon Gas to Aotearoa—Hydrogen Feasibility Study* [Summary Report]. https://gasischanging.co.nz/our-path-to-zero-carbon-gas/hydrogen-trial-results/

FirstGas. (2018, March 1). *Transmission security and reliability: Production outages*. https://www.gasindustry.co.nz/work-programmes/pipeline-security-and-reliability/developing/update-on-security-and-reliability-matters/document/5905

FirstGas. (2020). *Gas Transmission: Asset management plan 2020—Summary document* (No. J003564). https://firstgas.co.nz/wp-content/uploads/J003564-Firstgas-Transmission-AMP-2020-FINAL.pdf

Flesch, S., Pudlo, D., Albrecht, D., Jacob, A., & Enzmann, F. (2018). Hydrogen underground storage—Petrographic and petrophysical variations in reservoir sandstones from laboratory experiments under simulated reservoir conditions. *International Journal of Hydrogen Energy*, *43*(45), 20822–20835.

Folk, R. L., Andrews, P. B., & Lewis, D. W. (1970). Detrital sedimentary rock classification and nomenclature for use in New Zealand. *New Zealand Journal of Geology and Geophysics*, *13*(4), 937–968.

Freifeld, B. M., Daley, T. M., Hovorka, S. D., Henninges, J., Underschultz, J., & Sharma, S. (2009). Recent advances in well-based monitoring of CO2 sequestration. *Energy Procedia*, *1*(1), 2277–2284.

Furre, A.-K., Eiken, O., Alnes, H., Vevatne, J. N., & Kiær, A. F. (2017). 20 years of monitoring CO2-injection at Sleipner. *Energy Procedia*, *114*, 3916–3926.

Gajda, D., & Lutyński, M. (2021). Hydrogen Permeability of Epoxy Composites as Liners in Lined Rock Caverns—Experimental Study. *Applied Sciences*, *11*(9), 3885.

Gas Industry Co. (2021). *Annual Report 2020/2021*. https://www.gasindustry.co.nz/publications/

Gombert, P., Lafortune, S., Pokryszka, Z., Lacroix, E., de Donato, P., & Jozja, N. (2021). Monitoring Scheme for the Detection of Hydrogen Leakage from a Deep Underground Storage. Part 2: Physico-Chemical Impacts of Hydrogen Injection into a Shallow Chalky Aquifer. *Applied Sciences*, *11*(6), 2686.

Gray, V. R., & Macknight, F. J. (1986). The apparent relative density of New Zealand coals. *New Zealand Journal of Geology and Geophysics*, *29*(4), 463–470.

Grigoli, F., Cesca, S., Priolo, E., Rinaldi, A. P., Clinton, J. F., Stabile, T. A., Dost, B., Fernandez, M. G., Wiemer, S., & Dahm, T. (2017). Current challenges in monitoring, discrimination, and management of induced seismicity related to underground industrial activities: A European perspective. *Reviews of Geophysics*, *55*(2), 310–340.

Groenenberg, R., Juez-Larre, J., Goncalvez, C., Wasch, L., Dijkstra, H., Wassing, B., Orlic, B., Brunner, L., van der Valk, K., Hajonides van der Meulen, T., & others. (2020). *Techno-Economic Modelling of Large-Scale Energy Storage Systems*.

GSNZ SPV1. (2020). *Ahuroa B Gas Storage Facility Monitoring Programme Annual Report 2018-2019* (Technical Report 2019-93). Taranaki Regional Council. https://www.trc.govt.nz/assets/Documents/Environment/Monitoring-OGproduction/2019onwards/MR19-AhuroaGasStorage.pdf

Hassannayebi, N., Azizmohammadi, S., De Lucia, M., & Ott, H. (2019). Underground hydrogen storage: Application of geochemical modelling in a case study in the Molasse Basin, Upper Austria. *Environmental Earth Sciences*, *78*(5), 1–13. https://doi.org/10.1007/s12665-019-8184-5

Heinemann, N., Alcalde, J., Miocic, J. M., Hangx, S. J. T., Kallmeyer, J., Ostertag-Henning, C., Hassanpouryouzband, A., Thaysen, E. M., Strobel, G. J., Schmidt-Hattenberger, C., Edlmann, K., Wilkinson, M., Bentham, M., Haszeldine, R. S., Carbonell, R., & Rudloff, A. (2021). Enabling large-scale hydrogen storage in porous media – the scientific challenges. *Energy & Environmental Science*, *14*(2), 853–864. https://doi.org/10.1039/D0EE03536J

Heinemann, N., Scafidi, J., Pickup, G., Thaysen, E., Hassanpouryouzband, A., Wilkinson, M., Satterley, A., Booth, M., Edlmann, K., & Haszeldine, R. (2021). Hydrogen storage in saline aquifers: The role of cushion gas for injection and production. *International Journal of Hydrogen Energy*, *46*(79), 39284–39296.

Hemme, C., & Van Berk, W. (2018). Hydrogeochemical modeling to identify potential risks of underground hydrogen storage in depleted gas fields. *Applied Sciences*, *8*(11), 2282.

Henkel, S., Pudlo, D., Werner, L., Enzmann, F., Reitenbach, V., Albrecht, D., Würdemann, H., Heister, K., Ganzer, L., & Gaupp, R. (2014). Mineral reactions in the geological underground induced by H2 and CO2 injections. *Energy Procedia*, *63*, 8026–8035.

Higgs, K. E. (2007). *Reservoir and seal rock studies: Te Kiri-2* (Appendix 21 in NZP&M Petroleum Report 3635).

Higgs, K. E. (2012). *Mineralogical study of the Tariki Sadstone, PEP 51155 and adjacent areas, Onshore Taranaki* (NZP&M Petroleum Report PR4670). New Zealand Petroleum and Minerals.

Higgs, K. E., Browne, G. H., & Pollock, R. (2005). *Mudstone database, eastern margin, Taranaki Basin*. Institute of Geological & Nuclear Sciences.

Higgs, K. E., & Crundwell, M. P. (2008). *Seal rock studies, Mangamingi-1* (NZP&M Petroleum Report 3964).

Higgs, K. E., Strogen, D., Griffin, A., Ilg, B., & Arnot, M. (2012). Reservoirs of the Taranaki Basin, New Zealand. *GNS Science Data Series*, *2012/13a*.

Holm, T., Borsboom-Hanson, T., Herrera, O. E., & Mérida, W. (2021). Hydrogen costs from water electrolysis at high temperature and pressure. *Energy Conversion and Management*, *237*, 114106.

Hsieh, P. A., & Bredehoeft, J. D. (1981). A reservoir analysis of the Denver earthquakes: A case of induced seismicity. *Journal of Geophysical Research: Solid Earth*, *86*(B2), 903–920.

Huggett, J. M. (1986). An investigation of petrographic controls of poroperm in the McKee Sandstone Member of the Taranaki Basin. *Ministry of Economic Development New Zealand Unpublished Petroleum Report PR*, *1180*.

ICCC. (2019). *Accelerated electrification*. Interim Climate Change Committee. https://www.climatecommission.govt.nz/our-work/advice-to-government-topic/interim-climate-change-committee-reports/

IEA. (2019). The future of hydrogen: Seizing today's opportunities. *IEA Report Prepared for the G20*, 189–191.

Ilg, B. R., Hemmings-Sykes, S., Nicol, A., Baur, J., Fohrmann, M., Funnell, R., & Milner, M. (2012). Normal faults and gas migration in an active plate boundary, southern Taranaki Basin, offshore New Zealand. *AAPG Bulletin*, *96*(9), 1733–1756.

IRENA. (2018). *Hydrogen from renewable power; Technology outlook for the energy transition*. International Renewable Energy Agency (IRENA). https://www.irena.org/publications/2018/sep/hydrogen-from-renewable-power

Ivanova, A., Borzenkov, I., Tarasov, A., Milekhina, E., & Belyaev, S. (2007). A microbiological study of an underground gas storage in the process of gas injection. *Microbiology*, *76*(4), 453–460.

Jaeger, J., Cook, N., & Zimmermann, R. (2007). *Fundamentals of rock mechanics. Blackwell, Oxford*.

Jiang, G., Liu, L., Barbour, A. J., Lu, R., & Yang, H. (2021). Physics-based evaluation of the maximum magnitude of potential earthquakes induced by the Hutubi (China) underground gas storage. *Journal of Geophysical Research: Solid Earth*, *126*(4), e2020JB021379.

Katz, D. L. V., & Coats, K. H. (1968). *Underground storage of fluids*. Ulrich's Books.

King, P., Bland, K., Funnell, R., Archer, R., & Lever, L. (2009). Opportunities for underground geological storage of CO2 in New Zealand-Report CCS-08/5-Onshore Taranaki Basin overview. *GNS Science Report*, *58*.

King, P. R., & Thrasher, G. P. (1996). *Cretaceous-Cenozoic geology and petroleum systems of the Taranaki Basin, New Zealand* (Vol. 2). Institute of Geological & Nuclear Sciences.

Kittinger, F., Pilcher, M., Hassannayebi, N., Lehner, M., & Ott, H. (2017). *Underground Sun Storage* (No. 840705). RAG Austria AG. https://www.underground-sun-storage.at/fileadmin/bilder/SUNSTORAGE/Publikationen/UndergroundSunStorage_Publizierbarer_Endbericht_3.1_web.pdf

Körner, A., Tam, C., Bennett, S., & Gagné, J. (2015). "Technology roadmap-hydrogen and fuel cells." *International Energy Agency (IEA): Paris, France*.

Kruck, O., Crotogino, F., Prelicz, R., & Rudolph, T. (2013). Assessment of the potential, the actors and relevant business cases for large scale and seasonal storage of renewable electricity by hydrogen underground storage in Europe. *KBB Undergr. Technol. GmbH*.

Leuning, R., Etheridge, D., Luhar, A., & Dunse, B. (2008). Atmospheric monitoring and verification technologies for CO2 geosequestration. *International Journal of Greenhouse Gas Control*, *2*(3), 401–414.

Li, H., Zhang, L., Liu, L., & Shabani, A. (2020). Impact of rock mineralogy on reservoir souring: A geochemical modeling study. *Chemical Geology*, *555*, 119811.

Lord, A. S. (2009). *Overview of geologic storage of natural gas with an emphasis on assessing the feasibility of storing hydrogen.* Sandia National Laboratories.

Lord, A. S., Kobos, P. H., & Borns, D. J. (2014). Geologic storage of hydrogen: Scaling up to meet city transportation demands. *International Journal of Hydrogen Energy*, *39*(28), 15570–15582. https://doi.org/10.1016/j.ijhydene.2014.07.121

Louthan Jr, M. R., Caskey Jr, G. R., Donovan, J. A., & Rawl Jr, D. E. (1972). Hydrogen embrittlement of metals. *Materials Science and Engineering*, *10*, 357–368.

Majer, E. L., Baria, R., Stark, M., Oates, S., Bommer, J., Smith, B., & Asanuma, H. (2007). Induced seismicity associated with enhanced geothermal systems. *Geothermics*, *36*(3), 185–222.

Massiot, C., Seebeck, H., Nicol, A., McNamara, D. D., Lawrence, M. J., Griffin, A. G., Thrasher, G. P., O'Brien, G., & Viskovic, G. P. D. (2019). Effects of regional and local stresses on fault slip tendency in the southern Taranaki Basin, New Zealand. *Marine and Petroleum Geology*, *107*, 467–483.

MBIE. (2017). *Energy efficiency and Conservation Strategy 2017-2022*. Ministry of Business, Innovation and Employment. https://www.mbie.govt.nz/building-and-energy/energy-and-natural-resources/energy-strategies-for-new-zealand/

MBIE. (2019). *A vision for hydrogen in New Zealand | Green Paper*. https://www.mbie.govt.nz/building-and-energy/energy-and-natural-resources/energy-strategies-for-new-zealand/a-vision-for-hydrogen-in-new-zealand/

MBIE. (2021). *Gas statistics | Ministry of Business, Innovation & Employment*. https://www.mbie.govt.nz/building-and-energy/energy-and-natural-resources/energy-statistics-and-modelling/energy-statistics/gas-statistics/

McGarr, A. (2014). Maximum magnitude earthquakes induced by fluid injection. *Journal of Geophysical Research: Solid Earth*, *119*(2), 1008–1019.

Mehmeti, A., Angelis-Dimakis, A., Arampatzis, G., McPhail, S. J., & Ulgiati, S. (2018). Life Cycle Assessment and Water Footprint of Hydrogen Production Methods: From Conventional to Emerging Technologies. *Environments*, *5*(2), 24. https://doi.org/10.3390/environments5020024

Michael, K., Ricard, L., Stalker, L., & Hortle, A. (2021). The CSIRO In-Situ Laboratory: A field laboratory for derisking underground gas storage. *The APPEA Journal*, *61*(2), 438–441.

Moratto, L., Romano, M. A., Laurenzano, G., Colombelli, S., Priolo, E., Zollo, A., Saraò, A., & Picozzi, M. (2019). Source parameter analysis of microearthquakes recorded around the underground gas storage in the Montello-Collalto Area (Southeastern Alps, Italy). *Tectonophysics*, *762*, 159–168.

Muzny, C. D., Huber, M. L., & Kazakov, A. F. (2013). Correlation for the viscosity of normal hydrogen obtained from symbolic regression. *Journal of Chemical & Engineering Data*, *58*(4), 969–979.

Namdar, H., Khodapanah, E., & Tabatabaei-Nejad, S. A. (2020). Comparison of base gas replacement using nitrogen, flue gas and air during underground natural gas storage in a depleted gas reservoir. *Energy Sources, Part A: Recovery, Utilization, and Environmental Effects*, *42*(22), 2778–2793. https://doi.org/10.1080/15567036.2019.1618989

New Zealand Herald. (2021a, June 9). *Norske Skog to close Tasman Mill, 160 staf to lose jobs*.

New Zealand Herald. (2021b, August 26). *"August blackout 'an early warning' as Genesis warns Huntly will be needed for a long time*.

Nicol, A., Carne, R., Gerstenberger, M., & Christophersen, A. (2011). Induced seismicity and its implications for CO2 storage risk. *Energy Procedia*, *4*, 3699–3706.

Nogues, J. P., Nordbotten, J. M., & Celia, M. A. (2011). Detecting leakage of brine or CO2 through abandoned wells in a geological sequestration operation using pressure monitoring wells. *Energy Procedia*, *4*, 3620–3627.

Noir, J., Jacques, E., Bekri, S., Adler, P. M., Tapponnier, P., & King, G. C. P. (1997). Fluid flow triggered migration of events in the 1989 Dobi earthquake sequence of Central Afar. *Geophysical Research Letters*, *24*(18), 2335–2338.

NZP&M (2021). *New Zealand Petroleum Occurrences* [Map]. New Zealand Petroleum and Minerals.

OGJ. (2000). *Swift pursues more Taranaki prospects*.

Ozaki, M., Tomura, S., Ohmura, R., & Mori, Y. H. (2014). Comparative study of large-scale hydrogen storage technologies: Is hydrate-based storage at advantage over existing technologies? *International Journal of Hydrogen Energy*, *39*(7), 3327–3341.

Palmer, J. (2021). *Diagenetic clay minerals and fomation damage in deep reservoir targets, onshore Taranaki, New Zealand*. Geological Society of New Zealand Abstracts.

Palmer, J. A., & Beardman, J. (1983). *PR913* (Well Completion Report No. PR913). Ministry of Economic Development.

Panfilov, M., Gravier, G., & Fillacier, S. (2006). Underground storage of H2 and H2-CO2-CH4 mixtures. *ECMOR X-10th European Conference on the Mathematics of Oil Recovery*, cp-23.

Paterson, L. (1983). The implications of fingering in underground hydrogen storage. *International Journal of Hydrogen Energy*, *8*(1), 53–59. https://doi.org/10.1016/0360-3199(83)90035-6

Peaceman, D. W. (1983). Interpretation of well-block pressures in numerical reservoir simulation with nonsquare grid blocks and anisotropic permeability. *Society of Petroleum Engineers Journal*, *23*(03), 531–543.

Perez, A., Perez, E., Dupraz, S., & Bolcich, J. (2016, June 13). Patagonia Wind—Hydrogen Project: Underground Storage and Methanation. *21st World Hydrogen Energy Conference 2016*.

Petch, R. A., & Marshall, T. W. (1988). GROUND WATER RESOURCES OF THE TAURANGA GROUP SEDIMENTS IN THE HAMILTON BASIN, NORTH ISLAND, NEW ZEALAND. *Journal of Hydrology (New Zealand)*, *27*(2), 81–98.

PetroWiki. (2015a, June 3). *Isothermal compressibility of oil*. PetroWiki. https://petrowiki.spe.org/Isothermal_compressibility_of_oil

PetroWiki. (2015b, June 4). *Oil viscosity*. PetroWiki. https://petrowiki.spe.org/Oil_viscosity

Prinzhofer, A., Tahara Cissé, C. S., & Diallo, A. B. (2018). Discovery of a large accumulation of natural hydrogen in Bourakebougou (Mali). *International Journal of Hydrogen Energy*, *43*(42), 19315–19326. https://doi.org/10.1016/j.ijhydene.2018.08.193

Priolo, E., Romanelli, M., Linares, M. P., Garbin, M., Peruzza, L., Romano, M. A., Marotta, P., Bernardi, P., Moratto, L., & Zuliani, D. (2015). Seismic monitoring of an underground natural gas storage facility: The Collalto Seismic Network. *Seismological Research Letters*, *86*(1), 109–123.

Rajabi, M., Ziegler, M., Tingay, M., Heidbach, O., & Reynolds, S. (2016). Contemporary tectonic stress pattern of the Taranaki Basin, New Zealand. *Journal of Geophysical Research: Solid Earth*, *121*(8), 6053–6070.

Reilly, C., Nicol, A., Walsh, J. J., & Seebeck, H. (2015). Evolution of faulting and plate boundary deformation in the Southern Taranaki Basin, New Zealand. *Tectonophysics*, *651*, 1–18.

Renton, A. (2021). *Transpower, Personal Conversation* [Personal communication].

Rickard, P. (2000). A summary of data indicating increased reservoir complexity in the McKee Field. *2000 New Zealand Petroleum Conference Proceedings*.

RISC. (2021). *Hydrogen storage potential of depleted oil and gas fields in Western Australia: Literature review and scoping study* (No. 221). Geological Survey of Western Australia.

Rissmann, C., Nicol, A., Cole, J., Kennedy, B., Fairley, J., Christenson, B., Leybourne, M., Milicich, S., Ring, U., & Gravley, D. (2011). Fluid flow associated with silicic lava domes and faults, Ohaaki hydrothermal field, New Zealand. *Journal of Volcanology and Geothermal Research*, *204*(1–4), 12–26. Scopus. https://doi.org/10.1016/j.jvolgeores.2011.05.002

Saigustia, C., & Robak, S. (2021). Review of Potential Energy Storage in Abandoned Mines in Poland. *Energies*, *14*(19), 6272.

Scafidi, J., Wilkinson, M., Gilfillan, S. M., Heinemann, N., & Haszeldine, R. S. (2021). A quantitative assessment of the hydrogen storage capacity of the UK continental shelf. *International Journal of Hydrogen Energy*, *46*(12), 8629–8639.

Sherwood, A. M., Australasian Institute of Mining and Metallurgy, & New Zealand Petroleum & Minerals. (2019). *The geology and resources of New Zealand coalfields: Vol. 33;no. 33.;* The Australasian Institute of Mining and Metallurgy. https://go.exlibris.link/BcZh1H61

Shi, Z., Jessen, K., & Tsotsis, T. T. (2020). Impacts of the subsurface storage of natural gas and hydrogen mixtures. *International Journal of Hydrogen Energy*, *45*(15), 8757–8773.

Shimada, S. (2006). *Current State of Japanese Researches on Geological CO*.

Sim, C. Y., & Adam, L. (2016). Are changes in time-lapse seismic data due to fluid substitution or rock dissolution? A CO2 sequestration feasibility study at the Pohokura Field, New Zealand. *Geophysical Prospecting*, *64*(4-Advances in Rock Physics), 967–986.

SKM. (2012). *Australian groundwater modelling guidelines* (Waterlines Report Series). Sinclair Knight Merz.

Stagpoole, V., & Nicol, A. (2008). Regional structure and kinematic history of a large subduction back thrust: Taranaki Fault, New Zealand. *Journal of Geophysical Research: Solid Earth*, *113*(B1).

Stirling, M., McVerry, G., Gerstenberger, M., Litchfield, N., Van Dissen, R., Berryman, K., Barnes, P., Wallace, L., Villamor, P., & Langridge, R. (2012). National seismic hazard model for New Zealand: 2010 update. *Bulletin of the Seismological Society of America*, *102*(4), 1514–1542.

Tapuae Roa. (2019). *H2 Taranaki Roadmap—How hydrogen will play a key role in our new energy future*.

Tarasov, A., Borzenkov, I., Chernykh, N., & Belyayev, S. (2011). Isolation and investigation of anaerobic microorganisms involved in methanol transformation in an underground gas storage facility. *Microbiology*, *80*(2), 172–179.

Tarkowski, R. (2019). Underground hydrogen storage: Characteristics and prospects. *Renewable and Sustainable Energy Reviews*, *105*(C), 86–94.

Tarkowski, R., Uliasz-Misiak, B., & Tarkowski, P. (2021). Storage of hydrogen, natural gas, and carbon dioxide – Geological and legal conditions. *International Journal of Hydrogen Energy*, *46*(38), 20010–20022. https://doi.org/10.1016/j.ijhydene.2021.03.131

Teatini, P., Castelletto, N., Ferronato, M., Gambolati, G., Janna, C., Cairo, E., Marzorati, D., Colombo, D., Ferretti, A., Bagliani, A., & others. (2011). Geomechanical response to seasonal gas storage in depleted reservoirs: A case study in the Po River basin, Italy. *Journal of Geophysical Research: Earth Surface*, *116*(F2).

Tenthorey, E., Nguyen, D., & Vidal-Gilbert, S. (2011). Applying underground gas storage experience to geological carbon dioxide storage: A case study from Australia's Otway Basin. *Energy Procedia*, *4*, 5534–5540.

Thakur, K. A., & Flores, J. (1974). Influence Of Production Rate And Oil Viscosity On Water Coning. *Annual Technical Meeting*.

Thaysen, E. M., McMahon, S., Strobel, G., Butler, I., Ngwenya, B., Heinemann, N., Wilkinson, M., Hassanpouryouzband, A., McDermott, C., & Edlmann, K. (2020). *Estimating Microbial Hydrogen Consumption in Hydrogen Storage in Porous Media as a Basis for Site Selection*. https://eartharxiv.org/repository/view/1799/

Townsend, D., Nicol, A., Mouslopoulou, V., Begg, J. G., Beetham, R. D., Clark, D., Giba, M., Heron, D., Lukovic, B., & McPherson, A. (2010). Palaeoearthquake histories across a normal fault system in the southwest Taranaki Peninsula, New Zealand. *New Zealand Journal of Geology and Geophysics*, *53*(4), 375–394.

Truche, L., Berger, G., Destrigneville, C., Guillaume, D., & Giffaut, E. (2010). Kinetics of pyrite to pyrrhotite reduction by hydrogen in calcite buffered solutions between 90 and 180 C: Implications for nuclear waste disposal. *Geochimica et Cosmochimica Acta*, *74*(10), 2894–2914.

Truche, L., Jodin-Caumon, M.-C., Lerouge, C., Berger, G., Mosser-Ruck, R., Giffaut, E., & Michau, N. (2013). Sulphide mineral reactions in clay-rich rock induced by high hydrogen pressure. Application to disturbed or natural settings up to 250 C and 30 bar. *Chemical Geology*, *351*, 217–228.

Turner, M. B., Cronin, S. J., Bebbington, M. S., & Platz, T. (2008). Developing probabilistic eruption forecasts for dormant volcanoes: A case study from Mt Taranaki, New Zealand. *Bulletin of Volcanology*, *70*(4), 507–515.

Van der Lingen, G. J., Watters, W. A., & Smale, D. (1986). *Diagenetic features in sediments of the McKee Formation, Taranaki* (New Zealand Geological Survey report SL 16. 2v.). New Zealand Geological Survey.

Venture Taranaki. (2021). *Power to X: Transforming renewable electricity into green products and servicies* [Concept paper].

Wang, L., Link to external site, this link will open in a new window, Pei, P., & Link to external site, this link will open in a new window. (2021). Evaluation of the Influencing Factors of Using Underground Space of Abandoned Coal Mines to Store Hydrogen Based on the Improved ANP Method. *Advances in Materials Science and Engineering*, *2021*. http://dx.doi.org/10.1155/2021/7506055

Watkins, H., Butler, R. W., Bond, C. E., & Healy, D. (2015). Influence of structural position on fracture networks in the Torridon Group, Achnashellach fold and thrust belt, NW Scotland. *Journal of Structural Geology*, *74*, 64–80.

WorleyParsons. (2014). *Gas disruption study: Report on the potential impacts on the NZ gas market*.

Yamamoto, K., & Koide, H. (2006). Earthquake related fluid migrations: Mechanism, historical record and lessons learnt. *Eighth International Conference on Greenhouse Gas Control Technologies (GHGT-8)*.

Yates, E., Bischoff, A., Beggs, M., & Jackson, N. (2021). *Green Hydrogen Geostorage in Aotearoa—New Zealand*. https://doi.org/10.13140/RG.2.2.36303.82083

Yekta, A. E., Manceau, J.-C., Gaboreau, S., Pichavant, M., & Audigane, P. (2018). Determination of hydrogen–water relative permeability and capillary pressure in sandstone: Application to underground hydrogen injection in sedimentary formations. *Transport in Porous Media*, *122*(2), 333–356.

Yekta, A. E., Pichavant, M., & Audigane, P. (2018). Evaluation of geochemical reactivity of hydrogen in sandstone: Application to geological storage. *Applied Geochemistry*, *95*, 182–194. https://doi.org/10.1016/j.apgeochem.2018.05.021

Yergin, D. (2020). *The New Map: Energy, Climate, and the Clash of Nations*. Penguin Press.

Zgonnik, V. (2020). The occurrence and geoscience of natural hydrogen: A comprehensive review. *Earth-Science Reviews*, *203*, 103140.

Zheng, J., Zhang, X., Xu, P., Gu, C., Wu, B., & Hou, Y. (2016). Standardized equation for hydrogen gas compressibility factor for fuel consumption applications. *International Journal of Hydrogen Energy*, *41*(15), 6610–6617.

Zivar, D., Kumar, S., & Foroozesh, J. (2020). Underground hydrogen storage: A comprehensive review. *International Journal of Hydrogen Energy*. https://doi.org/10.1016/j.ijhydene.2020.08.138

Zvyoloski, G. (2007). *FEHM: A control volume finite element code for simulating subsurface multi-phase multi-fluid heat and mass transfer May 18, 2007 LAUR-07-3359*. https://www.lanl.gov/orgs/ees/fehm/pdfs/FEHM_LAUR-07-3359.pdf

Zyvoloski, G. A., Robinson, B. A., Dash, Z. V., & Trease, L. L. (1997). *Summary of the models and methods for the FEHM application-a finite-element heat-and mass-transfer code*. Los Alamos National Lab.(LANL), Los Alamos, NM (United States).

Appendix 1 Glossary

Table A1.1. Glossary of terms used in the report.

Term	Definition
UHS	*Underground Hydrogen Storage;* storage of **hydrogen gas** in an underground reservoir.
UGS	*Underground Gas Storage;* storage of **natural gas** in an underground reservoir.
Porosity	Proportion or percentage of available volume that can be occupied by fluid (natural gas, hydrogen, water, oil).
Permeability	Measure of the speed that fluid flows underground for given pressure gradient and viscosity.
Reservoir	Rock formation that is the primary storage site of economic fluid accumulation (natural gas, hydrogen)
Seal	Low permeability formation overlying a reservoir that inhibits pressure or buoyancy driven escape of fluid.
Trap	Structural (anticline, fault) or stratigraphic (pinch-out or onlapping beds) form that inhibits the lateral or vertical escape of fluid from a reservoir.
Relative permeability	Tendency of a fluid to move under a pressure gradient as a function of its saturation relative to other components present.
MICP	*Mercury injection capillary pressure;* a technique for measuring porosity, pore throat size distribution, and injection pressure.
Cushion gas	Gas introduced to the reservoir that compresses and expands, assists in maintaining pressure support during storage operation. Not generally recoverable.
Working gas	Economic gas injected and then later withdrawn from the reservoir.
Injection pressure	Wellhead or downhole pressure conditions relative to the reservoir that induces flow into or out of storage.
Solubility	Ability of hydrogen gas to become dissolved into in-situ pore water, oil or other reservoir fluid.
FEHM	*Finite Element Heat and Mass;* Multi-phase, multi-fluid reservoir simulator for hydrogen-water mixtures.
PMP/PML	*Petroleum Mining Permit/License;* exclusive rights to mine (extract and produce) petroleum

	from a discovered field. PML was renamed to PMP.
1P	Proven reserves, calculated by adding proved developed and undeveloped reserves.
2P	Probable reserves, calculated by adding proven (*1P*) reserves and probable reserves.
3P	Possible reserves, calculated by adding proven *(1P)* and possible *(2P)* reserves.

Appendix 2 - Geological Conditions

A2.1 - Reservoir rocks

In this appendix we provide detailed descriptions of the Tariki Sandstone Member, McKee Formation, Moki Formation and the Mt Messenger/Urenui formations. For additional information refer to the cited publications and reports.

A2.1.1 - Tariki Sandstone Member

The Tariki Member is divided into three groups which are described here.

1. Whaingaroan (Lwh)-aged sandstones from the main producing fields of the central peninsula region (Kahili-Tariki North-Tariki-Ahuroa; Toko-Waihapa included)
2. Whaingaroan (Lwh) & Duntroonian (Ld)-aged sandstones, periphery of producing fields (east & north; Beluga-1, Tuihu-1/1A)
3. Lwh- to Ld-aged sandstones from the southern Taranaki fields (Rimu-Kauri)

Lwh-sandstones, central peninsula

The Tariki Member from the main producing fields (Kahili-Tariki North-Tariki-Ahuroa) comprises a series of stacked sands of good reservoir quality. They are fine- to medium-grained, quartzose sandstones with variable but generally minor feldspar contents, and typically classify as subfeldsarenites or feldsarenites. Feldspar is mostly K-feldspar and the minor lithics are dominated by rigid plutonic fragments. Sandstone cuttings from wells Toko-1, Trapper-A1, and Waihapa-1 display similar textural and detrital composition to core samples from the central peninsula region (Table A2.1; Table A2.2).

Total clay volume is low in most samples from the Tariki Member in the central field area, with authigenic clay dominated by kaolinite and/or illite-smectite. However, carbonate is highly variable. Traces to minor skeletal calcite is recorded from most samples and pervasive calcite cement occurs locally. The amount of “competent sandstone” cuttings (i.e., probable cemented cuttings) is greater in samples from wells Toko-1, Trapper-A1, and Waihapa-1 compared to the producing fields, and is particularly high in samples from Toko-1. This suggests a higher carbonate content in these samples. In all samples pyrite is present in minor volumes (< 2% and average <1%).

Table A2.1 Summary of thin section point-count data, core or SWC from reservoir interval. Data have been normalised removing the porosity component; labile grains include mica, lithics and variably clay-replaced degraded grains, opaques are pyrite and leucoxene cements. Data sources Higgs et al. (2012 and references therein), Higgs, 2007, 2012).

McKee Formation (wells Manganui-2, McKee-6A, Ngatoro-1, Ohanga-2, Onaero-1, Stratford-1, Tariki-1, Toetoe-1, Tuhua-1). Carbonate cements are minor; pyrite is a locally minor component.

Tariki Member (Lwh central wells Ahuroa-1, 1A, Tariki North-1A, Tariki-4/4A. Toko-1. Waihapa-1; Ld-Lwh periphery wells Tuihu-1A; Lwh south wells Rimu-A1, A3, B1). High carbonate contents (dominantly calcite) occur locally and more often in lithologies from the periphery wells. Pyrite is a minor component. Onshore Mid-Miocene Moki Sandstone (wells Cardiff-1, Kaimiro-2, Kapuni-9, Mystone-1, Ngatoro-5, Te Kiri-1, -2). Locally pervasive carbonate contents (dominantly calcite). Pyrite is typically a minor component.

Late Miocene sandstones (wells Burgess-1, Cheal-2, Kaimiro-2, -16, -18, Kaipikari-1, Mako-1, Ngatoro-5, Okoki-1, Waihapa-1A, -2, -6 and outcrop). High carbonate contents (dominantly calcite) locally occur as cements in the Mount Messenger sandstones. Pyrite is a minor component.

	Matrix (vol%)			**Quartz (vol%)**			**Feldspar (vol%)**			**Lithics & Labile Grains (vol%)**			**Other Grains (vol%)**			**Auth Clay (vol%)**			**Opaques (vol%)**			**Carbonate (vol%)**			**Other Cement**
	Min	Max	**Mean**	Min	Max	**Mean**	Min	Max	**Mean**	Min	Max	**Mean**	Min	Max	**Mean**	Min	Max	**Mean**	Min	Max	**Mean**	Min	Max	**Mean**	**Mean**
McKee Formation																									
Overthrust	0.0	2.8	**0.7**	42.1	65.0	**54.7**	20.5	35.5	**26.0**	2.7	9.3	**5.7**	0.0	0.3	**0.1**	2.8	10.2	**4.4**	0.0	3.3	**1.1**	0.0	2.1	**0.5**	**6.6**
In situ	0.0	16.7	**3.4**	24.7	64.8	**49.7**	12.9	37.0	**23.3**	2.9	12.5	**5.9**	0.0	2.6	**0.4**	1.3	15.3	**6.9**	0.0	6.0	**1.9**	0.0	3.0	**1.0**	**7.5**
Total	0.0	16.7	**2.2**	24.7	65.0	**51.8**	12.9	37.0	**24.5**	2.7	12.5	**5.8**	0.0	2.6	**0.3**	1.3	15.3	**5.8**	0.0	6.0	**1.5**	0.0	3.0	**0.8**	**7.1**
Tariki Member																									
Lwh-central	0.0	28.5	**1.4**	35.0	75.3	**60.6**	11.3	27.0	**18.6**	1.9	19.5	**6.5**	0.5	7.0	**3.2**	0.0	6.3	**1.4**	0.0	1.5	**0.6**	0.3	31.8	**6.6**	**1.1**
Ld-Lwh periphery	n/a	n/a	**0.0**	n/a	n/a	**39.7**	n/a	n/a	**28.0**	n/a	n/a	**4.6**	n/a	n/a	**2.7**	n/a	n/a	**1.7**	n/a	n/a	**2.0**	n/a	n/a	**21.0**	**0.3**
Lwh-south	0.0	26.1	**5.1**	21.4	45.4	**36.2**	11.6	30.2	**18.7**	5.7	19.6	**12.4**	2.1	13.6	**7.1**	1.0	12.1	**7.3**	0.5	7.0	**1.7**	2.3	19.1	**10.0**	**1.4**
Total	0.0	28.5	**2.4**	21.4	75.3	**53.9**	11.3	30.2	**18.8**	1.9	19.6	**8.0**	0.5	13.6	**4.2**	0.0	12.1	**2.9**	0.0	7.0	**0.9**	0.3	31.8	**7.8**	**1.2**
Moki Formation																									
Moki	0.0	71.8	**6.5**	9.0	40.0	**25.2**	6.3	25.7	**14.6**	6.3	52.5	**33.3**	0.0	3.3	**1.1**	0.7	16.4	**10.8**	0.3	4.0	**2.0**	0.0	26.8	**5.5**	**0.9**
Late Miocene Sands																									
Urenui Fm	0.3	15.7	**3.1**	18.6	31.4	**22.3**	5.6	24.1	**13.4**	37.0	69.7	**56.9**	0.3	4.0	**1.5**	0.0	4.6	**1.4**	0.0	2.1	**0.4**	0.0	1.3	**0.2**	**0.7**
Mt Mess Fm	0.0	61.0	**5.3**	13.0	36.4	**27.0**	2.8	33.0	**16.1**	11.0	68.3	**39.3**	0.0	8.3	**2.6**	0.0	14.2	**4.6**	0.0	6.7	**1.2**	0.0	20.4	**2.6**	**1.3**

Table A2.2: Summary of bulk mineralogy from QEMSCAN, mostly cuttings (reservoir and intraformational baffles), with some core samples. Lithics not identified by QEMSCAN. Traces have been given a value of 0.01%, data have been normalised removing the porosity component. Data sources Higgs et al. (2012 and references therein), Higgs, 2007, 2012.

McKee Formation (wells Manganui-2, McKee-4, Ngatoro-1, Tuhua-1, Urenui-1). Carbonate (dominantly calcite) occurs as a local cement phase. Pyrite is a minor component.

Tariki Member (Lwh central wells Kahili-1B, Tariki North-1A, Tariki-4/4A. Toko-1. Trapper-A1, Waihapa-1; Ld-Lwh periphery wells Beluga-1, Tuihu-1/1A; Lwh south wells Rimu-A3). High carbonate contents (dominantly calcite) abundant in lithologies from the periphery wells. Pyrite is a very minor component.

Onshore Mid-Miocene sandstones (onshore wells Kaimiro-2, Kapuni-9, Ngatoro-5, Te Kiri-2). Carbonate (dominantly calcite) is present in all samples and locally abundant. Pyrite is a trace or minor component. Late Miocene sandstones (wells Burgess-1, Cheal-2, Kaimiro-2, Kaipikari-1, Mako-1, McKee-1, Ngatoro-5, Okoki-1, Pohokura South-1, Pohokura-2, Te Kiri-2, Waihapa-6). Carbonate (dominantly calcite) is present in all samples and locally abundant. Pyrite is a very minor component.

	Depth (m MD)			Quartz Size (microns)			Quartz (vol%)			Feldspar (vol%)			Clay (vol%)			Heavy Minerals & Others (vol%)			Pyrite (vol%)			Carbonate (vol%)		
	Min	Max	**Mean**	Min	Max	**Mean**	Min	Max	**Mean**	Min	Max	**Mean**	Min	Max	**Mean**	Min	Max	**Mean**	Min	Max	**Mean**	Min	Max	**Mean**
McKee Formation																								
Overthrust	2234	2401	**2321**	53	237	**112**	29.5	76.2	**47.1**	9.6	30.3	**17.2**	4.7	34.6	**20.7**	0.3	5.4	**2.4**	0.1	1.9	**0.9**	0.0	27.5	**11.7**
In situ	3152	3757	**3598**	45	212	**119**	29.1	82.6	**56.7**	8.8	43.3	**18.1**	6.7	17.7	**12.6**	0.3	4.2	**2.3**	0.2	1.1	**0.5**	1.6	27.7	**10.0**
Total	2234	3757	**3031**	45	237	**116**	29.1	82.6	**52.4**	8.8	43.3	**17.7**	4.7	34.6	**16.2**	0.3	5.4	**2.3**	0.1	1.9	**0.7**	0.0	27.7	**10.8**
Tariki Member																								
Lwh-central	2718	4055	**3221**	93	343	**224**	40.8	93.0	**71.6**	4.1	17.4	**9.0**	1.2	24.8	**8.8**	0.3	7.9	**1.7**	Tr	1.1	**0.2**	0.6	23.6	**8.6**
Ld-Lwh periphery	3485	4671	**4305**	31	243	**145**	25.2	72.8	**49.1**	6.7	25.5	**13.8**	4.9	21.9	**14.0**	0.4	4.5	**2.6**	Tr	0.7	**0.3**	7.4	50.4	**20.2**
Lwh-south	n/a	n/a	**3590**	n/a	n/a	**168**	n/a	n/a	**55.6**	n/a	n/a	**25.2**	n/a	n/a	**10.4**	n/a	n/a	**1.2**	n/a	n/a	**0.2**	n/a	n/a	**7.3**
Total	2718	4671	**3731**	31	343	**186**	25.2	93.0	**60.8**	4.1	25.5	**11.6**	1.2	24.8	**11.2**	0.3	7.9	**2.1**	Tr	1.1	**0.3**	0.6	50.4	**13.9**
Moki Formation																								
Moki	1866	3330	**2163**	19	70	**42**	16.7	44.1	**29.0**	7.5	32.3	**18.9**	19.9	50.7	**30.4**	2.1	8.4	**5.1**	0.0	1.8	**0.4**	1.3	47.3	**16.1**
Late Miocene Sands																								
Urenui Fm	500	2150	**1282**	22	88	**34**	16.3	52.7	**26.8**	15.9	26.3	**23.9**	14.1	52.2	**38.8**	1.9	3.9	**3.0**	0.0	1.5	**0.4**	1.0	40.4	**7.0**
Mt Mess Fm	990	2630	**1539**	24	69	**41**	14.0	48.0	**27.7**	16.1	30.9	**25.0**	13.5	53.9	**37.5**	2.4	8.9	**3.6**	0.0	1.2	**0.2**	0.7	26.6	**6.0**
Total	470	2630	**1544**	22	88	**38**	14.0	52.7	**27.4**	15.9	30.9	**24.6**	13.5	53.9	**37.9**	1.9	8.9	**3.4**	0.0	1.5	**0.3**	0.7	40.4	**6.3**

Reservoir quality of the Tariki Member in the producing fields is generally good (Table A2.4). Core-derived porosity and permeability measurements suggest the best quality at Tariki-4A (average porosity 15.3%, max 20.2%; average permeability 147 mD, max 574 mD) and Ahuroa-1 (average porosity 13.9%, max 18.6%; average permeability 62.5 mD, max 313 mD). Lower quality is recorded at Tariki North-1A (average porosity 13.4%, max 16.6%; average permeability 18 mD, max 102 mD). Core samples and therefore core analyses data are not available for the Lwh-aged sandstones south of the main producing fields (Toko-Waihapa). Compaction effects appear to be largely represented by mechanical compaction, with no significant pressure solution effects in the Tariki/Ahuroa region. Mechanical compaction and the locally occurring carbonate cementation are considered to be the main secondary controls that have been detrimental to reservoir quality.

Lwh & Ld-sandstones, periphery of Tariki/Ahuroa fields

An interval of Lwh-aged sandstone cuttings has been interpreted by (Higgs, 2012) from logs (well Beluga-1) to the north of the main producing fields. Results demonstrate the dominance of calcareous mudstone/siltstone lithologies at this wellsite. Loose detrital grains are rare, and competent sandstone cuttings are minor. It is possible that the ditch cuttings are not representative of the interval (i.e., sand/sandstone cuttings are washed out). However, all indications suggest that sandstones occurring at this well will have poor reservoir quality due to a very fine grain size and relatively abundant clay and carbonate content.

An interval of Ld-Lwh aged sandstone has also been interpreted east of the main producing fields (wells Tuihu-1/1A). In this area younger strata (Ld-sandstones) are less quartzose and more lithic rich, compared to the older strata (Lwh-sandstones) at the same wellsite. The type of feldspar changes up-hole from dominantly K-feldspar to dominantly plagioclase, and the lithic type is dominantly granitic in the Lwh interval and dominantly degraded volcanic in the Ld interval. Both the Ld and Lwh-aged sandstones at Tuihu-1/1A tend to have poorer reservoir quality compared to the correlative gas reservoirs in the central peninsula region, which is thought to be due to greater compaction (associated with greater burial), finer overall grain size, and greater carbonate concentration. The latter might be a response to deposition of more skeletal carbonate in the relatively proximal eastern wells.

It is notable that calcite is relatively common in all analysed samples from the periphery wells, but only minor pyrite has been observed (<2%).

Lwh- to Ld-sandstones, southern peninsula

Sandstones from the southernmost region (Rimu Field) are texturally and mineralogically distinct from other Tariki Member sandstones. The sandstones are much finer grained (very fine) than the main producing reservoir at Tariki-Ahuroa, the interval is much thinner, and reservoir quality is mostly poor to fair. being relatively feldspathic and lithic-rich. Sandstones classify as feldsarenites or lithic feldsarenites, feldspars are dominantly plagioclase, labile lithics are relatively common, and the heavy mineral suite includes more pyroxene. These

sandstones are therefore relatively mineralogically complex compared to their time-equivalent counterparts at Tariki-Ahuroa.

Thin section analysis shows the presence of locally significant degraded grains; these include degraded and variably clay-replaced plagioclase and labile lithics. Clays also occur as intergranular matrix and authigenic minerals, with the latter dominated by illite/smectite and subordinate kaolinite; XRD analysis also shows the presence of significant chlorite (Core Lab, 2003). Carbonate content is highly variable, but overall higher compared to the main producing reservoir at Tariki-Ahuroa. Carbonates include minor skeletal calcite and locally pervasive calcite cement. Pyrite is generally a minor component but is locally significant in some samples (Table A2.1; Table A2.3).

Reservoir quality of the Tariki Member is fair at Rimu-Kauri, with average porosity of 11.4% (max 23.3%) and average permeability of 7.4 mD (max 180 mD; Table A2.4). Based on petrophysical evaluation the average porosity/permeability is reported as 13.5%/10.7 mD for the upper Tariki plate (6 wells) and 13.3%/37.3 mD for the lower plate (3 wells; Core Lab, 2003). The relatively low permeability values for given porosity values are considered to be a response to 1) a finer grain size, resulting in smaller intergranular pores, 2) a higher clay content, resulting in greater microporosity (less macroporosity) and, 3) a higher carbonate cement volume, where cements have occluded pores. Reservoir quality is therefore largely controlled by the relative abundance of clay/matrix and carbonate, with mechanical compaction having a slightly more detrimental effect on reservoir quality in the relatively labile Rimu sandstones.

Table A2.3: Summary XRD data, core or SWC from reservoir interval. Minerals in wt% cannot be directly compared with thin section and QEMSCAN data. Data sources Core Lab, 2003. Tariki Member Lwh-south (wells Kauri-A1, Rimu-A2A; Core Lab, 2003). Generally low pyrite concentrations ≤2%, but significant calcite in most samples. Manutahi Sands (wells Kauri-A1, Kauri-B1; Core Lab, 2003).

	Depth (m MD)			Quartz (wt%)			Feldspar (wt%)			Clay (wt%)			Pyrite (wt%)			Carbonate (wt%)		
	Min	Max	**Mean**	Min	Max	**Mean**	Min	Max	**Mean**	Min	Max	**Mean**	Min	Max	**Mean**	Min	Max	**Mean**
Tariki Lwh-south	3399	3909	**3702**	30	67	**50**	9	30	**19.3**	3	19	**8.3**	1	5	**1.5**	1	56	**21.4**
Manutahi	1141	1391	**1214**	30	71	**43.5**	17	44	**31.4**	9	34	**24.1**	1	3	**1.3**	0	2	**0.4**

*Table A2.4: Summary core analysis data. Data sources for Manutahi Sands from Core Lab 2003, 2003b; other data from original well completion reports, compiled in Higgs et al. (2012), Higgs, 2007. McKee Formation (wells Manganui-1, -2, McKee-2, -3A, -4, 5A, -6A, Ngatoro-1. Ohanga-2, Pukemai-1, Stratford-1, Tariki-1, Toetoe-1, -3A, -4A, Tuhua-1). Tariki Member (wells Ahuroa-1, Kauri-A1, Rimu-A1, Rimu-A3, Tariki North-1A, Tariki-1, -4/4A). Moki Formation (wells Cardiff-1, Durham-1, Kaimiro-2, -3, Kapuni-1, -9, Mystone-1, Ngatoro-3, -5, Te Kiri-2). Late Miocene sandstones (wells Burgess-1, Cheal-2, Kaimiro-2, -15, -16, -18, Kaipikari-1, Mako-1, Ngatoro-2, -3, -4, -5, -7, -9, -11, Okoki-1, Te Kiri-2, Waihapa-6, Wingrove-1). Manutahi Sands * analogue data, (wells Kauri-A1, -A2, -A3, -A4, -B1, Manutahi-1).*

	Depth (m MD)			He Porosity (%)			Horizontal Permeability (mD)				GD (g/cc)
	Min	Max	**Mean**	Min	Max	**Mean**	Min	Max	**Mean**	**Geomean**	**Mean**
McKee Formation											
Overthrust	2131	2511	**2269**	1.1	22.2	**16.9**	0.004	1140	**99.4**	**35.0**	**2.64**
In situ	3028	4139	**3772**	0.3	12.5	**8.1**	0.01	101	**2.8**	**0.56**	**3.71**
Tariki Member											
Lwh-central	2706	3040	**2826**	1.3	20.2	**14.6**	0.01	574	**114.8**	**29.4**	**2.65**
Lwh-south	3399	4214	**3715**	1.7	23.3	**11.4**	0.003	180	**7.4**	**0.46**	**2.65**
Moki Formation											
Moki	1829	3215	**2206**	0.3	24.5	**14.5**	0.01	337	**14.3**	**1.7**	**2.71**
Mid Miocene Sands											
Urenui Fm	1362	2158	**1960**	3.5	27.3	**23.8**	0.02	1180	**543.7**	**101.9**	**2.71**
Mt Mess Fm	1134	2617	**1612**	0.4	32.6	**22.8**	0.01	1230	**97.4**	**25.2**	**2.70**

Manutahi Sands											
Analogue	1141	1401	**1218**	3.2*	26.6*	**22.2***	0.01*	644*	**183***	**41.8***	**nd**
Core Analysis	1124	1313	**1232**	24	32.9	**27.5**	nd	nd	**nd**	**nd**	**nd**

Table A2.5: Summary XRD data, selected Taranaki mudstones. Minerals in wt% cannot be directly compared with thin section and QEMSCAN data. Generally low pyrite concentrations ≤2%, but significant calcite in most samples. Data sources from Higgs et al., 2005, Field et al., 2011 and references therein.

Formation	Sample Location	Depth (m)			Quartz (wt%)			Feldspar (wt%)			Clay (wt%)			Pyrite (wt%)			Carbonate (wt%)			Other (wt%)		
		Min	Max	**Mean**	Min	Max	**Mean**	Min	Max	**Mean**	Min	Max	**Mean**	Min	Max	**Mean**	Min	Max	**Mean**	Min	Max	**Mean**
McKee/Mangahewa	Toetoe-4A	2248	2259	**2253.5**	31	40	**35.7**	10.4	15.4	**12.9**	31.9	33.7	**32.8**	0	5.6	**2.8**	15.7	16	**15.9**	0	0	**0**
Turi	Maui-6, Tangaroa-1	3032	3899	**3609**	28.5	70.3	**49**	0.5	8.5	**4**	23.8	50.5	**36**	1.1	11.5	**6**	0	12.7	**5**	0	3.3	**1**
Otaraoa	Onaero-1	3029	3029.3	**3029**	22.9	32.7	**27.8**	8.7	10.2	**9.4**	21.8	34.3	**28**	4	4.6	**4.3**	18.2	41.5	**29.9**	0	1.2	**0.6**
Manganui	Wingrove-1	1214	1231	**1222.5**	22.2	22.9	**22.5**	14.7	15	**14.8**	56.1	56.8	**56.5**	1.4	2	**1.7**	3.6	5.3	**4.5**	0	0	**0**
Mt Messenger	Kaimiro-2, outcrop	0	1360.2	**n/a**	20.3	35.3	**29.3**	12.5	20.6	**16.4**	36.5	56.3	**46.9**	0	2.1	**0.6**	0.9	28.4	**6.3**	0	3.2	**0.5**
Moki	Kaimiro-2, Te Kiri-2	2051.45	2821.35	**2436.4**	20.1	28.2	**24.1**	14.6	22.6	**18.6**	39.4	45.9	**42.6**	1.3	2.6	**1.9**	1.5	15.3	**8.4**	0	8.6	**4.3**

Table A2.6: Summary of MICP data, onshore Taranaki cap rocks.. Data sources for GNS compilation in Higgs et al., 2005, Field et al., 2011.

Well	Formation	MICP pressure	Por (Hg)	Reference
Toetoe-4A	Turi/McKee	8520-11900 psi	2-3.3%	GNS compilation
Onaero-1	Otaraoa	6965-8600 psi	1.7-2.2%	GNS compilation
Kaimiro-2	Mt Messenger & Moki	997-6055 psi	3.2-17.8%	GNS compilation
Toetoe-6B	Manganui	14-200 psi	7.1-39.2%	GNS compilation
Mangamingi-1	Manganui/Otunui	40-842 psi	23-26.3%	Higgs and Crundwell, 2008
Te Kiri-2	Moki 2821.23	3500 psi	1.53%	Higgs, 2007
Waihapa-6	Manganui	5011-5988 psi	7-8.5%	GNS compilation
Wingrove-1	Manganui	1001-1428 psi	19.2-19.6%	GNS compilation
North Taranaki outcrop	Mt Messenger	70-1731 psi	19.7-30.4%	GNS compilation

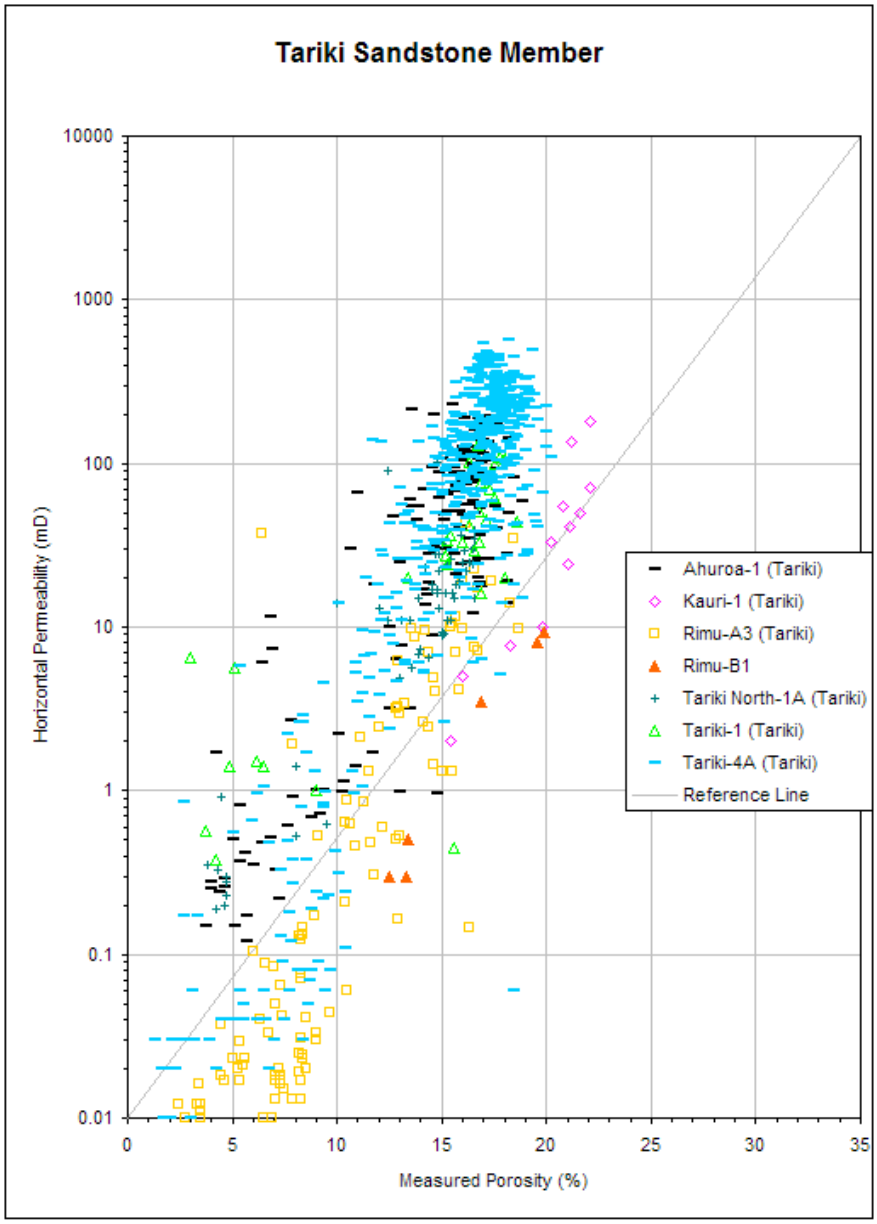

Figure A2.1: Porosity-permeability plot comparing overall better quality Tariki Member in the Ahuroa-Tariki fields compared to the Rimu-Kauri fields. From Higgs et al. (2012).

A2.1.2 - McKee Formation

The McKee Formation is characterised by fine- to medium-grained sandstones, commonly with moderately good sorting. Most sandstone samples from the McKee Formation classify as feldsarenites, with both thin section and QEMSCAN data demonstrating a quartzo-feldspathic composition through the reservoir interval (Table A2.1; Table A2.2). Feldspar includes both K-feldspar and plagioclase, with the proportion of feldspar varying significantly between samples at any single wellsite. Petrographic analysis shows that the lithic content is typically low and dominated by rigid quartz-feldspar grains, while degraded grains are a minor component and include degraded/altered plagioclase. Other grains are generally rare.

Total clay volume is higher in the QEMSCAN data than thin section data, recording clays in the labile grains and interbedded lithologies. Authigenic clay minerals are relatively minor in the overthrust McKee but are more abundant in in situ samples, which have undergone higher temperature diagenesis. Kaolinite and illite-smectite are the dominant clays with illite becoming more common in the deeper samples.

Carbonate (dolomite and siderite) is recorded as a very minor component of the thin section samples. However, calcite is abundant in some of the QEMSCAN samples demonstrating the presence of local cemented units. In most cases pyrite is present in minor volumes (up to ~2%), although it can be higher in some in situ samples.

Reservoir quality of the McKee Formation is variable; in many areas the reservoir is structurally complicated, with several fault compartments and steep stratal dips. Porosity within the producing field area typically ranges between 12-23% with permeabilities up to 1140 mD (Table A2.4). The quality of McKee reservoirs can be broadly subdivided into the overthrust plate, characterised by moderate to moderately good reservoir quality, and the in-situ plate, which commonly has poorer reservoir quality (Figure A2.2 & Table A2.4). These differences are largely due to burial depth, with the overthrust McKee Formation occurring at a much shallower burial depth than the in-situ McKee Formation. Locally, reservoir quality of McKee Sands have been reduced by diagenetic modification, principally through pressure solution of quartz (in the in situ samples), the development of clay (more advanced in the in situ samples), grain fracturing due to overthrusting (overthrust plate), and carbonate cementation (Higgs et al., 2012; Huggett, 1986; Van der Lingen et al., 1986). The presence of smectite in the McKee reservoir interval has been identified by Palmer (2021) as a possible explanation for formation damage whereby the clays have expanded in water-based drilling fluids. Geochemical modelling of rocks containing smectite predict very little reaction with hydrogen (Amid et al., 2016; Bo et al., 2021; Hassannayebi et al., 2019), although the presence of smectite and its potential on injection/recovery should be considered in any future drilling program.

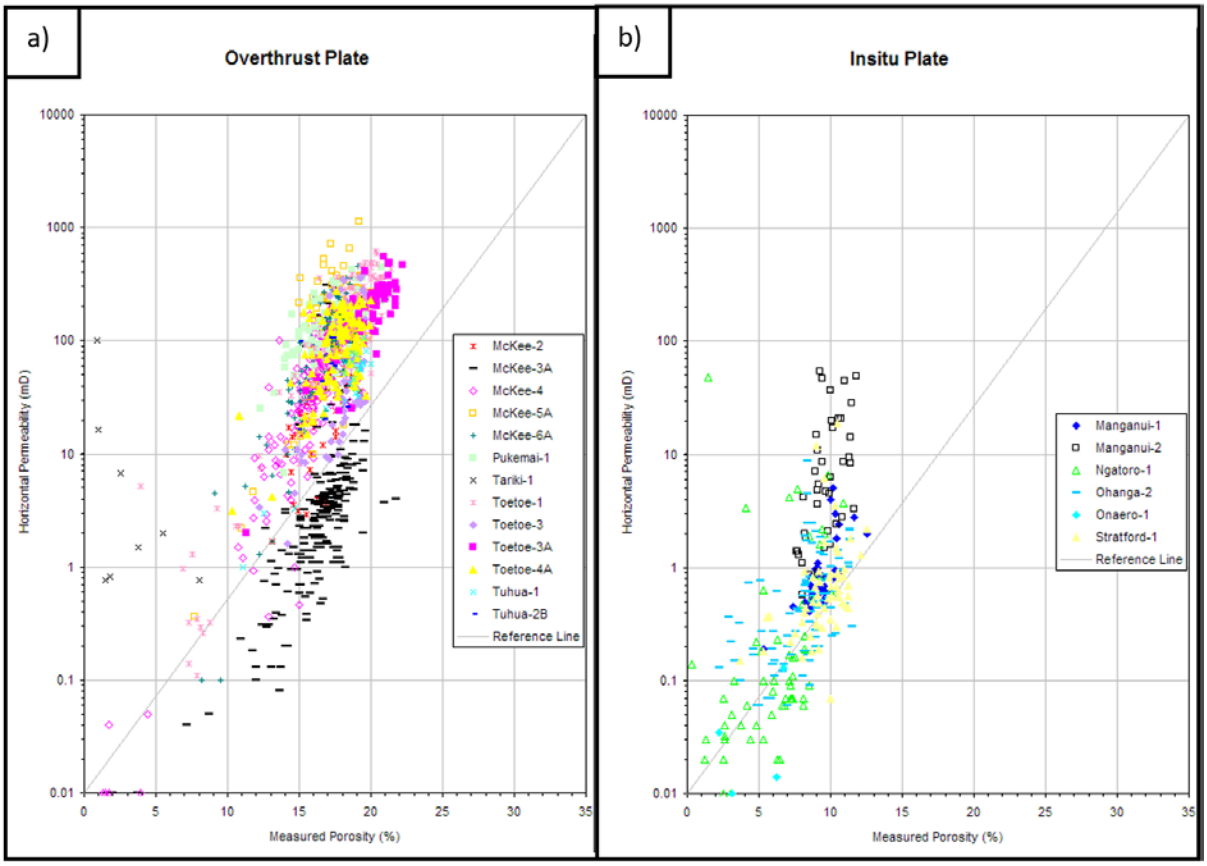

Figure A2.2: Porosity-permeability plot comparing overall better quality overthrust McKee (a) with the more deeply buried in situ (b) McKee. From Higgs et al. (2012).

A2.1.3 - Moki Formation

The Moki Formation is characterised by very fine- to fine-grained and moderately to well sorted sandstones, with onshore samples displaying a variable Q-F-L ratio, classifying as feldsarenite, lithic feldsarenites, feldspathic litharenites and litharenites. Compared to Paleogene reservoirs, the Moki Formation is characterised by low quartz and variable but fairly common feldspar and lithic fragments (Table A2.1; Table A2.2). Feldspar is mostly plagioclase, and lithics are mostly labile grains of metasedimentary and volcanic origin.

The sands are clay-rich, often with little detrital matrix but variable mica content and common clay-replaced grains. Total clay volume is higher in the QEMSCAN data than thin section data, recording clays in the labile grains and interbedded lithologies (Table A2.1; Table A2.2). Clay minerals are dominated by illite and mixed-layer clays of illite-smectite and chlorite-smectite composition that have formed from the decomposition and replacement of unstable lithic grains and feldspar; secondary kaolinite is also common in these samples.

Carbonates (mostly calcite) are the main cement type of the Moki sands, occurring as a trace to abundant phase. The carbonate-rich beds locally appear more common in thin beds, possibly due to a source of ions from the mudstones and/or from skeletal material, which occurs in minor amounts within the finer intervals (Higgs, 2007). Minor pyrite typically displays a framboidal morphology and locally replaces grains and clays; it is generally <2% by volume (Table A2.1; Table A2.2).

Reservoir quality of the cored sandstones is highly variable, typically with fair to moderately good, measured porosity and poor to locally moderately good permeability. Porosity of onshore samples ranges between 0.3-24.5% (average 14.5%) with permeabilities ranging up to 337 mD (average 14.3 mD; Table A2.4) The high proportion of labiles in the Moki Formation together with the fine grain size is a critical control on reservoir quality and heavily dependent on depth of burial. The amount of visible porosity, and reservoir quality is also likely linked to cement volume. Notably, the mineralogical composition of the Moki Formation has been shown to change in a southwesterly direction from relatively lithic-rich along the eastern basin margin to relatively quartz-rich westward and offshore (Higgs, 2007) (Figure A2.3a). However, Moki sands of slightly more mature composition on the western peninsula have poorer reservoir quality, possibly due to a higher carbonate cement content.

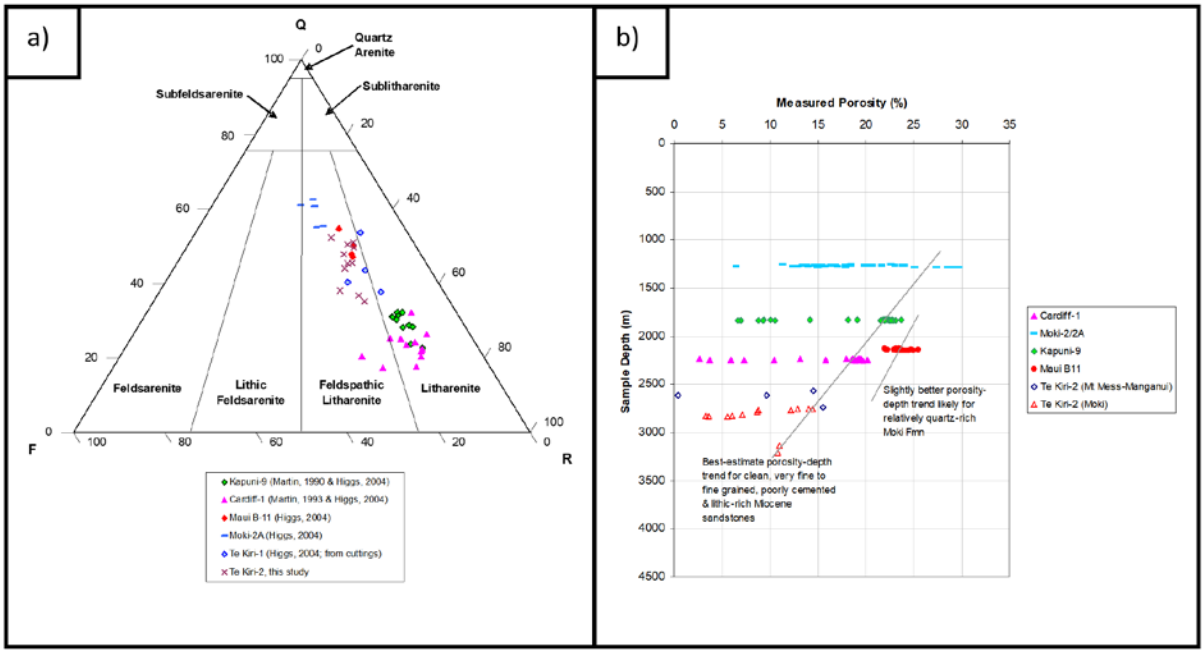

Figure A2.3: (a) Ternary diagram illustrating sandstone classification of the onshore Moki Formation from several wells (classification scheme of Folk et al., 1970). (b) Scatter plot of porosity versus sample depth for the onshore Moki Formation; the very poor to poor reservoir quality of the Miocene sandstones at Te Kiri-2 is due to relatively deep burial compared to Miocene sandstones from other Taranaki wells. From Higgs (2007).

A2.1.4 - Mount Messenger and Urenui formations

Late Miocene sandstones of the Mount Messenger and Urenui formations display similar mineralogical and petrophysical characteristics. They benefit from being at shallow burial depths (targets generally <2 km deep), with central and southern Taranaki peninsula wells currently close to maximum burial depths (<600 m Plio-Pleistocene uplift), but with progressively more uplift towards the eastern basin margin (~1 km e.g., Kamp et al., 2004). As such, most of the reservoirs have not undergone extensive compaction and diagenesis, resulting in good porosity-permeability. However, reservoir sandstones are typically thin-bedded (bed thicknesses often <30 cm at Kaimiro/Ngatoro), which for hydrogen gas storage may increase the surface area of gas-water-rock interactions and lead to fingering, cellar entrapment etc.

The majority of cored samples from the Mount Messenger and Urenui formations are very fine to locally fine grained and moderately well to well sorted sandstones, being overall slightly finer grained than the mid-Miocene Moki Formation. However, mineralogically the sands are similar to the Moki; they are feldspathic and lithic-rich (Table A2.2), and classify as feldsarenite, lithic feldsarenites, feldspathic litharenites and litharenites. Feldspar is mostly plagioclase, and lithics are mostly labile grains of metasedimentary and volcanic origin. Clay minerals are abundant and are mostly contained within the variably clay-replaced labiles and degraded grains; clays are slightly more abundant than the Moki Formation (Table A2.1; Table A2.2). Clay minerals are dominated by illite and mixed-layer clays of illite-smectite and chlorite-smectite composition, with subordinate kaolinite.

Pore-filling cements are generally minor in the Late Miocene reservoirs, with only local pervasive calcite cements that may occur as thin horizons and/or concretions; concretions are commonly observed in outcrop with sizes of <1 m to 10 m diameter (cf. King et al., 2007). Pyrite occurs as a minor component of the Late Miocene sandstones, but can be significant locally (>5%).

These reservoirs commonly display good porosity and permeability due to the shallow burial depths. Porosity in selected Mount Messenger wells is up to 32.6%, with an average of 22.8%, while permeability averages 97 mD (Table A2. 4); porosity in the more limited Urenui samples is up to 27.3%, with an average of 23.8%, and permeability average of 544 mD (Table A2. 4). However, outcrop studies on base-of-slope facies from the Mount Messenger Formation show that there is considerable variation in permeability both vertically and horizontally within individual thin beds (Browne and Slatt, 2002). Overall, thick- and thin-bedded basin floor sandstones display comparable reservoir properties, and it is suggested that the vertical and lateral changes in frequency and continuity of siltstones is likely to represent the most significant primary sedimentary heterogeneity to impact reservoir flow in the basin floor sandstones (Arnot et al., 2006).

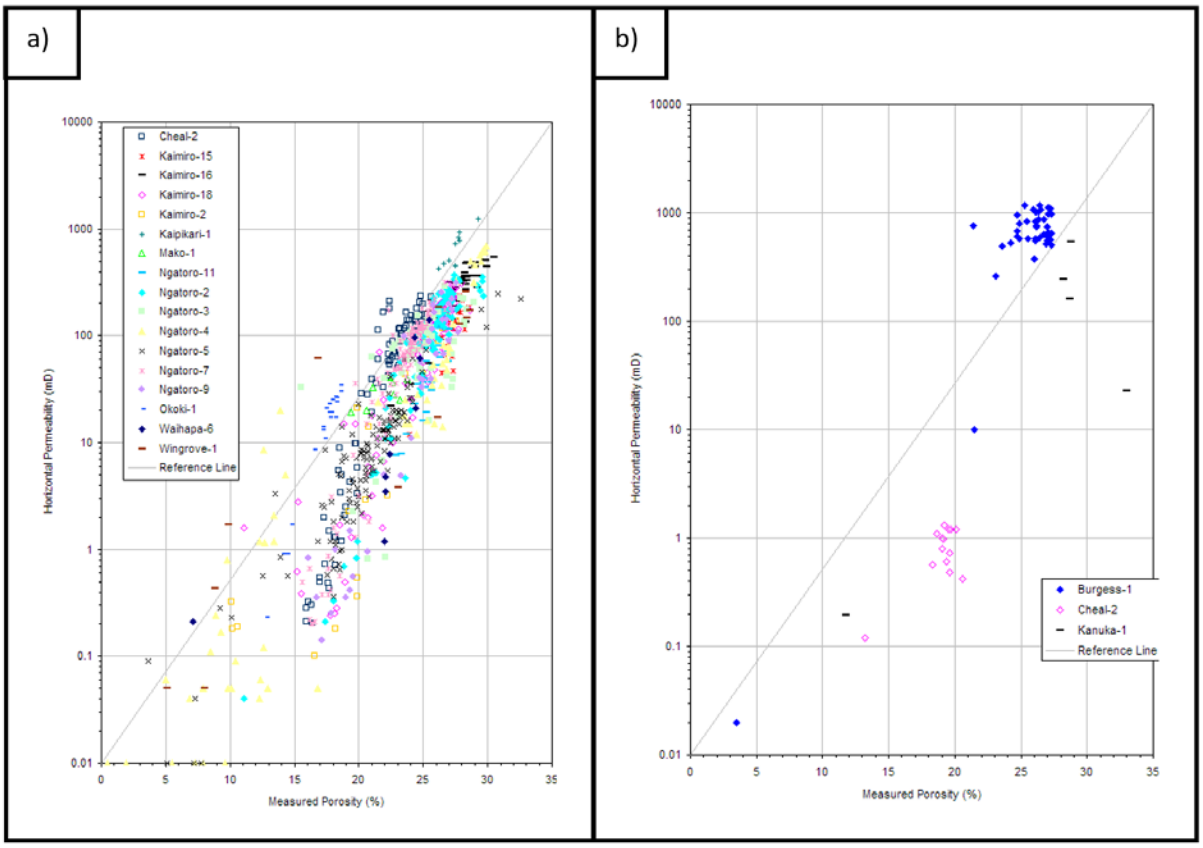

Figure A2.4: Porosity-permeability plot comparing (a) Mt Messenger and (b) Urenui sands. From Higgs et al. (2012).

A2.1.5 - Matemateaonga Formation; Manutahi Sands

Manutahi Sands have been petrographically analysed by Core Lab (2003) in the producing field, where they comprise poorly consolidated, very fine- to very coarse-grained (mostly fine-grained) and moderately sorted sands. Samples are mostly composed of quartz and plagioclase feldspar (Table A2.3), with common lithic fragments mostly of volcanic and sedimentary origin, and locally mica. Similar to other Miocene reservoirs (Moki, Mt Messenger, Urenui), the Manutahi Sands are clay-rich, with many of the clays associated with labile grains. This high labile content is compacted and considered to be one of the principal controls on reservoir quality (Core Lab, 2003).

Chlorite and mixed layer illite-smectite have been identified as the dominant clay minerals in the Manutahi Sands, occurring within labiles and as pore-lining and pore-filling clay; kaolinite occurs as an authigenic clay mineral and may pose a migrating fine problem (Core Lab, 2003). Cements include trace to minor carbonate (calcite, siderite and dolomite) and pyrite. Locally pervasive thin zones of calcite cement are recorded, although XRD analysis suggests that carbonates are rare in much of the reservoir interval (Table A2.3).

A2.2 - Cap rocks

A2.2.1 Turi Formation

It is likely that the **capillary seal capacity** of the Turi Formation will vary significantly due to the shelfal marine facies. There is a lack of capillary pressure data across the Taranaki peninsula, although XRD and MICP measurements are available from intraformational cap

rocks below the McKee reservoir at the Toetoe-4A well. These mudstone samples are relatively quartz-rich with lower feldspar and clay contents compared to other cap rocks (Table A2.5), and with clay minerals mostly composed of kaolinite and illite-mica with subordinate chlorite. Carbonates are relatively common (~16 wt%), although in these samples they are predominantly siderite. Two samples from Toetoe-4A illustrate the very good sealing potential, at least locally, with low porosities (2 – 3.3%) and high air mercury injection threshold pressures (8520–11900 psi, 2248–2259 m; Table A2.6). This is likely to be partly due to the high carbonate content; the dominant siderite is likely to be less reactive with hydrogen than other carbonates. Pyrite is locally present in significant amounts (up to 5.6 wt%), which potentially could react with hydrogen to form H_2S.

In the absence of onshore samples from the Turi Formation, cap rock quality in offshore wells is presented. XRD data at Maui-6 and Tangaroa-1 illustrates the potential for significant mineralogical variability from relatively quartz-rich (at Tangaroa-1) to clay-rich (at Maui-6). The clay mineralogy is similar to the intraformational onshore mudstones, with dominant kaolinite and illite-mica and subordinate chlorite. Carbonates are also variably common, but with the main phase occurring as calcite, dolomite or siderite. Notably, pyrite is also significant in two samples (Table A2.5) and will need to be considered when assessing cap rocks for UHS. Air mercury threshold pressures for samples in offshore Taranaki range from 1800–9980 psia (3024–3040 m at Maui-4), 1600 psia (3445 m at Tane-1), to 1500–2506 psia (3896–3899 m at Tangaroa-1). It is expected that overall quality may be poorer onshore, notwithstanding the Toetoe-4A data cited above, due to the more proximal palaeoenvironment.

A2.2.2 Otaraoa Formation

The Otaraoa Formation forms the top seal for the Oligocene Tariki Member and is part of the seal interval for the late Eocene McKee Formation. Two XRD and capillary seal measurements are available from the Otaraoa Formation at Onaero-1 (Table A2. 5 & 6). These samples are composed of quartz, clay and carbonate in similar quantities, with clay minerals mostly composed of illite-mica with subordinate kaolinite, chlorite and illite-smectite. Carbonates, forming 41 wt% of one sample, are mostly calcite, and pyrite is also present in significant amounts (~4 wt%); both these minerals may react with pore fluid during UHS (see Section 4.4).

The samples from Onaero-1 demonstrate the potential for very good sealing potential, at least locally, with low porosities (1.7–2.2%) and high air mercury threshold pressures (6965–8600 psi). This is likely in part to be due to the high carbonate content. The pore throat size plot (Figure A2.5) shows a bimodal distribution, with the larger mode possibly indicating micro-fracturing and hence a consideration for cap rock integrity.

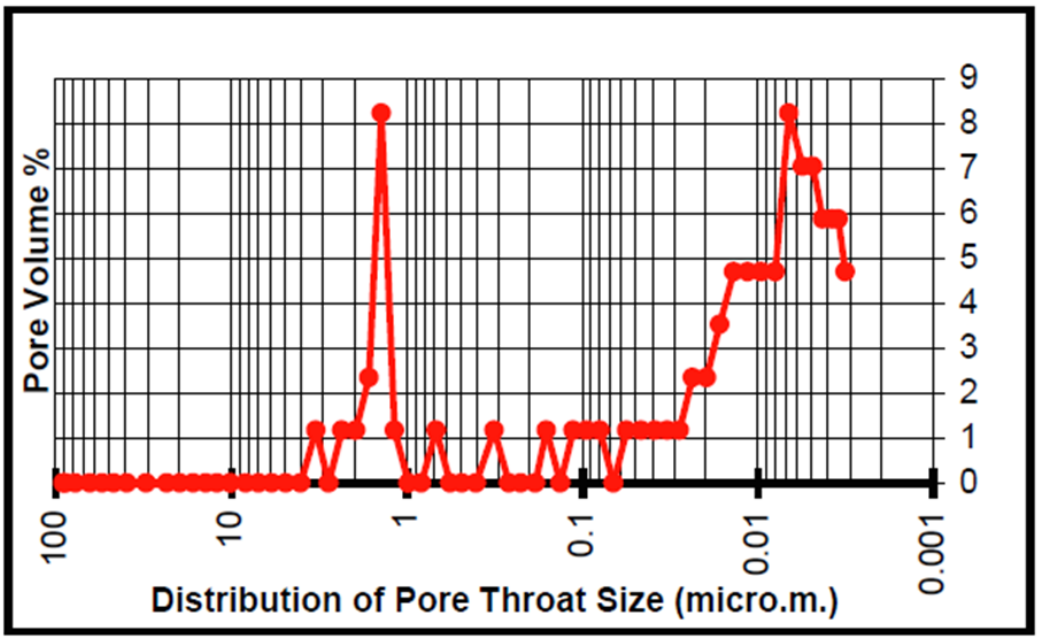

Figure A2.5: MICP pore throat distribution plot, Onaero-1, 3029 m, Otaraoa Formation. MICP Lab Australian School of Petroleum, Adelaide. MICP refers to Mercury Injection Capillary Pressure, while pore throat size is a measure of the connectivity of the pore space.

A2.2.3 Miocene (Manganui) Mudstone

The Manganui Formation is widespread and thick across the Taranaki peninsula, providing effective top and lateral seals for the Moki, Mount Messenger, and Urenui reservoirs. XRD mineralogy and/or cap rock properties of Miocene mudstones are available for Taranaki outcrop samples and sparce samples from onshore wells Kaimiro-2, Toetoe-6B, Mangamingi-1, Waihapa-6 and Wingrove-1. XRD data for samples of Manganui Formation and intra-Moki and Mount Messenger formations illustrate a lower quartz content and higher feldspar and clay content compared to the Eocene mudstones (Table A2.5). Feldspars are mostly plagioclase and clay minerals are dominantly illite/mica with subordinate chlorite and minor illite-smectite; minor kaolinite occurs in the Moki mudstones. Minor carbonate and pyrite occur in most samples, with locally significant calcite cement, and amorphous silica (opal-A) present in a Moki mudstone sample from Te Kiri-2; these phases all pose a risk of reaction with pore fluid during UHS.

Air mercury threshold pressures for samples of Manganui Formation from onshore wells range from 14 psia (1320 m at Toetoe-6B) to 6055psia (2051.45 m at Kaimiro-2) demonstrating a wide range of cap rock properties (Table A2. 6). Notably the three samples measured from Toetoe-6B are all low (1–200 psia), although these are the only analyses undertaken on cuttings. Air mercury threshold pressure measurements from outcrop samples of the Mount Messenger are also variable (70–1731 psi), although the mean of 719 psi (n=14) suggests overall good cap rock properties.

A comparison of the two measurements from Kaimiro-2 well show moderate seal potential for the Mount Messenger mudstone sample (997 psi at 1360.2 m), contrasting with good potential measured for the Moki Formation mudstone sample (6055 psi at 2051.45 m). This corresponds with potential gas columns of 117 and 711 m respectively. The better seal

potential in the Moki Formation sample is also illustrated by SEM examination, which showed the Moki sample to have an average pore diameter of 2 microns and average pore-throat diameter of 0.2 microns (3.2% porosity) compared to average pore and pore throat diameters of average 4 micron and 0.3–0.4 microns (17.8% porosity) respectively for the sample from the Mount Messenger Formation (Core Lab, 1996). Better seal quality in the Moki sample is largely attributed to carbonates, while poorer quality in the Mt Messenger sample is partly due to a higher abundance of silt and sand. These results illustrate how the cap rock mineralogy and capacity vary significantly, both spatially and stratigraphically (see also Figure A2.6).

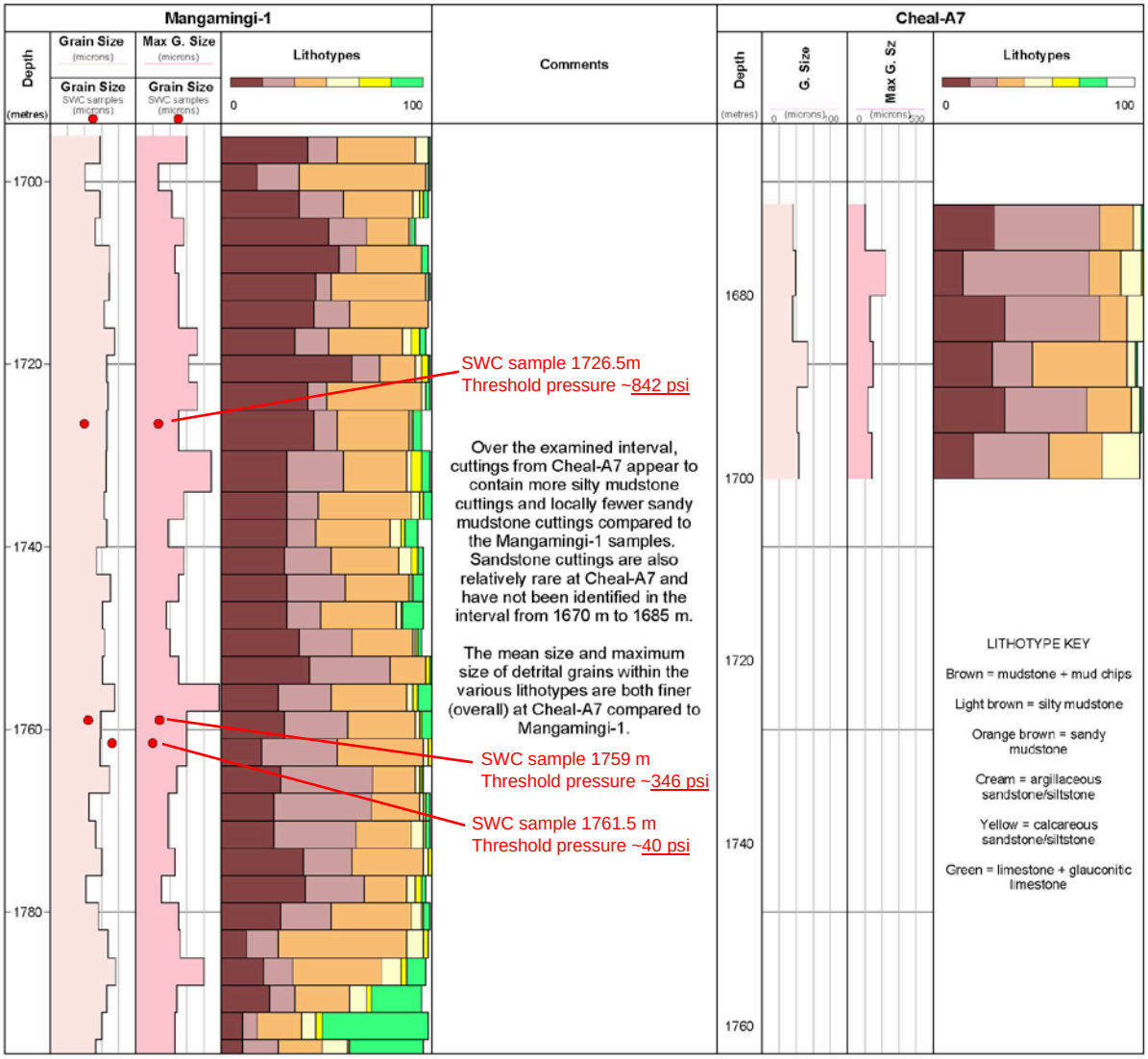

Figure A2.6: Comparison of grain size and lithotype abundance, cuttings samples from Miocene mudstones, Mangamingi-1 and Cheal-A7. From Higgs & Crundwell (2008). Significant variability in threshold pressure relating to stratigraphic changes in lithology (% lithotypes and associated differences in grain size and mineralogy).

A2.3 Geochemistry

Table A2.7: Geochemical Studies Reference Table. References 1) Bo et al. (2021), 2) Hassannayebi et al. (2019), 3) Amid et al. (2016), 4) Yekta et al (2018a), 5) Shi et al. (2020), 6) De Lucia et al. (2015), 7) Yekta et al. (2018b), 8) Henkel et al. (2014), 9) Flesch et al. (2018), 10) Truche et al. (2013).

Ref	Type of study	Rock Type	Results	Notes
1	Geochemical modelling varying temperature (30-200 °C), pressure (0.1-101 Mpa), salinity (distilled water, 5000-35000 ppm, formation brine), & mineralogy	Mondarra sandstone (wt%): quartz (76%), kaolinite (10%), K-feldspar (3%), muscovite (3%), pyrophyllite (3%), calcite (3%), chlorite (2%)	Very little reaction is modelled between the hydrogen-saturated aqueous solution and silicate and clay minerals; the presence of carbonate in the Mondarra sandstone (av. 3% in the models) triggers up to 9.5% hydrogen loss due to calcite dissolution induced hydrogen dissociation process.	
		Tubridgi sandstone (wt%): quartz (64.4%), muscovite (5.7%), tourmaline (5.4%), K-feldspar (4.9%), kaolinite (4.2%), pyrophyllite (4%), montmorillonite (3.6%), lithic (3%), pyrite (2.9%), chlorite (1.9%)		
2	Geochemical modelling to evaluate gas-brine-mineral interactions; equilibrium batch modelling and kinetic modelling; H_2 solubility assumed at equilibrium with gas phase	Clay and carbonate rich sandstone (nearby, vol%): quartz (20%), muscovite & clay (47%), plagioclase (4%), K-feldspar (2%), calcite (20%), dolomite (9%), ankerite (4%), siderite (2%), pyrite (1%). Clays comprise illite (59%), smectite (29%), chlorite (15%), kaolinite (3). Water chemistry provided in paper	Modelling suggests H_2 reactions will only become significant over long timescales (much greater than considered for storage cycles); equilibrium batch show increase of pH associated with formation of pyrrhotite from pyrite, dissolution of muscovite resulting in increase in K^+	Molasse Basin, Austria, suitable storage site for pilot study; 1.5 m thick reservoir, 22% porosity, 22% irreducible water saturation, T 40 °C. Mineralogical from XRD of a nearby well
3	Geochemical modelling of several different mineral assemblages in the presence of water, hydrogen, and in some cases hydrogen sulphide; pH 5	1) Sandstone: quartz, illite, kaolinite, chlorite, montmorillonite, sepiolite, K-feldspar, K-mica, anorthite, iron oxides 2) sulphur-containing minerals including anhydrite, gypsum, pyrite, sulphur	Clay-bearing sandstone and iron oxides were found to be stable under the reservoir conditions; sulphur assemblages were not stable suggesting conversion of H_2 to H_2S may occur	Leakage losses in the model were ~ 0.035% of the stored H_2 after 12 months (0.029% in the aquifer, 0.006% in the cap rock)
4	Experimental and modelling; 100, 200 °C, max H_2 pressure 100 bar, duration 1.5-6 months, pure H_2 and H_2-water	3 quartzose sandstones vol%: quartz (71.6-80.9%), K-feldspar (17.2-25.7%), mica (0.6-2.3%), oxide (0.3-0.9%), clay minerals (0.6-1%)	Limited reaction suggesting that H_2 can be considered as relatively inert; minor changes in the clays and Fe oxides - small reduction in FeO concentration of muscovite. New phases identified are Fe-bearing hydrous and anhydrous silicates and oxides	Most experiments performed in the absence of water
5	Incubation experiments with H_2/natural gas mixtures (13-15%/85-87%), 3 month period, representative storage reservoir T & P (353.15 °K, 26.2 Mpa)	Reservoir (wt%): quartz (31.3%), plagioclase (24.6%), K-feldspar (10.6%), gypsum (1.7%), pyrite (0.3%) total clay (31.5%)	Gypsum gone, other minerals show small increases or decreases in wt% (before and after incubation, but note destructive technique); larger changes in permeability but not consistent, decrease in cap rock potentially improving sealing quality	Reservoir, cap rock and cement samples from a California natural gas storage site
		Cap rock (wt%): quartz (12%), opal (40.5%), plagioclase (16%), K-feldspar (5.4%), gypsum (1.4%), pyrite (2.1%) total clay (22.6%)		
		Polymeric materials used in natural gas storage operations (wt%): quartz (55.6%), calcite (3.6%), portlandite (40.8%)	Swelling due to H_2 exposure but no direct evidence of geochemical reactions. Calcite actually increases (3.6 wt% to 7.9	Only mineralogical analysis was XRD on 3 samples (1 reservoir, 1 cap rock, 1 cement)

			wt%) but portlandite decreases (40.8 wt% to 29.8 wt%); permeability increase may impact quality	
6	Static batch experiments of H_2 solubility, salinity (up to 20% NaCl), temperatures (up to 373.15 °K) pressures (up to 200 bar); 1) pure H_2, 2) hydrogen and saline solution	N/A	Evaluation method to obtain PVT data and interpret solubility data. Experimental results of hydrogen solubility exceeded the values predicted by theoretical models	
7	Core-flood experiments for relative permeability and capillary pressure, H_2-water-rock, under 1) 55 bar 20 °C and 2) 100 bar 45 °C	Triassic sandstone	Relative permeability curves and capillary pressure data vary little for both sets of experimental conditions	Both shallow/low T conditions
8	Static batch experiments, 3% H_2 + 97% CO_2, sample specific reservoir conditions (p, T, Xfluid)	Sandstone and Cap rock from 25 wellsites in Germany and Austria, sandstone includes subarkoses, arkoses, lithic subarkoses and sublitharenites. Authigenic minerals locally include chlorite, carbonate, anhydrite, quartz,feldspar	Mineral dissolution and increase in permeability, specifically decrease in calcite & anhydrite cement resulting in increase in porosity	Note low H_2 high CO_2 gas content
9	Static batch experiments, H_2 and brine, 6 weeks, different reservoir specific conditions; 100% hydrogen	Tertiary sandstone	No chemical reactions	3 potential H_2 storage sites in Germany
		Permian, Triassic & Tertiary sandstones including lithic subarkoses, litharenites, sublitharenites, subarkoses, arkoses; starting mineralogy not provided	Before and after porosity and permeability measured with significant changes but increase in porosity (plug samples) mostly accompanied by small **decrease** in permeability (interpreted as sample-specific heterogeneities and ppt of salt and carbonates due to selective oversaturation). Increase in permeability was measured from CT analyses on smaller cube samples. Permeability changes (-60.5% to +38.5%) and porosity changes (-56 to +107.8%). Observations show severe carbonate and anhydrite dissolution although no quantiative data. No alteration observed for feldspar, quartz, mica, volcanic clasts, clay minerals (illite and chlorite)	21 samples from Germany and Austria: Molasse, >1.6 km; Emsland, >1.5 km; Altmark, > 3km. Pore-filling anhydrite and carbonate in Triassic samples (Emsland)
10	Batch experimental, 90 & 150-250 °C, hydrogen partial pressure 3-30 bar, ground sample, 5 month duration	Clay-rich rock with pyrite (1-2 wt%): clay fraction (48%), quartz (19%), calcite (22%), dolomite (7%), pyrite (1.4-1.9%)	Rapid precipitation of pyrrhotite due to reduction of pyrite in all high-T experiments (150-250 °C); pH remained at 7.5-8.2; no morphological modification of clay particles, quartz, calcite, dolomite and feldspar was observed at 150 °C. At lower temperatures (90 °C) no observed precipitation of pyrrhotite, major change in water chemistry or pH (7.6-7.7), although corrosion pits were observed on the pyrite	Higher hydrogen pressures in a storage site (50-100 bar) could result in pyrrhotite precipitation even at the lower temperatures.

Appendix 3 - UHS opportunities beyond Taranaki

The following screening assessment of North Island (excluding Taranaki) UHS opportunities is done using typical geology within these regions and the following assumptions:

1. Suitable geology, i.e. a porous reservoir with a suitable pore volume for the desired maximum volume of gas to be stored; an unambiguous crest within a containing structure; assurance as to effective cap rock and lateral boundaries whether structural (fold limbs and/or fault planes) or stratigraphic (i.e. depositional or diagenetic edges to the porous domain).
2. Proximity to a source of electricity, ideally renewable generation such as a wind farm, solar development, geothermal or hydroelectric plant, but potentially simply a point on the national grid.
3. Proximity to a hydrogen infrastructure hub, which might be the gas pipeline system as it is progressively de-carbonised; or a major industrial sink for hydrogen (e.g. methanol, ammonia).

In the North Island, UHS opportunity classes are broadly spread across the subdivisions of the gas pipeline network as summarised in Figure A3.1.

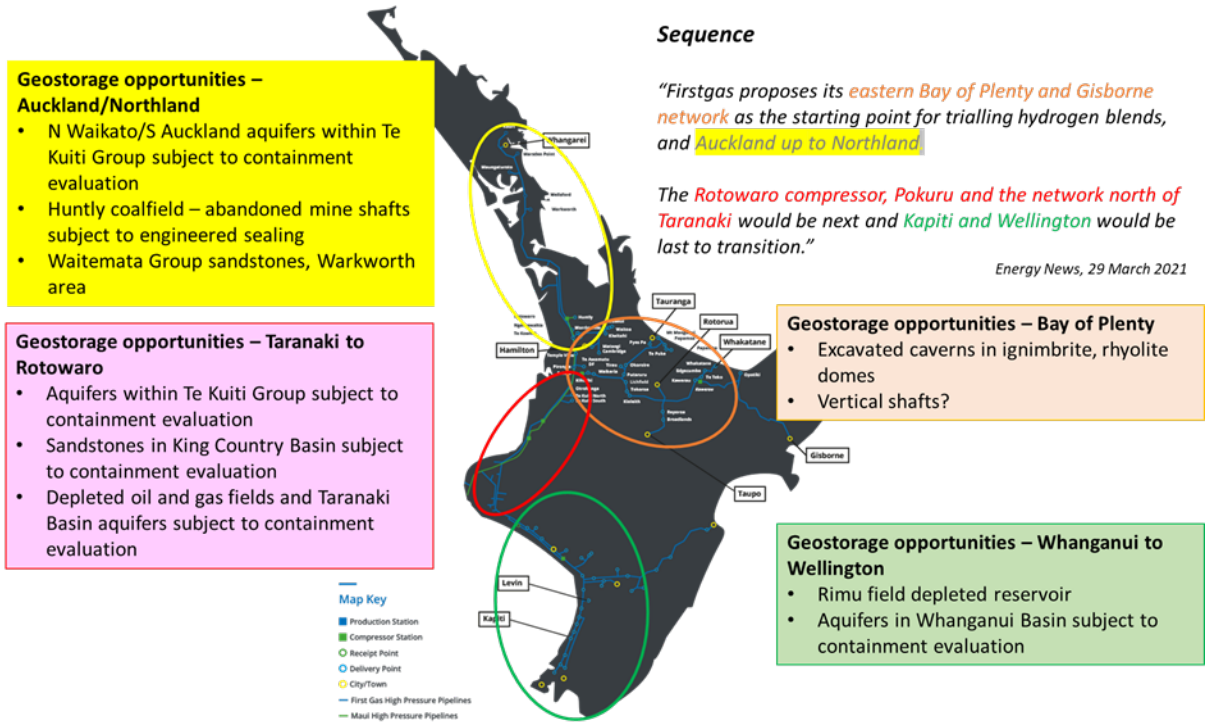

Figure A3.1: Gas transmission network and low-level UHS opportunities in the North Island. Figure adapted from FirstGas (2020).

The geological aspects are discussed briefly below.

East Coast

Opportunities on the East Coast of the North Island have not been given detailed consideration at this juncture, due to unfavourable aspects of the geology as well as the limited penetration of natural gas infrastructure.

Petroleum exploration over more than a century has failed to establish any commercial discovery despite widespread surface and subsurface manifestations of both oil and gas. The closest to success was declared a gas discovery at Kauhauroa-1 in the Wairoa district of northern Hawkes Bay, with gas tested at up to 11 million cubic feet per day in 1998. Considerable appraisal investment and wells on other structures in the area failed to prove up the prospect.

In general, the East Coast basin system has poor to moderate reservoir/aquifer quality apart from shallow limestone bodies which are widespread in outcrop but apparently rare in the subsurface. More significantly, intense active tectonic activity is a high risk to effective containment.

Bay of Plenty

The eastern branch of the gas pipeline network traverses the central volcanic region which contains several geothermal fields. The Tauranga–Taupo–Whakatane triangle within the eastern branch contains many gas distribution nodes (Figure A3.1) that could provide strategic medium-scale (small UHS) storage to either transmission or distribution networks in the area. This area is primarily composed of volcanic, volcaniclastic and alluvial sedimentary rocks. Sedimentary units within the Tauranga group have been known to be prolific aquifers (e.g., Petch & Marshall, 1988) and could be a possible target for UHS. The Tauranga group may be locally self-sealed by mudstones and faulting, however extensive subsurface mapping would be required to determine possible localities of interest. Low-temperature geothermal fields may act similarly to aquifers and may benefit from prior exploration of these resources; however the addition of geothermal mineral elements would require extensive research of hydrogen-rock interactions on a site-by-site basis.

Aquifers and low-temperature geothermal fields may also occur in non-welded ignimbrites that are common to this area. These present similar challenges to their sedimentary counterparts, although require further geochemical interactions to be assessed. Fractured lavas, including rhyolite domes may show high porosities and permeabilities and it is conceivable that they could prove to be effective reservoirs (Bischoff et al., 2021; Rissmann et al., 2011; Yates et al., 2021). As with geothermal reservoirs, volcanic UHS is novel and subject to further evaluation and should be treated as such.

Engineered caverns and vertical shafts might provide a more technically ready option for medium scale storage in the Bay of Plenty. Suitable rocks to investigate cavern storage could include coherent lavas, welded ignimbrites, shallow basement rocks and shallow lava domes. Although the Bay of Plenty may provide a strategic hub for hydrogen storage there is an exceptionally high degree of scientific and technical uncertainty surrounding UHS options presented above. Furthermore, extensive subsurface data either does not exist or is unpublished in the public domain and would require significant time and monetary costs for exploration and appraisal to establish the viability of UHS.

Waikato

The Huntly Coalfield could provide a strategic location for UHS in one or more of the several abandoned underground mines (Figure A3.2), including the massive Huntly East mine that

ceased operations in 2015 (Sherwood et al., 2019). The Huntly East mine reached a depth of 340 m below ground level and has produced well over 9 million tonnes of coal. The mine underwent a pilot coal gasification project to a depth of 380m in 2011 – 2012 (Sherwood et al., 2019).

The Huntly Coalfield exploits the Waikato Coal Measures, a 50–100 m thick unit with up to three coal seams, namely; the 3–24m thick Kupakupa Seam; the <6m overlying Renown Seam; and the Ngaro Seam that rarely exceeds 2m thickness (Sherwood et al., 2019). The Waikato Coal Measures are overlain by the Te Kuti Group that forms a barrier to the overlying Tauranga Group aquifer – another potential target for UHS. Despite previous tectonic activity, there are no known active faults nearby (GNS Science, 2020).

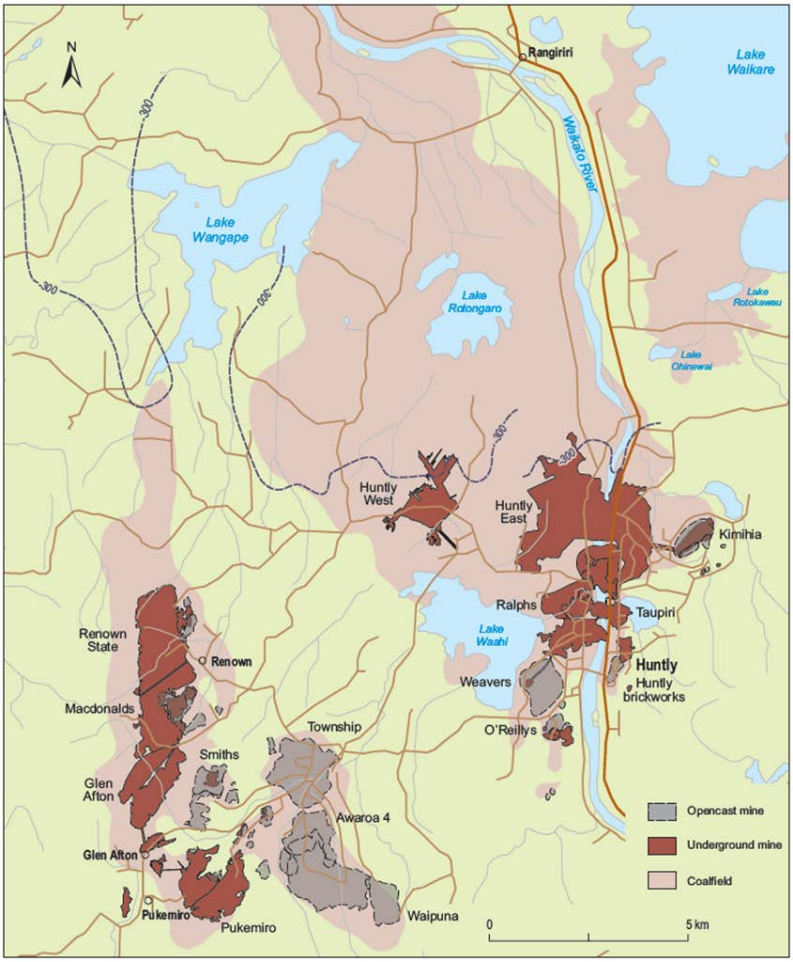

Figure A3.2: Map of historic and current coalmines in the Huntly and Rotowaro coalfields. The 300m depth interval of the major Kupakupa Seam is approximated by the dashed black line. Figure from Sherwood et al. (2019).

Using an assumed coal density of 1.25 t/m^3 from Gray and Macknight (1986) studies of New Zealand coal, an estimated void volume can be calculated (Table A3.1). Note that an estimated void should not be considered equivalent to total available volume as difficult working conditions including inclines created by coal compaction, deposition on uneven basement topography and syn- and post-depositional faulting have resulted in an irregular void space. Considerations about use of liners, maximum operating pressures and other

geochemical and geomechanical implications would require further research in a separate study before considering the feasibility of this storage type.

Table A3.1: Estimated void space of underground coal mines in the Huntly coalfields. Table adapted from Sherwood et al. (2019). Void space is estimated using the assumption that New Zealand coal density = 1.25 t/m3 from (Gray & Macknight, 1986).

Mine	Years worked	Production (t)	Estimated void (m^3)
Waikato (Kupakupa)	1876 – 1999	209,089	167,000
Taupiri Reserve	1887 – 1910	372,258	280,000
Taupiri Extended	1889 – 1924	3,110,064	2,488,000
Ralph's	1898 – 1916	1,268,236	1,015,000
Huntly West	1978 – 2001	1,200,000	960,000
Huntly East	1978 – 2015	9,780,000	7,824,000

Auckland/ Northland

In the south, the strata associated with the Waikato coal fields (Te Kuiti Group) include several sandstones with good porosity and permeability; containment may be problematic considering generally simple structure (lack of identified anticlinal folds) and uncertain integrity of cap rock top seal formations.

From Auckland northwards, the early Miocene Waitemata Group includes sandstones of moderate (at best) reservoir quality which would require considerable exploration/appraisal investment to establish the viability of UHS.

Planned expansion of large-scale solar power generation across Northland represents a potential synergy for green hydrogen, and UHS potential could be screened at sites especially where proximal to the gas pipeline system.

Appendix 4 - Reservoir Engineering

This section provides further details about reservoir engineering concepts introduced in Section 6.

A4.1.1 - UHS static modelling

Consider a mass of hydrogen, M, to be stored by UHS. At standard surface conditions (20°C, 1 atm), the hydrogen occupies a volume, V_{std}, given by

$$V_{std} = \frac{M}{\rho_{std}}$$

where ρ_{std}=0.083 kg/m^3 is hydrogen density at standard conditions. At reservoir conditions, the same gas occupies a pore volume, V_{pore}, given by

$$V_{pore} = \frac{M}{\rho_h(P,T)}$$

where ρ_h is the density at reservoir pressure, P, and temperature, T. Recognizing that available pore volume is only a fraction of the rock formation volume, the equivalent UHS volume is

$$V = \frac{V_{pore}}{\phi - \theta_{res}}$$

where ϕ is formation porosity and θ_{res} is the residual saturation of an immobile liquid phase (water, oil) that cannot be displaced by the injected hydrogen.

In the absence of direct observations, pressure and temperature at reservoir depth are estimated from linear relations

$$P = P_{atm} + \rho_w g z, \qquad T = T_{surf} + \frac{dT}{dz} z$$

where P_{atm} = 0.1 MPa (1 bar), ρ_w is the density of water [1000 kg/m^3], g is the acceleration of gravity [9.8 m^2/s], z is depth [m], T_{surf} is average surface temperature [°C] and dT/dz is the geothermal gradient [°C/km]. For Taranaki, we have used indicative values of 15°C and 29°C/km for the surface temperature and geothermal gradient respectively (Armstrong et al., 1996).

The equivalent energy content, E, of the stored hydrogen is

$$E = M \times LHV$$

where LHV is the lower heating value of hydrogen [120 MJ/kg] and is the readily available heat liberated through combustion.

A4.1.2 - UHS dynamic modelling

The mass rate at which fluids flow underground is governed by Darcy's law

$$\mathbf{q}_i = \frac{\rho_i k k_{ri}}{\mu_i}(\nabla P - \rho_i \mathbf{g})$$

Where $\mathbf{q}$ is the mass flow rate vector [kg/s], k is permeability [m^2], k_r is relative permeability [-], μ is viscosity [Pa s], ∇P is the pressure gradient vector [Pa/m], $\mathbf{g}$ is the gravitational acceleration vector [m^2/s], and the subscript i denotes the fluid component (e.g., h = hydrogen, w = water).

A numerical reservoir simulator solves the equations of mass conservation on a discretized grid of blocks representing the reservoir. The Darcy flow law, EQ (1), is an imposed constraint. The output of the reservoir model is pressure and fluid composition (fraction of hydrogen vs. water) time series for each of grid block. How these change over time depends on the imposed boundary conditions (injection/production of hydrogen), fluid and rock properties.

This compositional simulator FEHM used in this study does not implement an equation of state for an oil phase. Thus, when simulating injection into a depleted gas reservoir, water is used to approximate the displaced oil phase. Results should be interpreted with some caution. For instance, because, water has a lower viscosity than oil, displacement of the fluid phase by hydrogen will be overestimated. On the other hand, water is less compressible than oil, and so pore space availability for hydrogen storage will be underestimated. Although these errors will partly cancel each other, any subsequent analysis of site feasibility should be undertaken with a commercial hydrocarbon simulator that includes accurate phase properties, gas dissolution and gas-oil relative permeability.

A4.1.3 - Hydrogen properties

The simplest approximation for gas density is the ideal gas law:

$$\rho_{id} = \frac{PM}{rT}$$

where ρ_{id} is ideal gas density [kg/m^3], P is pressure [Pa], M is molecular weight [for hydrogen, 0.002016 kg/mol], r is the ideal gas constant [8.3145 J/kg/K] and T is temperature [K]. Modifications are necessary to describe the departure of real gases from ideal behaviour, particularly at high pressure. The density of a real gas can be described using a compressibility factor to modify EQ (2) above

$$\rho_h = \frac{\rho_{id}}{Z(P,T)}$$

where ρ_h is real gas density of hydrogen, and Z is the compressibility factor depending on P and T. Setting $Z = 1$ recovers the ideal gas law. In this study, we have used the polynomial model of Zheng et al. (2016), which agrees with NIST density data to within 0.01% in temperature and pressure ranges of interest (Figure A4.1).

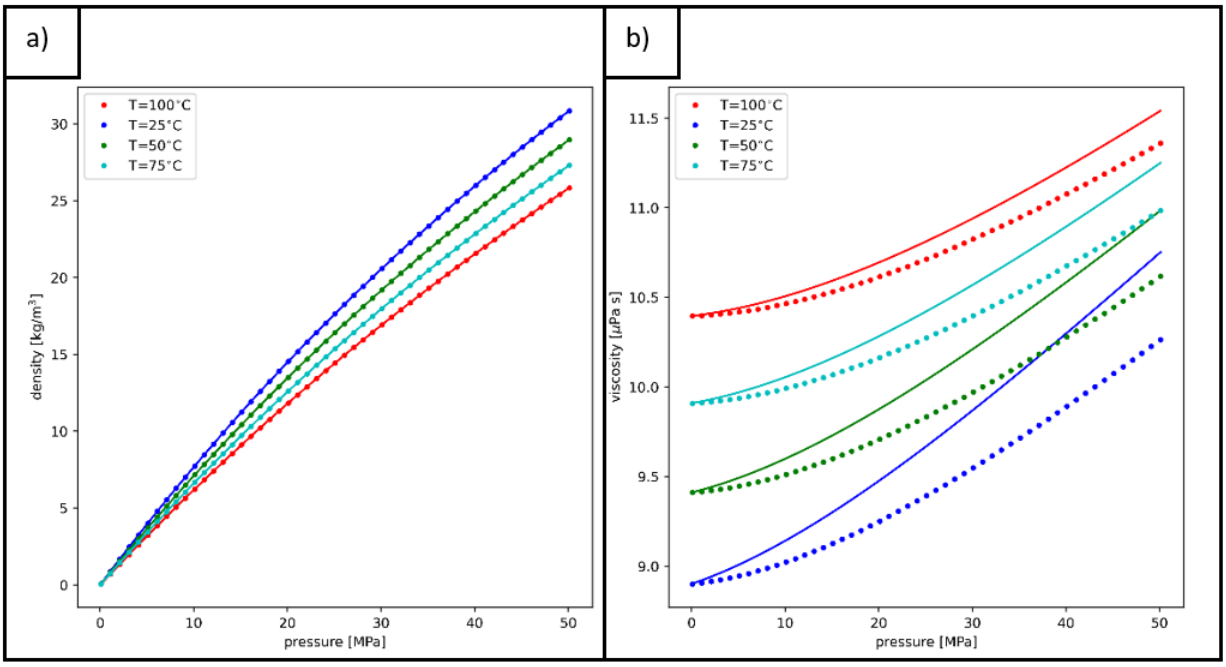

Figure A4.1: Hydrogen properties at possible reservoir pressures and temperatures. (a) Density, as given by a real gas model of Zheng et al. 2016 (lines) fitted to NIST data (dots), accurate to within 0.01%. (b) Viscosity, as given by the model of Muzny et al. 2013 (lines) fitted to NIST data (dots), accurate to within a few percent.

Hydrogen viscosity

Viscosity quantifies a fluid's resistance to flow through a porous medium. The range of hydrogen viscosity at UHS conditions (9-11 µPa s) is comparable to other gases (CO_2, 0.05-77; natural gas, 11-27 µPa s), and low compared to water (300-900 µPa s). Viscosity contrasts can result in the development of "fingers" at the front of a developing plume, as the less dense hydrogen displaces the in-situ fluid (natural gas, water or oil). Viscous fingering can reduce storage efficiency and recovery from a reservoir. However, the process is difficult to resolve in models and therefore rarely considered in site analyses. It has not been studied here.

Viscosity depends on both temperature and density, which in turn depends on pressure. To calculate viscosity in reservoir simulations, we used the correlation of Muzny et al. (2013), which was obtained from regression to a large experimental dataset. The model over predicts viscosity by a few percent in the reservoir conditions of interest (Figure A4.1)

Hydrogen solubility and losses

Hydrogen gas can dissolve into water at the gas-liquid interface. This might occur both on the lateral flanks of the injected plume as well as at the top surface where it contacts the cap rock, which is presumed to be water saturated. Hydrogen that dissolves into water is likely to be unrecoverable and therefore represents a loss from the UHS.

At reservoir conditions of interest, hydrogen solubility in water ranges between 0.001 and 0.006 mole fraction. For comparison, CO_2 solubility is much higher, ranging 0.006 to 0.027. In a numerical analysis of UHS, (Heinemann, Scafidi, et al., 2021) argued that H_2 dissolution can be neglected because it is an order of magnitude smaller than CO_2. Ennis-King et al. (2021) used an analytical diffusion model to approximate dissolution losses into the overlying cap

rock. For typical parameters, the scale of loss was estimated to be less than 1% of the injected volume over 25 years.

The relatively low solubility of hydrogen is an advantage for vertical containment of the buoyant H_2 plume by water saturated cap rock (Ennis-King et al., 2021).

Hydrogen is much more soluble in liquid hydrocarbons than in water. UHS in depleted oil reservoirs would need to develop appropriate dissolution relations specific to the oil in place if dissolution losses are to be estimated.

Relative permeability

The relative movement of co-existing hydrogen and water phases under a pressure gradient depends on how gas and water interact. In a reservoir model, this is captured by relative permeability curves, which rebalances the individual hydrogen and water flow rates to account for the saturation of each. For example, as the amount of water in a grid block decreases (say, because it is being displaced by hydrogen) the relative ability of the remaining water to move is diminished. Ultimately, this imposes a minimum residual saturation of pore water, which reduces the available storage volume.

Yekta, Manceau, et al. (2018) measured relative permeability of hydrogen-water mixtures in sandstone rocks. Exponential curves fitted to their experimental data have been used in models developed here (Figure A4.2).

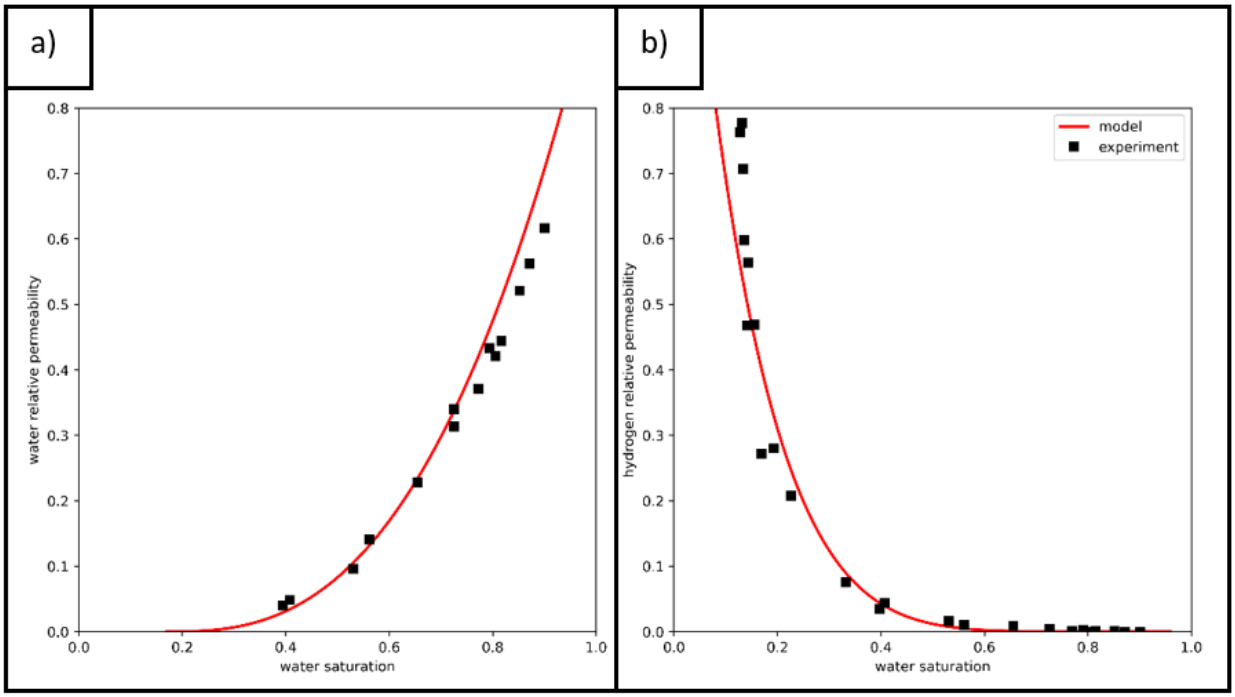

Figure A4.2: Relative permeability curve fits (red line) to experimental data (black squares) from Yekta et al. (2018). (a) water relative permeability, k_{rw}. (b) hydrogen relative permeability, k_{rh}.

Capillary pressure is a property of gas-water-rock interactions that controls, amongst other aspects of the hydrogen plume dynamics, entry of the buoyant gas phase into the overlying cap rock. A high capillary pressure will tend to inhibit hydrogen entry and therefore render

losses through the cap rock negligible. Ennis-King et al. (2021) modelled the relative buoyancy forces of hydrogen and methane (natural gas) entrapments, and showed that a cap rock that traps methane (as must be the case in depleted gas reservoirs) can trap at least as thick a column of hydrogen. Capillary pressure effects have not been considered in our simulations.

A4.1.4 - Wellbore model

When modelling an injection well, we can choose to specify either the rate or the pressure. Fixing either rate or pressure imposes a response on the other quantity, e.g., selecting a mass rate that is too large could cause DHP to exceed the fracture gradient or pump limit. To avoid this situation, it is more pragmatic to specify safe operating pressures (for injection and production) and calculate the flow rates consistent with these.

For reservoir models with large blocks, a Peaceman correction is used to represent unresolved wellbore pressure effects (Feldmann et al., 2016; Heinemann, Scafidi, et al., 2021; Peaceman, 1983). The alternative is to sufficiently discretize the near wellbore region, which is what has been done here.

For a wellbore fully penetrating the reservoir, the flow is calculated

$$Q = \frac{\rho_h k k_{rh}}{\mu_h} \times \frac{P_{DHP} - P_{res}(r)}{r} \times h \times 2\pi r_{well}$$

where h is reservoir thickness, P_{DHP} is downhole pressure maintained by the pump, r_{well} is the radius of the well, and P_{res} is pressure within the reservoir a short distance, r, from the well. The reservoir pressure will change over time in response to injection, production, and diffusive relaxation of overpressure (Heinemann et al., 2021). Thus, injection and production rates will tend to decline over time. Furthermore, larger diameter boreholes can accommodate greater transfer rates to and from storage for similar operating pressures.

There are several ways to choose the injection pressure. Heinemann et al. (2021) modelled storage in saline aquifers where high pressure is needed to displace water. They used an injection pressure that was 90% of the fracture pressure, i.e., the threshold where tensile hydraulic fractures would be opened in the reservoir. This can usually be estimated from depth considerations and a simple geomechanical model. During the production phase, they allowed pressure to drop by up to 100 bar.

The approach is different for a depleted reservoir. Feldmann et al. (2016) modelled UHS in a depleted reservoir that had experienced a pressure decline of 350 bar during earlier development. They first considered injection of H2 enabling a pressure recovery in the reservoir of 330 bar, i.e., pressure was still 20 bar below the pre-development pressure. They then considered an operating pressure range of 100 bar, which was the difference between maximum pressure during injection and minimum pressure during production.

The two injection pressure regimes are shown schematically in Figure A4.3.

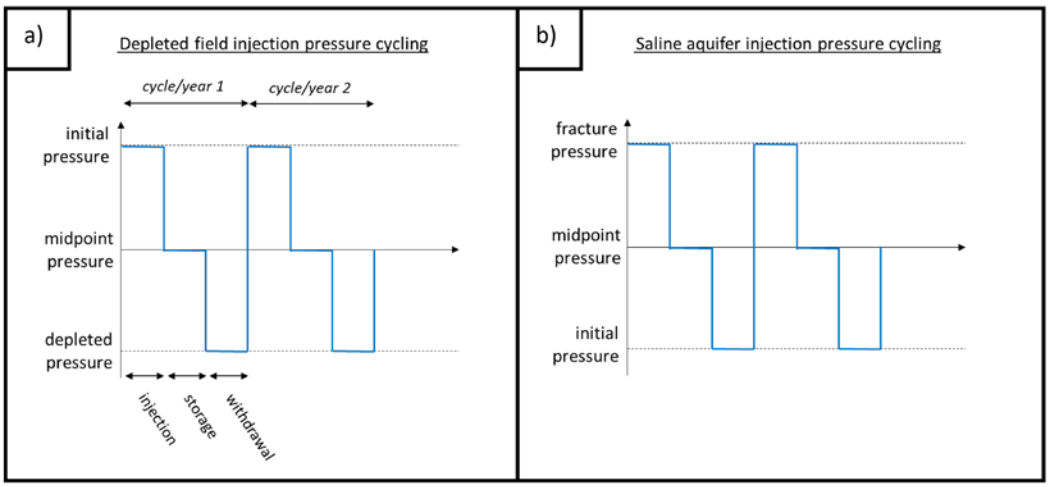

Figure A4.3: Schematic injection pressure cycling for (a) depleted reservoir scenarios, (b) saline aquifer scenarios.

A4.2 - Ahuroa U20 sand geomechanical calculation

The tectonic stress state in the vicinity of Ahuroa is most likely extensional with the possibility of some strike-slip component (Rajabi et al., 2016). In the absence of in-situ stress measurements, we can use frictional theory to estimate the minimum principal stress at reservoir depth and use this to constrain the safe injection pressure. Assuming an average overburden density of 2500 kg/m^3, the vertical stress at reservoir depth is 25 MPa. In an extensional tectonic setting, this is the maximum principal stress. For a corresponding hydrostatic reservoir pressure of 10 MPa, the effective vertical stress, σ_v', is 15 MPa.

For a system at the limit of frictional failure, maximum and minimum principal stresses are related by (Jaeger et al., 2007)

$$\sigma_v' = \left(f_s + \sqrt{1 + f_s^2}\right)^2 \sigma_{h,min}'$$

For typical rock friction values (f_s=0.6 – 0.8), an indicative range for $\sigma_{h,min}{}'$ is 3.4 to 4.8 MPa. Hydraulic fractures will open when fluid pressure is raised high enough that the minimum principal effective stress reaches 0. Thus, injection pressures should not exceed 3.4 MPa and the modelled pressure range is $\pm$1.7 MPa.

Table A4.1: Hydrogen quantity conversion table.

kg	kt	PJ	TWh	Volume at standard conditions (15°C, 1 bar) [Nm^3]	V at typical reservoir conditions (80°C, 250 bar, density = 15.4 kg/m^3) [m^3]
1	10^{-6}	1.2×10^{-7}	3.3×10^{-8}	11.9	0.065
10^6	1	0.12	0.033	1.2×10^6	6.5×10^4
	8.33	1			
			1		
				1	
					1

Appendix 5 - Geophysical monitoring

Table A5.1: Geophysical techniques that may be used to monitor stored hydrogen and associated rock deformation in the subsurface.

Technique	Capabilities	Detection limits	Where applicable	Limitations
3D seismic	Images seismic wave reflectivity, for a volume beneath a 3D surface array. Can be used in a time-lapse (4D) mode, by repeated surveying over the same area.	Vertical resolution controlled by the wavelength of the seismic waves (~10-100m), and wave speeds of sediments. Good horizontal resolution ~20-50m.	Both onshore and offshore. Costs are significantly cheaper offshore.	In 4D mode repeat measurements require high accuracy to reduce artefacts.
Distributed Acoustic Sensing (DAS)	Images seismic reflectivity and microseismicity. Uses optical fibre to record seismic waves. Fibre can be left on the ground for the duration of the monitoring campaign for high repeatability.	Same vertical resolution as described above, but horizontal resolution customisable due to the nature of the fibre. In passive mode, a low error of 10-30m seismic event could be expected in optimum conditions.		The DAS is calibrated to either active source (reflectivity) or passive microseismic recordings, meaning one of the two methods will have a lower sensitivity.
Passive-seismic	Records microseismicity which may indicate induced fractures or movement of natural fractures due to hydrogen injection.	5-10 metre accuracy obtainable, depending on whether borehole or surface sensors are used, and the design of the sensor array.	Primarily onshore, although seafloor passive seismic recording is routinely carried out over North Sea oil reservoirs, using OBS's and seafloor ocean-bottom cables.	Usually requires downhole sensors in separate monitoring well. Optimally this would involve an array of downhole sensors, rather than just a single sensor.
VSP	Forms high-resolution image of seismic reflectivity, in the vicinity of the hydrogen plume.	High seismic resolution (vertical ~5-50m), but usually only acquired in 2D geometry. Can involve multi-component recording, offering potential for pressure/saturation discrimination and anisotropy characterisation.	Both onshore and offshore.	Requires monitoring well close to hydrogen plume, and a well-designed acquisition geometry.

Downhole logging	Measures rock-fluid properties immediately surrounding the measurement well, with very high (cm) resolution. Routinely used in the oil-gas industry.	Very high resolution providing a range of rock properties, including resistivity, density, sonic velocity, nuclear magnetic resonance, among others. Each log has the potential to discriminate different lithologies/properties.	Onshore and offshore.	Penetration of different signals is only tens of cm (other than for resistivity). Seldom used to monitor fluid plume movement. Costly to run in a time-lapse sense.
Gravimetry	Detects density changes in volume, which can be used to track the migration of the hydrogen.	Detects density contrast with 100s of m resolution.	Primarily onshore, although offshore work has been carried out, using seafloor plinths and ROV's.	Poor vertical and lateral resolution and limited to strong density contrast between the hydrogen and surrounding material.
Cross-well EM	Utilises time-variant source field to derive information about subsurface electrical structure	Potentially ca. 5 m resolution, but dependent on the separation of transmitters and receivers (in adjacent monitoring wells)	Primarily onshore	Dependent on positioning of transmitters and receivers (in relation to the plume). Really requires cross-hole seismic to be also carried out, for joint interpretations.
Cross-well Electrical Resistivity, EM or Seismic Tomography	Measurement of direct or induced electrical currents or wave propagation between two boreholes.	Depending on electrical electrodes, magnetometers and geophone configurations hydrogen accumulations more than ~30m thick could be imaged with borehole instruments.	Primarily onshore.	Technique limited to detection of lateral changes (not changes with depth). Requires two wells setup with equipment: one with sources and the other with receivers.
Surface Electromagnetics (EM)	Electrical and magnetic fields induced in the subsurface. Created and received via electromagnetic sources and receivers. Data translated into electrical resistivity images of the subsurface.	EM methods suitable for monitoring storage in water-bearing formations, where hydrogen displaces more conductive formation waters. Technique could be sensitive to thin resistive anomalies at depths 100s m to several km.	Offshore, involving repeated surveys using seafloor EM instruments, recording from ship-source.	Poor vertical and lateral resolution. Hard to achieve repeatability for 4D studies. Resistivity models non-unique.
Satellite interferometry	Repeated radar surveys detect changes in elevation potentially caused by hydrogen injection.	InSAR can detect millimetre-scale changes in elevation.	Onshore	Changes in elevation may not occur, or may occur seasonally (e.g., via water saturation or freezing/thawing).